

**MECHANICAL CHARACTERIZATION AND SOILD PARTICLE  
EROSION RESPONSE OF PARTICULATE FILLED  
JUTE-EPOXY COMPOSITES**

A THESIS SUBMITTED IN PARTIAL FULFILLMENT OF  
THE REQUIREMENTS FOR THE DEGREE OF

**MASTER OF TECHNOLOGY**

IN

**MECHANICAL ENGINEERING**

[Specialization: Machine Design and Analysis]

By

**ALOK KUMAR JHA**

207-ME-116



Department of Mechanical Engineering

**NATIONAL INSTITUTE OF TECHNOLOGY  
ROURKELA**

MAY, 2009

**MECHANICAL CHARACTERIZATION AND SOILD PARTICLE  
EROSION RESPONSE OF PARTICULATE FILLED  
JUTE-EPOXY COMPOSITES**

A THESIS SUBMITTED IN PARTIAL FULFILLMENT OF  
THE REQUIREMENTS FOR THE DEGREE OF

**MASTER OF TECHNOLOGY**

IN

**MECHANICAL ENGINEERING**

[Specialization: Machine Design and Analysis]

By

**ALOK KUMAR JHA**

**Roll No. 207-ME-116**

Under the supervision of

**Prof. Alok Satapathy**

Department of Mechanical Engineering, N.I.T. Rourkela

and

**Mr. Sisir Mantry**

Advanced Materials Department,  
Institute of Minerals & Materials Technology  
Bhubaneswar



Department of Mechanical Engineering  
**NATIONAL INSTITUTE OF TECHNOLOGY**  
**ROURKELA**  
MAY, 2009



**National Institute of Technology**

**Rourkela**

## CERTIFICATE

This is to certify that the work in this project report entitled **Mechanical Characterization and Solid Particle Erosion Response of Particulate Filled Jute-Epoxy Composites** by **Alok Kumar Jha** has been carried out under our supervision in partial fulfillment of the requirements for the degree of **Master of Technology** in *Mechanical Engineering with Machine Design and Analysis* specialization during session 2008 - 2009 in the Department of Mechanical Engineering, National Institute of Technology, Rourkela.

To the best of our knowledge, this work has not been submitted to any other University/Institute for the award of any degree or diploma.

**Dr. Alok Satapathy**

(Supervisor)

**Asst. Professor**

Dept. of Mechanical Engineering

National Institute of Technology,  
Rourkela - 769008

**Mr. Sisir Mantry**

(Co-Supervisor)

**Scientist B**

Dept. of Advanced Materials

Institute of Minerals & Materials Technology,  
Bhubaneswar - 751013

## ACKNOWLEDGEMENTS

Setting an endeavor may not always be an easy task, obstacles are bound to come in this way & when this happens, help is welcome & needless to say without help of the those people whom I am going to address here, this endeavor could not have been successful & I owe my deep sense of gratitude & warm regards to my Supervisor **Dr. Alok Satapathy** Assistant Professor, Mechanical Engineering Department , NIT Rourkela for his in depth supervision and guidance, constant encouragement and co-operative attitude for bringing out this thesis work.

I further cordially present my gratitude to my Co-Supervisor **Mr Sisir Mantry** Scientist B Dept. of Advanced Materials Institute of Minerals & Materials Technology, Bhubaneswar for his indebted help and valuable suggestion for accomplishment of my dissertation work.

I extend my sincere thanks to **Dr. R.K. Sahoo**, Professor and Head of Department, Mechanical Engineering Department, NIT Rourkela for his valuable suggestion for bringing out this thesis in time.

I greatly appreciate & convey my heartfelt thanks to my colleague's flow of ideas, dear ones & all those who helped me in completion of this work.

Special thanks to my parents & elders without their blessings & moral enrichment I could not have landed with this outcome.

**ALOK KUMAR JHA**

# CONTENTS

<b>Certificate</b>	<b>i</b>
<b>Acknowledgement</b>	<b>ii</b>
<b>Contents</b>	<b>iii</b>
<b>List of figures</b>	<b>vi</b>
<b>List of tables</b>	<b>vii</b>
<b>Abstract</b>	<b>viii</b>
<b>Chapter 1 Introduction</b>	<b>1</b>
Background and Motivation	2
Naturals Fibers	2
Types of Natural Fibers	3
Thesis Outline	5
<b>Chapter 2 Literature Review</b>	<b>6</b>
On fiber Reinforced Polymer Composites	
On Particulate Filled Polymer Composites	8
On Multiphase Hybrid Composites	9
On Rice Husk and Formation of SiC from it	10
On Erosion Wear Characteristics of Composites	10
On Erosion Wear Modeling	17
On Implementation of Design-of-Experiment (DOE)	19
Chapter Summary	21
<b>Chapter 3 Materials and Methods</b>	
Materials	23
Matrix Material	23
Fiber Material	23

Particulate Filler Material	23
Synthesis of SiC from Rice Husk in a Plasma Reactor	24
Composite Fabrication	25
Mechanical Characterization	26
Density and Void Fraction	26
Tensile Strength	27
Flexural and Inter Laminar Shear Strength	27
Scanning Electron Microscopy	28
Erosion Test Apparatus	28
Parametric Appraisal and Taguchi Method	30
Taguchi Experimental Design	31
Chapter Summary	34
<b>Chapter 4 Mechanical Characterization of the Composites</b>	<b>35</b>
Mechanical Characterization	36
Density and Volume Fraction of Voids	36
Micro Hardness	37
Tensile and Flexural Strength	38
Inter Laminar Shear Strength (ILSS)	40
Surface Morphology of Un-eroded Composite samples	41
Chapter Summary	41
<b>Chapter 5 Development of a Theoretical Model for Erosion</b>	
<b>Wear Rate Estimation</b>	42
Theoretical Model	43
Nomenclature	43
Chapter Summary	48

<b>Chapter 6 Erosion Wear Characteristics of Jute-Epoxy Composites</b>	49
Erosion Test Results	50
Part I For Unfilled Jute-Epoxy Composites (A <sub>1</sub> , B <sub>1</sub> and C <sub>1</sub> )	50
Steady State Erosion	50
Surface Morphology	50
Taguchi Analysis of Erosion Test Results	52
Factor Settings for Minimum Erosion Rate	55
Part II For Jute-Epoxy Composites Filled with	
SiC Particulates (C <sub>1</sub> , C <sub>2</sub> & C <sub>3</sub> )	55
Steady State Erosion	55
Surface Morphology	56
Taguchi Analysis of Erosion Test Results	58
Factor Settings for Minimum Erosion Rate	61
Chapter Summary	61
<b>Chapter 7 Summary and Conclusions</b>	63
Summary	64
Conclusions	66
Recommendation for Future Work	67
<b>References</b>	68
<b>Appendices</b>	77

# LIST OF FIGURES

<b>Figure 3.1</b>	Photograph of the machine (Instron 1195) for tensile and 3-point bend Test	27
<b>Figure 3.2</b>	Loading arrangement for the specimens	28
<b>Figure 3.3</b>	Scanning Electron Microscope JEOL JSM-6480LV	29
<b>Figure 3.4</b>	A schematic diagram of the erosion test rig	29
<b>Figure 3.5</b>	Solid Particle Erosion Test Set Up	29
<b>Figure 4.1</b>	Micro-hardness values of composites with different fiber and filler content	37
<b>Figure 4.2</b>	Effect of fiber loading on tensile & flexural strength of JF-epoxy Composites	39
<b>Figure 4.3</b>	Effect of filler content on tensile & flexural strength of JF-epoxy Composites	39
<b>Figure 4.4</b>	Comparison of Inter-laminar shear strength of different composites	40
<b>Figure 4.5</b>	Surface morphology of un-eroded composite samples	41
<b>Figure 5.1</b>	SEM Micrograph of the erodent used	44
<b>Figure 5.2</b>	Scheme of material removal mechanism	45
<b>Figure 5.3</b>	Resolution of impact velocity in normal and parallel directions	46
<b>Figure 6.1</b>	Erosion rate vs. angle of impingement for different fiber loading	51
<b>Figure 6.2</b>	SEM micrograph of eroded jute-epoxy composite surface	51
<b>Figure 6.3</b>	Comparison of Theoretical and Experimental Values of Erosion Rate	53
<b>Figure 6.4</b>	Effect of control factors	54
<b>Figure 6.5</b>	Erosion rate vs. Angle of impingement for different weight fraction of SiC	56
<b>Figure 6.6</b>	SEM micrograph of SiC filled jute-epoxy composite surface	57
<b>Figure 6.7</b>	Comparison of Theoretical and Experimental Values of Erosion Rate	59
<b>Figure 6.8</b>	Effect of control factors on erosion rate	60



# LIST OF TABLES

<b>Table 3.1</b>	Designation and detailed composition of the composites	25
<b>Table 3.2</b>	Parameters considered during erosion test	30
<b>Table 3.3</b>	Levels for various control factors	32
<b>Table 3.4</b>	Orthogonal array for L <sub>9</sub> Taguchi Design for composites A <sub>1</sub> ,B <sub>1</sub> ,C <sub>1</sub>	32
<b>Table 3.5</b>	Orthogonal array for L <sub>9</sub> Taguchi Design composites C <sub>1</sub> , C <sub>2</sub> , C <sub>3</sub>	33
<b>Table 4.1</b>	Measured and Theoretical densities of the composites	36
<b>Table 4.2</b>	Mechanical properties of the composites	38
<b>Table 6.1</b>	Erosion Test Results for Jute-Epoxy Composites	52
<b>Table 6.2</b>	S/N ratio and Erosion Rate for Different Test conditions	53
<b>Table 6.3</b>	Response Table for Signal to Noise Ratio (Smaller is better)	54
<b>Table 6.4</b>	Erosion Test Results for particulate filled Jute-Epoxy Composites	58
<b>Table 6.5</b>	S/N ratio and Erosion Rate for Different Test conditions	59
<b>Table 6.6</b>	Response Table for Signal to Noise Ratios (Smaller is better)	60

# ABSTRACT

Fiber reinforced polymer composites are now considered as an important class of engineering materials. This thesis depicts the processing and mechanical characterization of a new class of multi-phase composites consisting of epoxy resin reinforced with jute fiber and filled with silicon carbide (SiC) particulates. The SiC used as filler material in this work has been prepared from rice husk through plasma processing technique. The effect of filler in modifying the physical and mechanical properties of jute-epoxy composites has been studied. Rice husk is considered as an agricultural waste and it is thus interesting to explore the utilization potential of SiC derived from rice husk in composite making. Moreover, being cheap, inexhaustible and easily available, it would hopefully provide a cost effective solution to composite manufacturers.

With the increased use of these materials in erosive work environments, it has become extremely important to investigate their erosion characteristics intensively. In view of this, erosion trials are carried out at various test conditions. For this, an air jet type erosion test rig and Taguchi's orthogonal arrays are used. Significant control factors influencing the erosion wear rate are identified. This thesis also presents the development of a theoretical model for estimating erosion damage caused by solid particle impact on the composites. The model is based upon conservation of particle kinetic energy and relates the erosion rate with some of the material properties and test conditions. The theoretical results are compared and are found to be in good agreement with the experimental values.

The research reported in this thesis reveals that successful fabrication of multi-component hybrid jute-epoxy composites with reinforcement of SiC derived from rice husk by plasma processing route is possible. Incorporation of these SiC fillers modifies the micro-hardness, density, tensile, flexural and inter-laminar shear strengths of the composites. Hence, while fabricating a composite of specific requirements, there is a need for the choice of appropriate filler material and for optimizing its content in the composite system. It is demonstrated that if supported by an appropriate magnitude of erosion efficiency, the proposed theoretical model can perform well for epoxy based hybrid composites for normal as well as oblique impacts. The presence of particulate fillers in these composites improves their erosion wear resistance and this improvement depends on the weight content of the filler. Erosion characteristics of these composites have been successfully analyzed using Taguchi experimental design. Significant control factors affecting the erosion rate have been identified through successful implementation of this technique. Impact velocity, fiber/filler content and impingement angle in declining sequence are found to be significant for minimizing the erosion rate of all the composites. Erodent size is identified as the least influencing control factor for erosion rate.

# Chapter 1

## Introduction

### **Background and Motivation**

Composites are materials consisting of two or more chemically distinct constituents, on a macro-scale, having a distinct interface separating them. One or more discontinuous phases therefore, are embedded in a continuous phase to form a composite. The discontinuous phase is usually harder and stronger than the continuous phase and is called the *reinforcement*, whereas, the continuous phase is termed the *matrix*. The matrix material can be metallic, polymeric or can even be ceramic. When the matrix is a polymer, the composite is called polymer matrix composite (PMC). The reinforcing phase can either be fibrous or non-fibrous (particulates) in nature and if the fibers are derived from plants or some other living species, they are called natural-fibers. The fiber reinforced polymers (FRP) consist of fibers of high strength and modulus embedded in or bonded to a matrix with distinct interface between them. In this form, both fibers and matrix retain their physical and chemical identities. In general, fibers are the principal load carrying members, while the matrix keeps them at the desired location and orientation, acts as a load transfer medium between them, and protects them from environmental damages [1].

### **Natural Fibers**

Natural fibers have recently attracted the attention of scientists and technologists because of the advantages that these fibers provide over conventional reinforcement materials, and the development of natural fiber composites has been a subject of interest for the past few years. These natural fibers are low-cost fibers with low density and high specific properties. These are bio-degradable and nonabrasive, unlike other reinforcing fibers. Also, they are readily available and their specific properties are comparable to those of other fibers used for reinforcements. However, certain drawbacks such as incompatibility with the hydrophobic polymer matrix, the tendency to form aggregates during processing, and poor resistance to moisture greatly reduce the potential of natural fibers to be used as reinforcement in polymers.

## Types of Natural Fibers

Natural fibers are grouped into three types: seed hair, bast fibers, and leaf fibers, depending upon the source. Some examples are cotton (seed hairs), ramie, jute, and aflax (bast fibers), and sisal and abaca (leaf fibers). Of these fibers, jute, ramie, flax, and sisal are the most commonly used fibers for polymer composites. Natural fibers in the form of wood flour have also been often used for preparation of natural fiber composites.

On the basis of the source which they are derived from natural fibers can be grouped as:

- Fibers obtained from plant/vegetable  
(cellulose: sisal, jute, abaca, bagasse)
- Fibers derived from animal species  
(sheep wool, goat-horse hair, rabbit hair, angora fiber)
- Fibers from bird / aqueous species  
(bird feathers, fish scale)

A judicious selection of matrix and the reinforcing phase can lead to a composite with a combination of strength and modulus comparable to or even better than those of conventional metallic materials [2]. The physical and mechanical characteristics can further be modified by adding a solid filler phase to the matrix body during the composite preparation. The improved performance of polymers and their composites in industrial and structural applications by the addition of particulate filler materials has shown a great promise and so has lately been a subject of considerable interest. A possibility that the incorporation of both particles and fibers in polymer could provide a synergism in terms of improved properties and performance has not been adequately explored so far. However, some recent reports suggest that by incorporating filler particles into the matrix of fiber reinforced composites, synergistic effects may be achieved in the form of higher modulus and reduced material costs, yet accompanied with decreased strength [3-8]. Such multi-component composites consisting of a matrix reinforced with fiber as well as particulate matters are termed as *hybrid* composites.

Polymer composites are often used in places where they are subjected to different kind of wear situations. A progressive loss of material from the surface of any component is called wear. It is a material response to the external stimulus and can be mechanical or chemical in nature. Wear is unwanted and the effect of wear on the reliability of

industrial components is recognized widely; also, the cost of wear has also been recognized to be high. Systematic efforts in wear research were started in the 1960's in industrial countries. The direct costs of wear failures, i.e., wear part replacements, increased work and time, loss of productivity, as well as indirect losses of energy and the increased environmental burden, are real problems in everyday work and business. In catastrophic failures, there is also the possibility of human losses. Although wear has been extensively studied scientifically, in the 21st century there are still wear problems present in industrial applications. This actually reveals the complexity of the wear phenomenon [9].

Solid particle erosion (SPE), a typical wear mode, is the loss of material that results from repeated impact of small, solid particles. In some cases SPE is a useful phenomenon, as in sandblasting and high-speed abrasive water jet cutting, but it is a serious problem in many engineering systems, including steam and jet turbines, pipelines and valves carrying particulate matter, and fluidized bed combustion (FBC) systems. Solid particle erosion is to be expected whenever hard particles are entrained in a gas or liquid medium impinging on a solid at any significant velocity. In both cases, particles can be accelerated or decelerated, and their directions of motion can be changed by the fluid.

Polymer composites are often used as engineering as well as structural components where erosive wear occurs. Due to the operational requirements in dusty environments, the study of solid particle erosion characteristics of the polymeric composites becomes highly relevant. Differences in the erosion behaviour of various types of composite materials are caused by the amount, type, orientation and properties of the reinforcement on the one hand and by the type and properties of the matrix and its adhesion to the fibers/fillers on the other. A full understanding of the effects of all system variables on the wear rate is necessary in order to undertake appropriate steps in the design of machine or structural component and in the choice of materials to reduce wear [10].

The subject of erosion wear of polymer composites has not received substantial attention in past two decades. Interest in this area is commensurate with the increasing utilization of composites in aerospace, transportation and process industries, in which they can be subjected to multiple solid or liquid particle impact. Examples of these applications are pipe lines carrying sand slurries in petroleum refining, helicopter rotor blades [11], pump impeller blades, high speed vehicles and aircrafts operating in desert environments, water

turbines, aircraft engines [12], missile components, canopies, radomes, wind screens [13] and outer space applications [14]. Resistance to rain and sand erosion is called among the major issues in the defence application of non-metallic materials [14]. Although a great amount of work has already been devoted to this topic many questions are still open. A comprehensive and systematic investigation of erosion in polymer composites has not been performed yet. Studies made on the erosive wear of composites refer more on fiber-reinforced polymer (FRP) and less on filler-reinforced-systems. The effect of fillers is considered more as modification of the matrix and less as reinforcement, possibly because of the low percentage of fillers. As a result, the effect of particulate fillers on erosion characteristics of hybrid composites has hardly received any research attention.

Against this background the present work has been undertaken to investigate the erosion characteristics of epoxy based hybrid composites. The focus has been on fabrication of a series of hybrid composites (Jute-fiber-reinforced epoxy composites filled with SiC derived from rice husk), evaluation of their mechanical properties, and development of a theoretical erosion model, assessment of their relative wear performance and on statistical interpretation of the various test results.

### **Thesis Outline**

The remainder of this thesis is organized as follows:

Chapter 2: Includes a literature review designed to provide a summary of the base of knowledge already available involving the issues of interest.

Chapter 3: Includes a detailed description of the raw materials, test procedures, and design of experiments methodology.

Chapter 4: Presents the physical and mechanical properties of the composites under study.

Chapter 5: Proposes a theoretical model for estimation of erosion wear rate.

Chapter 6: Includes the test results related to erosion of these composites

Chapter 7: Provides summary, specific conclusions drawn from both the experimental and analytical efforts and recommendations for future research.

\*\*\*\*

# Chapter 2

## Literature Review



### LITERATURE REVIEW

---

The purpose of this literature review is to provide background information on the issues to be considered in this thesis and to emphasize the relevance of the present study. This treatise embraces various aspects of polymer composites with a special reference to erosion wear characteristics. The topics include brief review:

- On Fiber/ Particulate Reinforced Polymer Composites
- On Multiphase Hybrid Composites
- On Mechanical Properties of Composites
- On Erosion Wear Characteristics of Composites
- On Erosion Wear Modeling
- On Implementation of DOE

At the end of the chapter a summary of the literature survey and the knowledge gap in the earlier investigations are presented.

#### **On Fiber Reinforced Polymer Composites**

Fiber reinforced polymer composites are now considered as an important class of engineering materials. They offer outstanding mechanical properties, unique flexibility in design capability and ease of fabrication. Additional advantages include light weight, corrosion and impact resistance and excellent fatigue strength. Today, fiber composites are routinely used in such diverse applications as automobiles, aircraft, space vehicles, off-shore structures, containers and piping, sporting goods, electronics and appliances. A fiber reinforced composite is not simply a mass of fibers dispersed within a polymer. It consists of fibers embedded in or bonded to a polymer matrix with distinct interfaces between the two constituent phases. The fibers are usually of high strength and modulus and serve as the principal load carrying members. The matrix acts as the load transfer medium between fibers and in less ideal cases where loads are complex, the matrix may even have to partly bear loads. The matrix also serves to protect the fibers from environmental damage before, during and after composite processing. In a composite,

both fibers and matrix largely retain their identities and yet result in many properties that cannot be achieved with either of the constituents acting alone. A wide variety of fibers are available for use in composites. The most commonly used fibers are various types of carbon, glass and aramid fibers. Besides, natural fibers such as: jute, sisal and ceramic fibers like alumina, silicon carbide, mullite and silicon nitride are also used in composite making. The unique combinations of properties available in these fibers provide the outstanding functional and structural characteristics such as: high specific strength and specific stiffness to the fiber reinforced composites.

A key feature of fiber composites that makes them so promising as engineering materials is the opportunity to tailor the materials properties through the control of fiber and matrix combinations and the selection of processing techniques. In principle, an infinite range of composite types exists, from randomly oriented chopped fiber based materials at the low property end to continuous, unidirectional fiber composites at the high performance end. A judicious selection of matrix and the reinforcing phase can lead to a composite with a combination of strength and modulus comparable to or even better than those of conventional metallic materials . The physical and mechanical characteristics can further be modified by adding a solid filler phase to the matrix body during the composite preparation. The improved performance of polymers and their composites in industrial and structural applications by the addition of particulate filler materials has shown a great promise and so has lately been a subject of considerable interest.

### **On particulate filled polymer composites**

Hard particulate fillers consisting of ceramic or metal particles and fiber fillers made of glass are being used these days to dramatically improve the wear resistance, even up to three orders of magnitude [15]. Various kinds of polymers and polymer matrix composites reinforced with metal particles have a wide range of industrial applications such as heaters, electrodes [16], composites with thermal durability at high temperature [17] etc. These engineering composites are desired due to their low density, high corrosion resistance, ease of fabrication, and low cost [18-20]. Similarly, ceramic filled polymer composites have been the subject of extensive research in last two decades. The inclusion of inorganic fillers into polymers for commercial applications is primarily aimed at the cost reduction and stiffness improvement [21, 22]. Along with fiber-reinforced composites, the composites made with particulate fillers have been found to

perform well in many real operational conditions. When silica particles are added into a polymer matrix to form a composite, they play an important role in improving electrical, mechanical, and thermal properties of the composites [23, 24]. Currently, particle size is being reduced rapidly, and many studies have focused on how single-particle size affects mechanical properties [25]. The shape, size, volume fraction, and specific surface area of such added particles have been found to affect mechanical properties of the composites greatly. Yamamoto et al. [26] reported that the structure and shape of silica particle have significant effects on the mechanical properties such as fatigue resistance, tensile and fracture properties. Nakamura et al. [27-29] discussed the effects of size and shape of silica particle on the strength and fracture toughness based on particle-matrix adhesion, and also found an increase of the flexural and tensile strength as specific surface area of particles increased.

It has also been reported that the fracture surface energies of epoxy and polyester resin and their resistance to crack propagation are relatively low. But if particulate filler is added to these brittle resins, the particles inhibit crack growth. As the volume fraction of filler is varied, the fracture energy increases up to a critical volume fraction and then decreases again. Srivastava and Shembekar [30] showed that the fracture toughness of epoxy resin could be improved by addition of fly ash particles as filler. The fillers also affect the tensile properties according to their packing characteristics, size and interfacial bonding. The maximum volumetric packing fraction of filler reflects the size distribution and shapes of the particles [31].

### **On Multiphase Hybrid Composites**

Garcia et al. [32, 33] are the first to suggest this kind of composite technique for improving the matrix-dominated properties of continuous fiber reinforced composites. In this technique, a supplementary reinforcement such as particulates, whiskers, or micro fibers is added to the matrix prior to resin impregnation. Jang et al. [34, 35] found a significant improvement in impact energy of hybrid composites incorporating either particulates or ceramic whiskers. Attempts to understand the modifications in the tribological behaviour of the polymers with the addition of fillers or fiber reinforcements have been made by a few researchers [36, 37]. The enhancement in tribological properties of Poly-phenylene-sulfide (PPS) has been reported with the addition of inorganic fillers [38] and fibers [39]. Bahadur et al. [40, 41] reported that the fillers such

as CuS, CuF<sub>2</sub>, CaS, and CaO reduced the wear rate of polyamide but many other types of filler such as CaF<sub>2</sub> increased the wear rate. But most of the above studies are confined to dry sliding and abrasive wear behaviour of composites. The erosive wear behaviour of epoxy based composites reinforced with a natural fiber along with particulate has not yet been reported in the literature.

### **On Rice husk and formation of SiC from it**

India is one of the largest rice producing countries in the world. Therefore, a large quantity of rice husk is generated as a by-product of rice milling. It has been estimated that 18×3 million tons of rice husk is produced every year (Panigrahi and Overand 1997).[42] At present the rice husk is considered as an agricultural waste. Burning has been the primary means of disposal. Not only does burning create pollution problems but the extremely fine silica ash is also toxic and thus constitutes a health hazard. Even careful incineration procedures cannot completely eliminate this airborne silica. Thus, burning with its attendant problems of air pollution and ash disposal has proven to be an unsatisfactory solution. Fortunately, rice husk contains the necessary carbon and silica, intimately dispersed, to provide a nearly ideal source material for production of SiC, an industrially important ceramic material. Rice husk was first used by Cutler [43] (1973) as a starting material for the production of silicon carbide. Since the rice husk route appears to be promising, much attention has been paid to it (Mansour and Hanna [44] 1979; Nutt [45] 1988; Patel [46] 1991; Ray *et al* [47] 1991; Singh *et al* [48] 1993, [49] 1995; Romera and Reinso [50] 1996; Moustafa *et al* [51] 1997; Krishnarao *et al* 1998; Padmaja and Mukunda [52] 1999; Janghorban and Tazesh [53] 1999; Panigrahi *et al* [54] 2001). Almost all the processes investigated so far involve two process steps i.e. (i) cooking at lower temperature (400–800°C) in a controlled manner to remove volatiles and (ii) reacting the cooked rice husk at high temperature (> 1300°C) to form SiC. In a novel approach, Singh *et al.* attempted to prepare SiC from rice husk in a single step [55].

### **On Erosion Wear Characteristics of Composites**

To ensure the durability of FRPs for industrial applications, it is necessary to discuss the degradation behaviour and mechanism under various conditions such as stress, corrosion and erosion, etc. Several parts and equipments are exposed to erosive conditions, for example pipes for hydraulic or pneumatic transportation [56–58], nozzle and impeller for sand-blasting facility [59], internal surface of vessels used for fluidized bed or with

catalysis [60], nose of high-velocity vehicle [61], blades/propellers of planes and helicopters [62], etc. Some of them are made from fibrous composites. Due to the operational requirements in dusty environments, the study of solid particle erosion characteristics of the polymeric composites is of high relevance.

Polymers are finding an ever increasing application as structural materials in various components and engineering systems. The high specific strength and stiffness of polymers are primarily responsible for their popularity. However, the resistance of polymers to solid particle erosion has been found to be very poor [63], and in fact it is two or three orders of magnitude lower than metallic materials [64]. One possible way to overcome such a shortcoming is to introduce a hard second phase in the polymer to form polymer matrix composites (PMCs). A number of investigators [65-70] have evaluated the resistance of various types of PMCs to solid particle erosion. Tilly [63] and Tilly and Sage [66] tested Nylon and epoxy reinforced with various fibers such as graphite, glass and steel and concluded that the reinforcement can either increase or decrease the erosion resistance depending on the type of fibers. Zahavi and Schmitt [64] tested a number of PMCs for erosion resistance and concluded that glass-reinforced epoxy composite had a particularly good erosion resistance. Pool *et al.* [11], conducted erosion tests on four PMCs and inferred that wee-handled, ductile fibers in a thermoplastic matrix should exhibit the lowest erosion rates. The above study was extended further by Tsiang [67]. He carried out sand erosion tests on a wide range of thermoset and thermoplastic PMCs having glass, graphite and Kevlar fibers in the forms of tape, fabric and chopped mat as reinforcements. Kevlar fibers in an epoxy resin provided the best erosion resistance. In a recent study, Mathias *et al.* [68] and also Karasek *et al* [70] have evaluated the erosion behaviour of a graphite-fiber-reinforced bismaleimide polymer composite. These investigators observed the erosion rates of the PMC to be higher than the unreinforced polymer. Many of the investigators [63-67] also consistently noted that the erosion rates of the PMCs were considerably larger than those obtained in metallic materials. In addition, composites with a thermosetting matrix invariably exhibited a maximum erosion rate at normal impact angles (i.e. a brittle erosion response) while for the thermoplastic polymer composites the erosion rate reached a maximum at an intermediate impact angle in the range  $40^{\circ}$ - $50^{\circ}$ , signifying a semi-ductile erosion response.

The wear behaviour of composite materials has received much less attention than that of conventional materials. However, as composites are utilized to an increasing extent in the aerospace, transportation and process industries, their durability may become a prime consideration. In erosion, material is removed by an impinging stream of solid particles. Studies to develop an understanding of the mechanisms of erosive wear have been motivated by reduced lifetimes and failures of mechanical components used in erosive environments, e.g. in pipelines carrying sand slurries, in petroleum refining [71, 72] and in aircraft gas turbine/compressor blades [73]. In addition to these studies, which were conducted to understand erosion behaviour in isotropic materials, there is increasing interest in understanding the erosion behaviour of anisotropic materials. Because of their very high specific stiffness and strength, composites are now used extensively in aircraft structures. The understanding of erosive wear behaviour is obviously important for such structures, e.g. helicopter rotor blades. While polymeric coatings have been developed to protect composite aircraft structures from rain erosion [74, 75], there is little understanding of the mechanisms of erosive wear in these materials. For polymers and composite materials, Tilly and Sage [66] investigated the influence of velocity, impact angle, particle size and weight of impacted abrasive for nylon, carbon-fiber-reinforced nylon, epoxy resin, polypropylene and glass-fiber-reinforced plastic. Their results showed that, for the particular materials and conditions of their tests, composite materials generally behaved in an ideally brittle fashion (*i.e.* maximum erosion rate occurred at normal impact). Fiber reinforcement may improve or worsen the resistance to erosion, depending on the type of fibers used. Zahavi and Schmitt [76] performed erosion tests on a quartz-polyimide composite and a quartz-Polybutadiene composite and again determined their behaviour to be like that of nearly ideally brittle materials. One interesting result was the behaviour of an E-glass-reinforced epoxy composite which exhibited erosion rates that were less than those of the other composites by a factor of 5. This was attributed to better adhesion between the matrix and the fibers and the lower porosity of this composite in comparison with the others studied.

The response of materials to solid particle erosion can be categorized as ductile or brittle depending on the variation in the erosion rate ( $E_r$ ) with impact angle [77-78]. The impact angle is usually defined as the angle between the trajectory of the eroding particles and the sample surface. If  $E_r$  goes through a maximum at intermediate impact angles, typically in the range  $15^0$ - $30^0$ , the response of the eroding material is considered ductile.

In contrast, if  $E_r$  continuously increases with increasing impact angle and attains a maximum at  $90^0$  (normal impact), the response of the eroding material is brittle. In addition, under ideally brittle erosion conditions the magnitude of  $E_r$  is determined only by the normal component of the impact velocity, and the size of the eroding particle strongly influences the erosion rate [79]. It is to be noted, however, that the above categorization of material behaviour as ductile or brittle is not absolute. For example, if spherical particles are used as the erodent instead of angular particles, the erosion rate exhibits a maximum at  $90^0$  even in the case of ductile materials such as copper and mild steel [80, 81]. Similarly, even a brittle material such as an inorganic glass exhibits ductile behaviour when impacted with very fine particles [82]. Erosion as well as abrasion experiments on metallic materials, ceramics and polymers have clearly indicated that the hardness of the eroding or abrading material by itself cannot adequately explain the observed behaviour [83]. As a result, combined parameters involving both hardness and fracture toughness have been utilized to correlate the erosion data of metals [84], ceramics [85] and polymers [86]. In addition, correlation between the fatigue and the erosion or wear resistance has also been observed in the case of polymers [87]. The hardness is unable to provide sufficient correlation with erosion resistance, largely because it determines only the volume displaced by each impacting erodent particle and not really the volume removed (eroded). Thus a parameter which will reflect the efficiency with which the volume that is displaced is removed should be combined with hardness to obtain a better correlation.

Erosion tests have been performed under various experimental conditions (erodent flux conditions, erosive particle characteristics) on different target composites. It has been concluded that composite materials present a rather poor erosion resistance [88]. A crucial parameter for the design with composites is the fiber content, as it controls the mechanical and thermo-mechanical responses. In order to obtain the favoured material properties for a particular application, it is important to know how the material performance changes with the fiber content under given loading conditions. The erosive wear behaviour of polymer composite systems as a function of fiber content has been studied in the past [89–90]. It was concluded that the inclusion of brittle fibers in both thermosetting and thermoplastic matrices leads to compositions with lower erosion resistance. Nevertheless, no definite rule is available to describe how the fiber content affects the ER of a composite. An analytical approach was presented by Hovis et al. [91]

which presumed that the ER of a multiphase material depends on the individual ER of its constituents. The linear (LROM) and inverse (IROM) rules of mixture were proposed and evaluated for a multiphase Al-Si alloy. The same rules of mixture were adopted by Ballout et al. [92] for a glass-fiber reinforced epoxy composite. These two rules of mixture were also proposed to model the abrasive wear of unidirectional (UD) fiber reinforced composite materials [93, 94].

Erosion of ductile materials by the impact of hard solid particles at low and moderate velocities (2-100 m/sec) can cause significant damage to structural components in many industrial applications. For example, erosion by non-combustible fly-ash particles causes premature material failures in the power generation industry [95]. During impact on the elastic-plastic target, particle energy transfers into rebound and plastic deformation of the target [96]. Rebound of the particle is caused by the elastic energy stored in the particle and target material, and the magnitude of this energy is determined by the ratio of the rebound to the initial particle velocity. This ratio, called the restitution coefficient ( $e$ ), depends on the mechanical properties of the target material and erodent, and impact parameters (i.e. velocity, impact angle, and particle size). The extent of erosion damage is related to the ability of the material to elastically recover and therefore, it is important to understand the effect of target mechanical properties, such as hardness, on the restitution coefficient. Several studies have been conducted to measure the restitution coefficient of various target-erodent systems [96, 97]. However, these measurements are complicated and often inaccurate because of the difficulties involved in measuring rebound velocity of the particle.

In general, the erosive wear behaviour of material depends on various operating parameters, such as velocity and angle of impact, particle size, shape, flux rate, etc. [98]. Literature on the effect of velocity of erodent on wear performance is sparse as compared to that on other parameters [99-101]. Earlier studies have shown that the value of the velocity exponent depends on the nature of both the target and the erodent. Tilly and Sage [71] reported a value of velocity exponent of 2.3 for 125–150  $\mu\text{m}$  quartz erodents impacting a range of materials from metals to plastics. They also reported that the velocity exponent decreased with decreasing size of the erodent. In contrast, Finnie [102] reported a high velocity exponent of 6.5 for 575  $\mu\text{m}$  steel spheres impacting glass. While studying the erosive wear behaviour of glass eroded by 300  $\mu\text{m}$  size iron spheres, Bitter [103] postulated that there was a threshold velocity value below which deformation was



elastic and hence no damage occurred. Tilly [104] proposed that the threshold velocity depended on the particle size of the erodent and obtained a value of 2.7 m/s for 225  $\mu\text{m}$  quartz against 11% chromium steel. Wiederhorn et al. [105] documented the velocity exponents for seven types of target materials having a wide range of brittleness indices and microstructures. Scattergood and Routbort [106] found that the velocity exponent increased with decreasing particle size of the erodent. While studying the erosive wear behaviour of amorphous polystyrene, Thai et al. [107] found that the velocity exponent was 3.69. Karasek et al. [108] observed almost linear correlation between the erosion rate of graphite fiber reinforced bismaleimide composite and the impinging velocity. Arnold and Hutchings found that the erosion rate of natural rubber and epoxidized natural rubber had very strong dependence on the impinging velocity above 70 m/s. Rao et al. [109] reviewed the effect of impact velocity on the erosive wear of various polymers and composites.

Erosion due to the impact of solid particles can either be constructive (material removal desirable) or destructive (material removal undesirable), and therefore, it can be desirable to either minimize or maximize erosion, depending on the application. Constructive applications include sand blasting, high-speed water-jet cutting, blast stripping of paint from aircraft and automobiles, blasting to remove the adhesive flash from bonded parts, erosive drilling of hard materials, and most recently, in the abrasive jet micromachining of Si and glass substrates for optoelectronic applications, and the fabrication of components for MEMS and micro-fluidic applications. Solid particle erosion is destructive in industrial applications such as erosion of machine parts, surface degradation of steam turbine blades, erosion of pipelines carrying slurries, and particle erosion in fluidized bed combustion systems. In most erosion processes, target material removal typically occurs as the result of a large number of impacts of irregular angular particles, usually carried in pressurized fluid streams. The fundamental mechanisms of material removal, however, are more easily understood by analysis of the impact of single particles of a known geometry. Such fundamental studies can then be used to guide development of erosion theories involving particle streams, in which a surface is impacted repeatedly.

Available reports on the research work carried out on erosion can be classified under three categories; experimental investigations, erosion model developments and numerical simulations. Tilly [104] presented a thorough analysis of the various parameters affecting

erosion, including particle properties, impact parameters, particle concentration, material temperature and tensile stress. He also reviewed the different mechanisms of erosion, which were categorized into brittle and ductile behaviours. Wiederhorn [105] presented another review of the solid particle erosion phenomena considering single and multiple particle models on erosion of metals and ceramics. The significant parameters for eroding particles and material characteristics were also presented. Humphrey [110] reported a more comprehensive review of the fundamentals of fluid motion and erosion by solid particles. The review includes a discussion of the experimental techniques and the various fundamental considerations relating to the motion of solid particles. An assessment of the fluid mechanics phenomena that can significantly influence erosion of material surfaces by impinging particles was also presented. Because of its direct relevance to gas and oil industries, erosion of pipes and pipe fittings attracted many researchers. Several experimental studies were conducted with the main objective being to determine the rate of erosion in such flow passages and its relation with the other parameters involved in the process. Among these studies are the works by Rochester and Brunton [111], True and Weiner [112], Glaeser and Dow [113], Roco et al. [114], Venkatesh [115], and Shook et al. [116]. Soderberg et al. [117] and Hutchings [118] reported the advantages and disadvantages of such experiments. The recent experimental study by McLaury et al. [119] on the rate of erosion inside elbows and straight pipes provided correlations between the penetration rate and the flow velocity at different values of the elbow diameter, sand rate and size. Edwards et al. [120] reported the effect of the bend angle on the normalized penetration rate. The objective of most of these experimental studies was to provide data for establishing a relationship between the amount of erosion and the physical characteristics of the materials involved, as well as the particle velocity and angle of impact. Blanchard et al. [121] carried out an experimental study of erosion in an elbow by solid particles entrained in water. The elbow was examined in a closed test loop. Electroplating the elbow surface and photographing after an elapsed period of time were carried out to show the wear pattern.

Information on the solid particle erosion of materials has been available for many years now [122]. Two erosion modes are often distinguished in the literature: brittle and ductile erosion. Brittle erosion deals with material removal due to crack formation, while ductile erosion deals with material removal due to cutting and ploughing. The difference manifests itself in the impact angle dependent erosion rate. When a brittle material is

impacted by a hard sharp particle, the contact area is plastically deformed due to the high compressive and shear stresses and a radial crack is formed. After the impact, the plastic deformation leads to large tensile stresses that result in lateral cracks causing the material removal. As has been observed by some researchers, the composite materials present a rather poor erosion resistance. Thus, in order to obtain the desired material characteristics for a particular application, it is important to know how the composite performance changes with the fiber content under given loading conditions. The erosive wear behaviour of FRP composite systems as a function of fiber content has been studied in the past [88]. Miyazaki and Hamao [89] have examined the effect of fiber inclusion on the erosion behaviour by comparing the erosion rate of an FRP with that of a neat resin, which is the matrix material of the FRP. It was observed that the inclusion of brittle fibers in both thermosetting and thermoplastic matrices leads to compositions with lower erosion resistance. They have also studied the erosion behaviour of treated and untreated glass fiber reinforced epoxy resin composites. The results show the clear correlation between interfacial strength and erosion rate.

### **On Erosion Wear Modeling**

Several erosion models/correlations were developed by many researchers to provide a quick answer to design engineers in the absence of a comprehensive practical approach for erosion prediction. The theoretical model developed by Rabinowicz [123] was used to calculate the volume of material removed from the target surface due to impact of solid particles entrained in a liquid jet. The results indicated that the sand particle trajectories appeared to be governed by the secondary flows and that there was no simple liquid velocity profile that can be used to calculate the particle trajectories in order to make an accurate prediction of the location of the point of maximum wear. One of the early erosion prediction correlations is that developed by Finnie [124] expressing the rate of erosion in terms of particle mass and impact velocity. In that correlation, the rate of erosion was proportional to the impact velocity squared. In a recent study, Nestic [125] found that Finnie's model over-predicts the erosion rate and presented another formula for the erosion rate in terms of a critical velocity rather than the impact velocity. The erosion model suggested by Bitter [126] assumed that the erosion occurred in two main mechanisms; the first was caused by repeated deformation during collisions that eventually results in the breaking loose of a piece of material while the second was caused by the cutting action of the free-moving particles. Comparisons between the

obtained correlations and the test results showed a good agreement. It was concluded that cutting wear prevails in places where the impact angles are small (such as in risers and straight pipes) and it is sufficient to use hard material in such places to reduce erosion. Tilly [104] suggested another two-stage mechanism for explaining different aspects of the erosion process for ductile materials. In the first stage, the particles indent the target surface, causing chips to be removed and some material to be extruded to form vulnerable hillocks around the scar. The second stage was the one in which the particles break up on impact causing fragments to be projected radially to produce a secondary damage. A correlation was presented relating erosion to the energy required to remove a unit mass and the particle velocity and size. The calculated values of erosion were compared with the experimental data for different particle sizes and a reasonable agreement was found, however, the validity of the work was limited to ductile materials and could not be generalized to include other materials. Other erosion models were suggested by Laitone [127], Salama and Venkatesh [128], Bourgoyne [129], Chase et al. [130], McLaury [131], Svedeman and Arnold [132], and Jordan [133].

In most erosion processes, target material removal typically occurs as the result of a large number of impacts of irregular angular particles, usually carried in pressurized fluid streams. The fundamental mechanisms of material removal, however, are more easily understood by analysis of the impact of single particles of a known geometry. Such fundamental studies can then be used to guide development of erosion theories involving particle streams, in which a surface is impacted repeatedly. Single particle impact studies can also reveal the rebound kinematics of particles, which are very important for models which take into account the change in erosive potential due to collisions between incident and rebounding particles [134].

In order to develop a mathematical model, it is important to understand the mechanism responsible for solid-particle erosion of composite materials. For a composite material, its surface damage by solid-particle erosion depends on many factors, including the impact velocity, particle size and shape of the erodent, mechanical properties of both the target material and the erodent, and the volume fraction, size and properties of the reinforcing phase as well as the bonding between the matrix and the reinforcing phase. The synergism of these factors makes it difficult to experimentally investigate the erosion mechanism for composite materials. Fortunately, computer simulation provides an effective and economic approach for such investigation. Computer models proposed

to simulate wear process may be classified into two groups: macro-scale models and atomic-scale models. The macro-scale models were proposed based on various assumptions or theories such as the cutting mechanism [124] and the platelet mechanism [135]. The cutting mechanism is based on the assumption that individual erodent particle impinges a target surface, cutting out a swath of the material. However, this mechanism is only suitable for ductile materials. Even for ductile materials, SEM observation of eroded surfaces has shown that erosion processes of metals involve extrusion, forging and fracture, and that micro-cutting does not often occur [136].

Another method, finite element analysis (FEM), is also used for erosion simulation [137]. The FEM can provide information on the stress/strain distribution in surface layer, which helps to predict the initiation of surface failure. However, continuous changes in surface geometry during erosion lead to the difficulty in simulation of an entire erosion process using FEM. Although many models have been proposed to simulate erosion processes, lack of generality, flexibility or feasibility make these models difficult to be used to simulate erosion under different conditions and to investigate microstructural effects on erosion. As a matter of fact, many wear models were proposed for mechanical design rather than for prediction of material performance. Therefore, they are not suitable for studying erosion processes in detail and for fundamentally investigating erosion mechanisms..

### **On Implementation of Design-of-Experiment (DOE)**

Wear processes in composites are complex phenomena involving a number of operating variables and it is essential to understand how the wear characteristics of the composites are affected by different operating conditions. Although a large number of researchers have reported on properties, performance and on wear characteristics of composites, neither the optimization of wear processes nor the influence of process parameters on wear rate has adequately been studied yet. Selecting the correct operating conditions is always a major concern as traditional experiment design would require many experimental runs to achieve satisfactory result. In any process, the desired testing parameters are either determined based on experience or by use of a handbook. It, however, does not provide optimal testing parameters for a particular situation. Thus, several mathematical models based on statistical regression techniques have been constructed to select the proper testing conditions [138–140]. The number of runs

required for full factorial design increases geometrically whereas fractional factorial design is efficient and significantly reduced the time. This method is popular because of its simplicity, but this very simplicity has led to unreliable results and inadequate conclusions. The fractional design might not contain the best design point. Moreover, the traditional multi-factorial experimental design is the “change-one-factor-at-a-time” method. Under this method only one factor is varied, while all the other factors are kept fixed at a specific set of conditions. To overcome these problems, Taguchi and Konishi [141] advocated the use of orthogonal arrays and Taguchi [142] devised a new experiment design that applied signal-to-noise ratio with orthogonal arrays to the robust design of products and processes. In this procedure, the effect of a factor is measured by average results and therefore, the experimental results can be reproducible. Phadke [143], Wu and Moore [144] and others [145, 146] have subsequently applied the Taguchi method to design the products and process parameters. This inexpensive and easy-to-operate experimental strategy based on Taguchi’s parameter design has been adopted to study effect of various parameters and their interactions in a number of engineering processes. It has been successfully applied for parametric appraisal in erosion wear process for glass polyester composites [147-156].

The exhaustive literature survey presented above reveals that:

- Though much work has been reported on various wear characteristics of metals, alloys and homogeneous materials, comparatively less has been reported on the erosive wear performance of polymers and composites and in fact no study has been found particularly on epoxy based natural fiber / particulate reinforced composites.
- A possibility that the incorporation of both particles and fibers in polymer could provide a synergism in terms of improved wear resistance has not been adequately addressed so far and there is inadequate data available about phenomena behind the modified wear behaviour due to the addition of particulate fillers to the fiber reinforced polymer composites.
- As far as erosion study of polymer matrix composites is concerned, no specific theoretical model based on the assumption that the kinetic energy of the erodent is utilized to cause micro-indentation leading to material loss has been developed.

- Studies carried out worldwide on erosion behaviour of composites have largely been experimental and use of statistical techniques in analyzing wear characteristics is rare.
- Taguchi method, in spite of being a simple, efficient and systematic approach to optimize designs for performance, quality and cost, is used only in a limited number of applications worldwide. Its implementation in parametric appraisal of wear process has hardly been reported.

It is thus clear that the effect of fiber reinforcement and ceramic particulate filling on erosion characteristics of epoxy composites has still remained a less studied area. It is felt that, a further study in this respect is needed particularly with the inclusion of ceramic fillers both in view of the scientific understanding and commercial importance.

In view of the above, the present work is undertaken to investigate the solid particle erosion wear characteristics of epoxy based hybrid composites under multiple impact conditions. The objectives of this work are outlined as follows:

1. Fabrication of a series of jute fiber reinforced epoxy matrix composites filled with and without SiC derived from rice husk.
2. Mechanical characterization of these composites
3. Development of a theoretical model for estimation of erosion wear rate under multiple impact condition.
4. Parametric appraisal of erosion wears process of unfilled jute-epoxy composites using Taguchi experimental design.
5. Parametric appraisal of erosion wears process of particulate filled hybrid jute-epoxy composites using Taguchi experimental design.
6. Development of predictive equations for wear rate based on Taguchi approach

### **Chapter Summary:**

This chapter has provided an exhaustive review of research works on fiber and particulate reinforced polymer composites reported by various investigators. It has also clearly outlined the objectives of the present work. The next chapter discusses experimental planning, characterization details and the Taguchi experimental design technique.

\*\*\*\*\*

# Chapter 3

## **Materials and Methods**



## MATERIALS AND METHODS

---

This chapter describes the materials and methods used for the processing of the composites under this investigation. It presents the details of the characterization and erosion tests which the composite samples are subjected to. The methodology related to the design of experiment technique based on Taguchi method is also presented in this part of the thesis.

### MATERIALS

#### Matrix Material

Epoxy LY 556 is the resin which is used as the matrix material. Its common name is Bisphenol-A-Diglycidyl-Ether and it chemically belongs to the 'epoxide' family. The epoxy resin and the hardener are supplied by Ciba Geigy India Ltd.

#### Fiber Material

Jute is a long, soft, shiny vegetable fiber that can be spun into coarse, strong threads. It is produced from plants in the genus *Corchorus*, family Tiliaceae. Jute is one of the cheapest natural fibers and is second only to cotton in amount produced and variety of uses. Jute fibers are composed primarily of the plant materials cellulose (major component of plant fiber) and lignin (major components wood fiber). It is thus a ligno-cellulosic fiber that is partially a textile fiber and partially wood. It falls into the bast fiber category (fiber collected from bast or skin of the plant) along with kenaf, industrial hemp, flax (linen), ramie, etc. The industrial term for jute fiber is *raw jute*. The fibers are off-white to brown, and 1–4 meters (3–12 feet) long. Woven mats of this fiber have been used as the reinforcing phase in the composites used in this work.

#### Particulate Filler Material

Silicon carbide (SiC) is a ceramic material that has the potential to be used as filler in various polymer matrices. It is an excellent abrasive and has been produced and made into grinding wheels and other abrasive products for over one hundred years. It is the only chemical compound of carbon and silicon. It was originally produced by a high temperature electro-chemical reaction of sand and carbon. Today the material has been

developed into a high quality technical grade ceramic with very good mechanical properties. It is used in abrasives, refractories, ceramics, and numerous high-performance applications. The material can also be made an electrical conductor and has applications in resistance heating, flame igniters and electronic components. Structural and wear applications are constantly developing. Silicon carbide is composed of tetrahedra of carbon and silicon atoms with strong bonds in the crystal lattice. This produces a very hard and strong material. It is not attacked by any acids or alkalis or molten salts up to 800°C. The high thermal conductivity coupled with low thermal expansion and high strength gives this material exceptional thermal shock resistant qualities. Silicon carbide has low density of about 3.1 gm/cc, low thermal expansion, high elastic modulus, high strength, high thermal conductivity, high hardness, excellent thermal shock resistance and superior chemical inertness.

SiC produced from rice husk by plasma processing route has been used as filler in the composites used in the present investigation.

### **Synthesis of SiC from rice husk in a plasma reactor**

A single step is adopted to prepare SiC directly from raw rice husk in an indigenously developed pot type extended arc plasma reactor using graphite electrodes. A graphite crucible containing the charge acts as the bottom electrode. The extended arc is formed by the movement of the top graphite electrode with an axial hole through which the argon plasma forming gas is introduced. Experiments are carried out in batch operations and experimental conditions such as power and time are varied. A typical experimental condition is as follows: Argon gas flow, 2 lpm; current, 300 A; load voltage, 50 V. After the end of the experiment argon gas is allowed to pass for 1 h and then the crucible is allowed to cool to room temperature. The plasma treated sample is found to be green in colour and fragile in nature, thus could easily ground in a mortar and pestle. Rice husk contains silica in hydrated amorphous form and cellulose which yields carbon when thermally decomposed. When such a product is further heated at high temperature (> 1400°C) a reaction occurs between silica and carbon resulting in the formation of SiC. Thermal plasma can reduce the reaction time significantly as the formation of SiC is observed in a short time of 5 min. The details of SiC preparation from rice husk by this route is described elsewhere [157].

## Composite fabrication

Cross plied jute fibers are reinforced in epoxy resin in three different weight proportions (20 wt%, 30 wt% and 40 wt%) to prepare the composites A<sub>1</sub>, B<sub>1</sub> and C<sub>1</sub> respectively. Jute fibers and epoxy resin have modulus of about 55 GPa and 3.42 GPa respectively and possess density of 1300 kg/m<sup>3</sup> and 1100 kg/m<sup>3</sup> respectively. No particulate filler is used in these composites.

The other composite samples C<sub>2</sub> and C<sub>3</sub> with silicon carbide fillers of fixed weight percentage are fabricated by the same technique. The low temperature curing epoxy resin and corresponding hardener (HY951) are mixed in a ratio of 10:1 by weight as recommended. The mix is stirred manually to disperse the particulate fillers in the matrix. The mixing is done thoroughly before the jute-fiber mats (40 wt%) are reinforced in the matrix body. Composites C<sub>2</sub> and C<sub>3</sub> contain SiC particles in 10 wt% and 20 wt% proportions respectively. Each ply of jute-fiber is of dimension 200 mm × 200 mm. The composite slabs are made by conventional hand-lay-up technique followed by light compression moulding technique. A stainless steel mould having dimensions of 210 × 210 × 40 mm<sup>3</sup> is used. A releasing agent (Silicon spray) is used to facilitate easy removal of the composite from the mould after curing. Care is taken to ensure a uniform sample since particles have a tendency to clump and tangle together when mixed. The cast of each composite is cured under a load of about 25kg for 24 h before it removed from the mould. Then this cast is post cured in the air for another 24 h after removing out of the mould. Specimens of suitable dimension are cut using a diamond cutter for physical characterization and mechanical testing. Utmost care has been taken to maintain uniformity and homogeneity of the composite. The designation and detailed composition of the composites are given in Table 3.1.

Designation	Composition
A <sub>1</sub>	Epoxy + 20 wt% jute fiber
B <sub>1</sub>	Epoxy + 30 wt% jute fiber
C <sub>1</sub>	Epoxy + 40 wt% jute fiber
C <sub>2</sub>	Epoxy + 40 wt% jute fiber + 10wt% SiC
C <sub>3</sub>	Epoxy + 40 wt% jute fiber + 20wt% SiC

Table 3.1 Designation and detailed composition of the composites

## MECHANICAL CHARACTERIZATION

### Micro-hardness

Micro-hardness measurement is done using a Leitz micro-hardness tester. A diamond indenter, in the form of a right pyramid with a square base and an angle  $136^{\circ}$  between opposite faces, is forced into the material under a load  $F$ . The two diagonals  $X$  and  $Y$  of the indentation left on the surface of the material after removal of the load are measured and their arithmetic mean  $L$  is calculated. In the present study, the load considered  $F = 24.54\text{N}$  and Vickers hardness number is calculated using the following equation.

$$H_v = 0.1889 \frac{F}{L^2} \quad (3.1)$$

$$\text{and } L = \frac{X + Y}{2}$$

Where  $F$  is the applied load (N),  $L$  is the diagonal of square impression (mm),  $X$  is the horizontal length (mm) and  $Y$  is the vertical length (mm).

### Density and Void Fraction

The theoretical density of composite materials in terms of weight fraction can easily be obtained as for the following equations given by Agarwal and Broutman [1].

$$\rho_{ct} = \frac{1}{(W_f / \rho_f) + (W_m / \rho_m)} \quad (3.2)$$

Where,  $W$  and  $\rho$  represent the weight fraction and density respectively. The suffix  $f$ ,  $m$  and  $ct$  stand for the fiber, matrix and the composite materials respectively.

The composites under this investigation consists of three components namely matrix, fiber and particulate filler. Hence the modified form of the expression for the density of the composite can be written as

$$\rho_{ct} = \frac{1}{(W_f / \rho_f) + (W_m / \rho_m) + (W_p / \rho_p)} \quad (3.3)$$

Where, the suffix ' $p$ ' indicates the particulate filler materials.

The actual density ( $\rho_{ce}$ ) of the composite, however, can be determined experimentally by simple water immersion technique. The volume fraction of voids ( $V_v$ ) in the composites is calculated using the following equation:

$$V_v = \frac{\rho_{ct} - \rho_{ce}}{\rho_{ct}} \quad (3.4)$$

### Tensile strength

The tensile test is generally performed on flat specimens. The commonly used specimens for tensile test are the dog-bone type and the straight side type with end tabs. During the test a uniaxial load is applied through both the ends of the specimen. The ASTM standard test method for tensile properties of fiber resin composites has the designation D 3039-76. The length of the test section should be 200 mm. The tensile test is performed in the universal testing machine (UTM) Instron 1195 and results are analyzed to calculate the tensile strength of composite samples is shown in Figure 3.1.

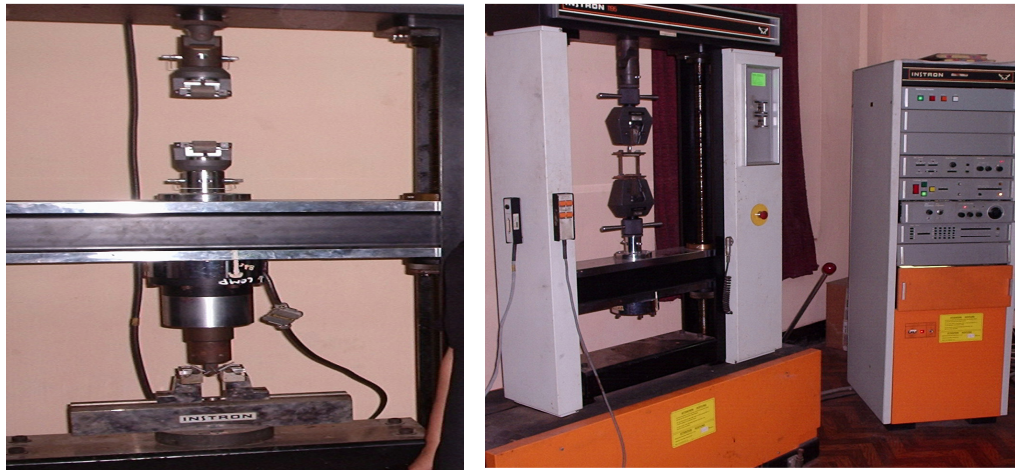


**Figure 3.1** Photograph of the machine (Instron 1195) for tensile and 3-point bend Test

### Flexural and Inter-laminar shear strength

The short beam shear (SBS) tests are performed on the composite samples at room temperature to evaluate the value of inter-laminar shear strength (ILSS). It is a 3-point bend test, which generally promotes failure by inter-laminar shear. The SBS test is conducted as per ASTM standard (D2344-84) using the same UTM. The loading arrangement is shown in Figure 3.2. Span length of 40 mm and the cross head speed of 10 mm/min are maintained. The ILSS values are calculated as follows,

$$ILSS = \frac{3P}{4bt} \quad (3.5)$$

Where,  $P$  is maximum load,  
 $b$  the width of specimen, and  
 $t$  the thickness of specimen

The data recorded during the 3-point bend test is used to evaluate the flexural strength also. The flexural strength (F.S.) of any composite specimen is determined using the following equation.

$$F.S = \frac{3PL}{2bt^2} \quad (3.6)$$

Where,  $L$  is the span length of the sample.

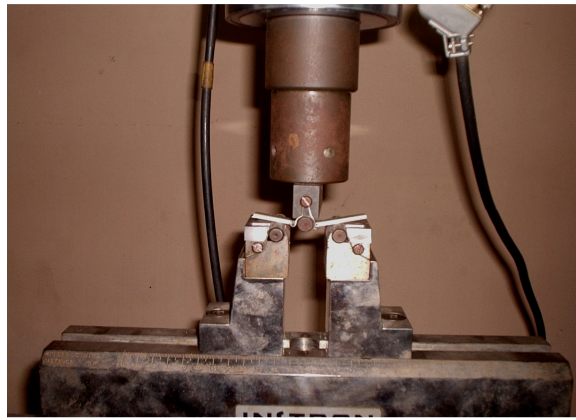


**Figure 3.2** Loading arrangement for the specimens

### **Scanning electron microscopy**

The surfaces of the specimens are examined directly by scanning electron microscope JEOL JSM-6480LV. The composite samples are mounted on stubs with silver paste. To enhance the conductivity of the samples, a thin film of platinum is vacuum-evaporated onto them before the photomicrographs are taken.

### **Erosion Test Apparatus**

The set up used in this study for the solid particle erosion wear test is capable of creating reproducible erosive situations for assessing erosion wear resistance of the prepared composite samples. It consists of an air compressor, an air particle mixing chamber and

accelerating chamber. The schematic diagram of the erosion test rig is given in Figure 3.4 and pictorial view is presented in Figure 3.5.



**Figure 3.3** Scanning Electron Microscope JEOL JSM-6480LV

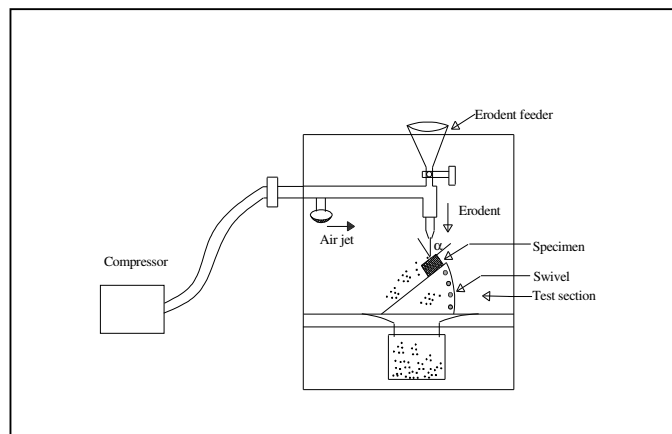


**Figure 3.4** A schematic diagram of the erosion test rig



**Figure 3.5** Solid Particle Erosion Test Set Up

Dry compressed air is mixed with the erodent particles which are fed at constant rate from a sand flow control knob through the nozzle tube and then accelerated by passing the mixture through a convergent brass nozzle of 3mm internal diameter. These particles impact the specimen which can be held at different angles with respect to the direction of erodent flow using a swivel and an adjustable sample clip. The velocity of the eroding particles is determined using standard double disc method [158]. The conditions (confirming to ASTM G 76 test standards) under which erosion tests are carried out are listed in Table 3.2. In the present study, dry silica sand of different particle sizes (200 $\mu$ m, 300  $\mu$ m and 400 $\mu$ m) are used as erodent. The samples are cleaned in acetone, dried and weighed to an accuracy of  $\pm 0.1$  mg before and after the erosion trials using a precision electronic balance. The weight loss is recorded for subsequent calculation of erosion rate. The process is repeated till the erosion rate attains a constant value called *steady state erosion rate*. The ratio of this weight loss to the weight of the eroding particles causing the loss is then computed as a dimensionless incremental erosion rate. The erosion rate is defined as the weight loss of the specimen due to erosion divided by the weight of the erodent causing the loss.

Control Factors	Symbols	Fixed parameters	
Velocity of impact	Factor A	Erodent	Silica sand
Impingement angle	Factor B	Erodent feed rate (g/min)	10.0 $\pm$ 1.0
Erodent size	Factor C	Test temperature	RT
Fiber/Filler loading	Factor D	Nozzle diameter (mm)	3
		Length of nozzle (mm)	80
		Stand-off distance (mm)	100

**Table 3.2** Parameters considered during erosion test

### **Parametric Appraisal and Taguchi Method**

Statistical methods are commonly used to improve the quality of a product or process. Such methods enable the user to define and study the effect of every single condition possible in an experiment where numerous factors are involved. Solid particle erosion is such a process in which a number of control factors collectively determine the performance output i.e. the erosion rate. Hence, in the present work a technique called Taguchi method is used to optimize the process parameters leading to minimum erosion



of the polymer composites under study. This part of the chapter presents the Taguchi experimental design methodology in detail.

### **Taguchi Experimental Design**

Every single discipline has researchers carrying out experiments to observe and understand a certain process or to discover the interaction and effect of different variables. From a scientific viewpoint, these experiments are either one or a series of tests to either confirm a hypothesis or to understand a process in further detail. Experiments from a manufacturing point of view, however, are concerned with finding the optimum product and process, which is both cost effective and of a high quality. In order to achieve a meaningful end result, several experiments are usually carried out. The investigator needs to know the factors involved, the range these factors are varied between, the levels assigned to each factor as well as a method to calculate and quantify the response of each factor. This *one-factor-at-a-time* approach will provide the most favorable level for each factor but not the optimum combination of all the interacting factors involved. Thus, experimentation in this scenario can be considered as an iterative process. Although it will provide a result, such methods are not time or cost effective. But the design of experiments is a scientific approach to effectively plan and perform experiments, using statistics. In such designs, the combination of each factor at every level is studied to determine the combination that would yield the best result. The advantage of such design schemes is that it will always determine the effect of factors and possible interactions (between factors) on the performance output.

Taguchi design of experiment is a powerful analysis tool for modeling and analyzing the influence of control factors on performance output. The most important stage in the design of experiment lies in the selection of the control factors. Therefore, initially a large number of factors are included so that non-significant variables can be identified at earliest opportunity. Exhaustive literature review on erosion behaviour of polymer composites reveal that parameters viz., impact velocity, impingement angle, fiber loading, filler content, erodent size etc largely influence the erosion rate of polymer composites [147-156]. In the present work, the impact of four such parameters are studied using  $L_9$  ( $3^4$ ) orthogonal design. The operating parameters and the selected levels are given in Table 3.3. The tests are conducted at room temperature as per experimental designs given in Table 3.4 (for  $A_1, B_1, C_1$ ) and Table 3.5 (for  $C_1, C_2, C_3$ ) which gives the operating conditions under which each erosion test has been carried out.

Control factor	Level			Units
	I	II	III	
A: Velocity of impact	32	44	58	m/sec
B: Impingement angle	30	60	90	degree
C: Erodent size	200	300	400	μm
D: Fiber loading (for composites A <sub>1</sub> ,B <sub>1</sub> ,C <sub>1</sub> )	20	30	40	wt%
Filler content (for composites C <sub>1</sub> ,C <sub>2</sub> ,C <sub>3</sub> )	0	10	20	wt%

**Table 3.3** Levels for various control factors

Four parameters viz., impact velocity, impingement angle, erodent size, and fiber/filler loading, each at three levels, are considered in this study. In Tables 3.5 and 3.6, each column represents a test parameter and a row gives a test condition which is nothing but combination of parameter levels. Four parameters each at three levels would require  $3^4 = 81$  runs in a full factorial experiment. Whereas, Taguchi's factorial experiment approach reduces it to 9 runs only offering a great advantage in terms of cost and time.

Test Run	Erodent Velocity	Impingement	Erodent	Fiber Content
	(m/s)	Angle (Degrees)	Size (μm)	(wt %)
	A	B	C	D
1	32	30	200	20
2	32	60	300	30
3	32	90	400	40
4	44	30	300	40
5	44	60	400	20
6	44	90	200	30
7	58	30	400	30
8	58	60	200	40
9	58	90	300	20

**Table 3.4** Orthogonal array for L<sub>9</sub> Taguchi Design for composites A<sub>1</sub>,B<sub>1</sub>,C<sub>1</sub>

Test Run	Erodent Velocity (m/s) A	Impingement Angle (Degrees) B	Erodent size (µm) C	Filler Content (wt %) D
1	32	30	200	0
2	32	60	300	10
3	32	90	400	20
4	44	30	300	20
5	44	60	400	0
6	44	90	200	10
7	58	30	400	10
8	58	60	200	20
9	58	90	300	0

**Table 3.5** Orthogonal array for L<sub>9</sub> Taguchi Design composites C<sub>1</sub>, C<sub>2</sub>, C<sub>3</sub>

The plan of the experiments is as follows: the first column is assigned to impact velocity (A), the second column to impingement angle (B), third column to erodent size (C), and the last column to fiber/filler loading (D).

The experimental observations are transformed into a signal-to-noise (S/N) ratio. There are several S/N ratios available depending on the type of characteristics. The S/N ratio for minimum erosion rate coming under *smaller-is-better* characteristic, which can be calculated as logarithmic transformation of the loss function as shown below.

$$\text{Smaller is the better characteristic: } \frac{S}{N} = -10 \log \frac{1}{n} \left( \sum y^2 \right) \quad (3.7)$$

where n the number of observations, and y the observed data. “Lower is better” (LB) characteristic, with the above S/N ratio transformation, is suitable for minimizations of erosion rate.

## **Chapter Summary**

This chapter has provided:

- The descriptions of materials used in the experiments
- The details of fabrication and characterization of the composites
- The description of erosion wear test
- An explanation of the Taguchi experimental design.

The next chapter presents the physical and mechanical properties of the polymer composites under study.

\*\*\*\*

# Chapter 4

## **Mechanical Characterization of the Composites**

## MECHANICAL CHARACTERIZATION OF THE COMPOSITES

---

This chapter presents the physical and mechanical properties of the jute fiber reinforced epoxy composites of different compositions prepared for this work. The interpretation of the results and the comparison among various composite samples are also presented in this part of the thesis, which deals with: the jute-epoxy composites without particulate filling (A<sub>1</sub>, B<sub>1</sub> and C<sub>1</sub>) and the silicon carbide filled ones (C<sub>1</sub>-C<sub>3</sub>).

### MECHANICAL CHARACTERIZATION

#### Density and volume fraction of voids

The theoretical and measured densities of the composites along with the corresponding volume fraction of voids are presented in Table 4.1. It may be noted that the composite density values calculated theoretically from weight fractions using Eq.(3) are not equal to the experimentally measured values. This difference is a measure of voids and pores present in the composites. It is clearly seen that with the increase in fiber content from 20 wt% to 40 wt%, there is a increase in the void fraction. However, in all the three composites A<sub>1</sub>, B<sub>1</sub> and C<sub>1</sub>, the volume fractions of voids are reasonably small (< 1.5%) and this can be attributed to the absence of particulate fillers in these composites. With the addition of silicon carbide as the filler material, more voids are found in the composites. As the filler content increases from 0 wt% to 10 wt% and subsequently from 10 wt% to 20 wt% the volume fraction of voids is found to be increasing. This trend is observed in both the particulate filled composites (C<sub>2</sub> and C<sub>3</sub>).

Composites	Measured density (gm/cc)	Theoretical density (gm/cc)	Volume fraction of voids (%)
A <sub>1</sub>	1.127	1.135	0.71
B <sub>1</sub>	1.139	1.153	1.35
C <sub>1</sub>	1.157	1.172	1.28
C <sub>2</sub>	1.199	1.258	4.68
C <sub>3</sub>	1.287	1.358	5.22

**Table 4.1** Measured and Theoretical densities of the composites

Density of a composite depends on the relative proportion of matrix and reinforcing materials and this is one of the most important factors determining the properties of the composites. The void content is the cause for the difference between the values of true density and the theoretically calculated one. The voids significantly affect some of the mechanical properties and even the performance of composites in the workplace. Higher void contents usually mean lower fatigue resistance, greater susceptibility to water penetration and weathering [1]. The knowledge of void content is desirable for estimation of the quality of the composites. It is understandable that a good composite should have fewer voids. However, presence of void is unavoidable in composite making particularly through hand-lay-up route.

### Micro-hardness

The variation of composite micro-hardness with the weight fraction of jute fiber and SiC particulates is shown in Figure 4.1. For the composite A<sub>1</sub> (20 wt% of JF), the micro-hardness value is recorded as 57 Hv while for C<sub>1</sub> (40 wt% of JF) this value is 63 Hv. It is thus seen that with the increase in fiber content in the composite, the hardness improves although the increment is marginal. Similarly, with the incorporation of filler particulates into the composites, the mean hardness is seen to have improved.

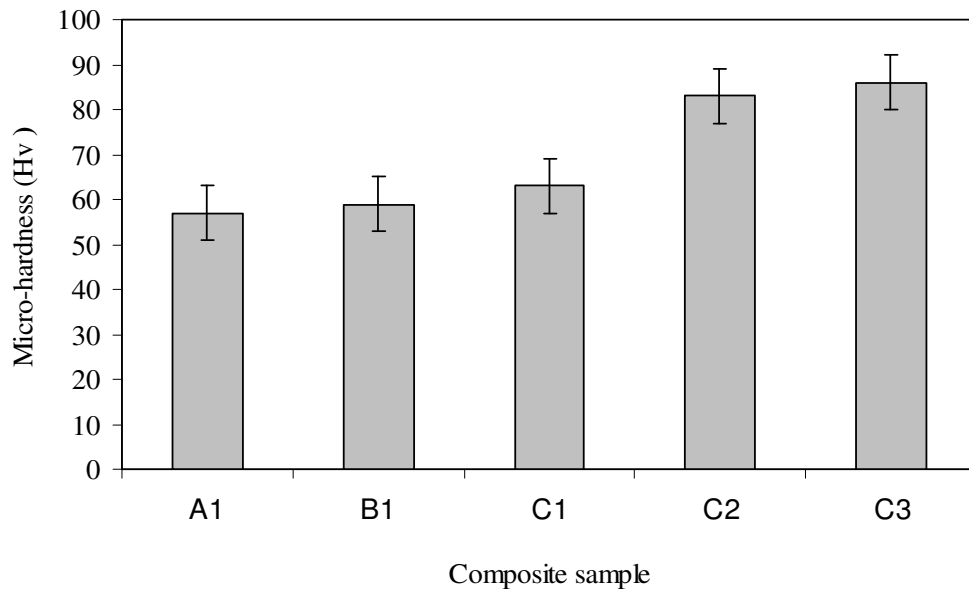


**Figure 4.1** Micro-hardness values of composites with different fiber and filler content

Composites	Mean Hardness (Hv)	Tensile strength (MPa)	Flexural strength (MPa)	ILSS (MPa)
A <sub>1</sub>	57	302.8	312.6	20.52
B <sub>1</sub>	59	331.5	345.8	19.32
C <sub>1</sub>	63	349.6	368.6	18.42
C <sub>2</sub>	83	304.5	357.8	22.57
C <sub>3</sub>	86	279.4	353.2	28.99

**Table 4.2** Mechanical properties of the composites

### **Tensile and flexural strength**

It is well known that the strength properties of composites are mainly determined by the fiber content and the fiber strength. So variation in composite strength with different fiber loading is obvious. These variations in tensile and flexural strengths of the composites A<sub>1</sub>, B<sub>1</sub> and C<sub>1</sub> are presented in Table 4.2 and are shown in Figure 4.2. A gradual increase in both tensile strength as well as flexural strength with the fiber weight fraction is noticed. It clearly indicates that inclusion of jute fiber improves the load bearing capacity and the ability to withstand bending of the composites. Similar observations have been reported by Harsha et al. [159] for fiber reinforced thermoplastics such as poly-aryl-ether-ketone composites. It may be mentioned here that both tensile and flexural strengths are important for recommending any composite as a candidate for structural applications.

The test results for tensile and flexural strengths for the particulate filled composites C<sub>1</sub>, C<sub>2</sub> and C<sub>3</sub> are shown in Figure 4.3. It is seen that the tensile strength of the composite decreases with increase in the filler content. The unfilled jute epoxy composite has a strength of 349.6 MPa in tension and it may be seen from Table 4.2 that this value drops to 304.5 MPa and 279.4 MPa with addition of 10 wt% and 20 wt% of silicon carbide respectively. Similar trend is observed in case of flexural strength of these composites.

There can be two reasons for this decline in the strength properties of these particulate filled composites compared to the unfilled one. One possibility is that the chemical reaction at the interface between the filler particles and the matrix may be too weak to transfer the tensile stress; the other is that the corner points of the irregular shaped



particulates result in stress concentration in the epoxy matrix. These two factors are responsible for reducing the tensile strengths of the composites so significantly. Similar property modification has been previously reported for SiC particles in polyester composites and Al<sub>2</sub>O<sub>3</sub> particles reinforced in polyurethane matrix [145, 159].

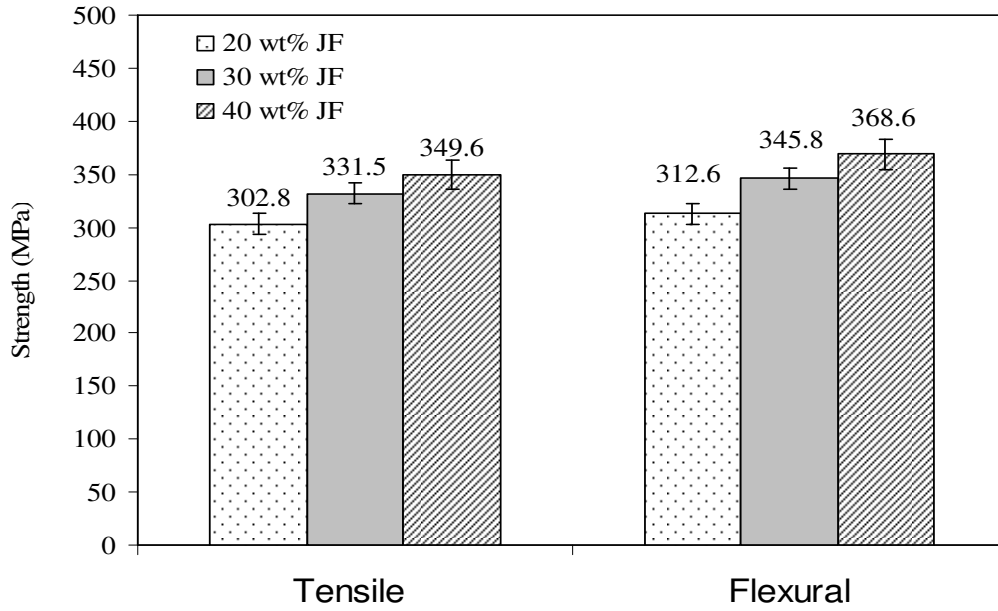


**Figure 4.2** Effect of fiber loading on tensile & flexural strength of JF-epoxy composites

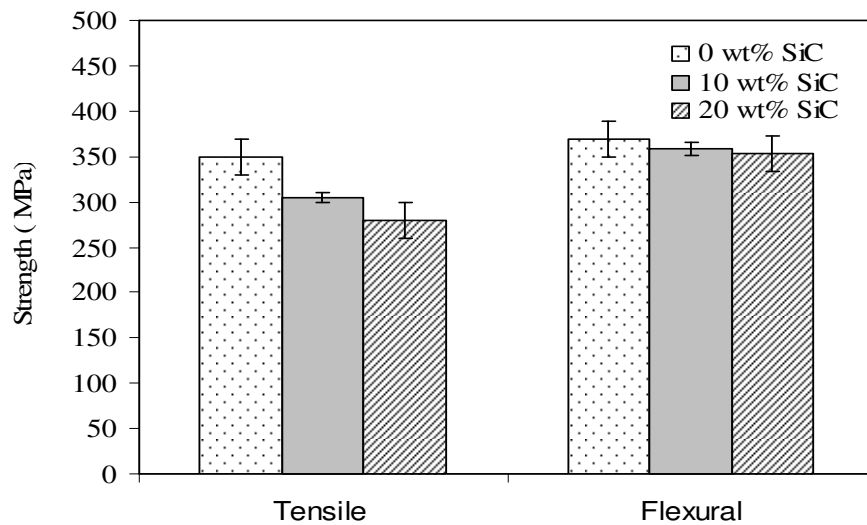


**Figure 4.3** Effect of filler content on tensile & flexural strength of JF-epoxy composites

### Inter laminar shear strength (ILSS)

The stresses acting on the interface of the two adjacent laminae in a layered composite are called inter-laminar stresses. These stresses cause relative deformations between the consecutive laminae and if these are sufficiently high they may cause failure along the mid-plane between two adjacent laminae. It is therefore of considerable interest to evaluate inter-laminar shear strength through tests in which failure of the laminates of the composite initiates in a shear (delamination) mode. In the present work the ILSS values are measured for unfilled jute-epoxy composites A<sub>1</sub>, B<sub>1</sub> and C<sub>1</sub> and no improvement is recorded in the ILSS of the composites with increase in the fiber content in them. The values are illustrated graphically in Figure 4.4.

The inter-laminar shear strength values of the particulate filled composites are shown along with that of the unfilled jute epoxy composite (C<sub>1</sub>) in the same Figure 4.4. It is seen that there is improvement of ILSS of jute-epoxy composites with particulate filling. Incorporation of silicon carbide is seen to have caused the substantial increase in the inter-laminar shear strength.

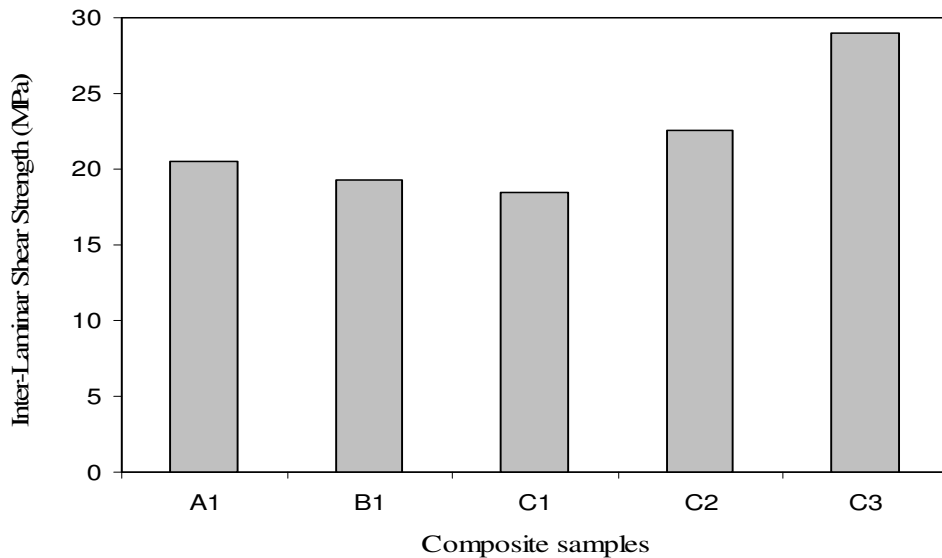


**Figure 4.4** Comparison of Inter-laminar shear strength of different composites

In the present investigation, during flexural test, the span length is very short (40 mm). A large span to depth ratio in bending test increases the maximum normal stress without affecting the inter-laminar shear stress and thereby increases the tendency for

longitudinal failure. If the span is short enough, failure initiates and propagates by inter-laminar shear failure. The maximum shear stress in a beam occurs at the mid plane. So in the shear test, failure consists of a crack running along the mid plane of the beam so that crack plane is parallel to the longitudinal plane.

### Surface morphology of un-eroded composite samples

The surface micro-structures of some of the composite samples are observed under scanning electron microscope to get an insight to the features.

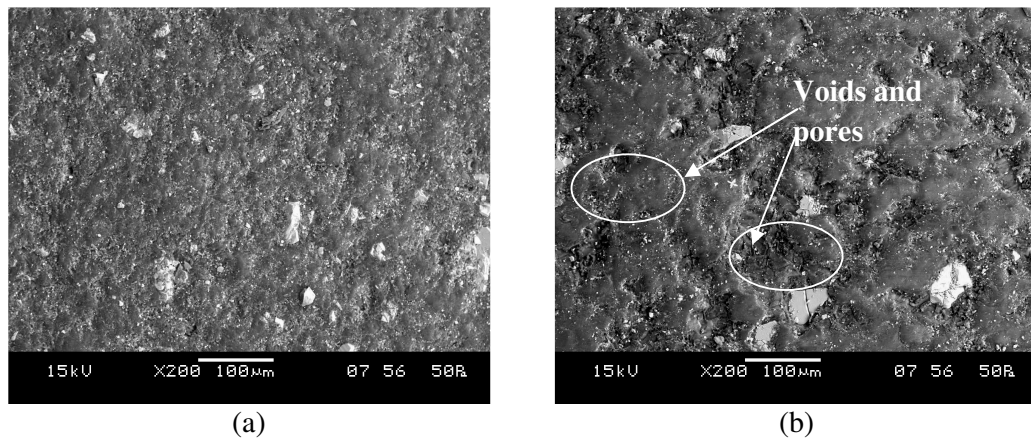


**Figure 4.5** Surface morphology of un-eroded composite samples

As seen in Figures 4.5 (a) and 4.5 (b), the surfaces are reasonably homogeneous. No cracks are seen although some voids and pores are visible even at this lower magnification. SiC particles are not seen in clusters within the matrix body.

### Chapter Summary

This chapter summarizes that:

- Successful fabrication of jute-epoxy composites with reinforcement of SiC derived from rice husk is possible.
- Incorporation of SiC as a filler modifies the micro-hardness, density, tensile, flexural and inter-laminar shear strengths of the jute epoxy composites.

The next chapter presents the development of a theoretical model for estimation of wear rate of polymer composites during solid particle erosion.

\*\*\*\*\*

# Chapter 5

## **Development of a Theoretical Model for Erosion Wear Rate Estimation**

## DEVELOPMENT OF A THEORETICAL MODEL FOR EROSION WEAR RATE ESTIMATION

---

This chapter presents the development of a mathematical model for estimating the rate of erosion wear caused by solid particle impact.

### THEORETICAL MODEL

#### Nomenclature

The following symbols are used in this paper:

$a$	erodent height and base length (m)
$\delta$	indentation depth (m)
$e_v$	volumetric wear loss per particle impact ( $m^3$ )
$E_v$	total volumetric erosion wear rate ( $m^3/sec$ )
$\alpha$	angle of impingement (degree)
$U$	impact velocity (m/sec)
$P$	force on the indenter (N)
$H$	hardness ( $N/m^2$ )
$m$	mass of single erodent particle (kg)
$M$	mass flow rate of the erodent (kg/sec)
$N$	number of impact per unit time ( $sec^{-1}$ )
$\rho_c$	density of composite ( $kg/m^3$ )
$\rho$	density of erodent ( $kg/m^3$ )
$\eta_{nor}$	erosion efficiency with normal impact
$\eta$	erosion efficiency
$E_{rth}$	erosion wear rate (kg/kg)

Solid particle erosion is a wear process in which the material is removed from a surface by the action of a high velocity stream of erodent particles entrained in a high velocity fluid stream. The particles strike against the surface and promote material loss. During flight, a particle carries momentum and kinetic energy which can be dissipated during the impact due to its interaction with a target surface. As far as erosion study of polymer matrix composites is concerned, no specific model has been developed and thus the study of their erosion behaviour has been mostly experimental. However, Mishra [160] proposed a mathematical model for material removal rate in abrasive jet machining process in which the material is removed from the work piece in a similar fashion. This model assumes that the volume of material removed is same as the volume of indentation caused by the impact. This has a serious limitation as in a real erosion process the volume of material removed is actually different from the indentation volume. Further, this model considers only the normal impact i.e.  $\alpha = 90^\circ$  whereas in actual practice, particles may impinge on the surface at any angle ( $0^\circ \leq \alpha \leq 90^\circ$ ). The proposed model addresses these shortcomings in an effective manner. It considers the real situation in which the volume of material removed by erosion is not same as the volume of material displaced and therefore, an additional term “erosion efficiency ( $\eta$ )” is incorporated in the erosion rate formulation. In the case of a stream of particles impacting a surface normally (i.e. at  $\alpha=90^\circ$ ), erosion efficiency ( $\eta_{normal}$ ) defined by Sundararajan et. al [161] is given as

$$\eta_{normal} = \frac{2ErHv}{\rho U^2} \quad (5.1)$$

But considering impact of erodent at any angle  $\alpha$  to the surface, the actual erosion efficiency can be obtained by modifying Eq. (5.1) as

$$\eta = \frac{2ErHv}{\rho U^2 \sin^2 \alpha} \quad (5.2)$$

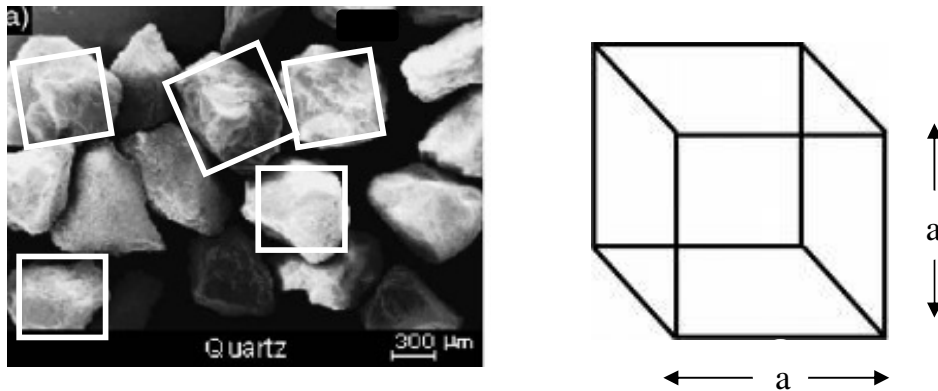


**Figure 5.1** SEM Micrograph of the erodent used

Besides, while all previous models have been developed assuming the shape of erodent to be spherical, in the real situation, the erodent particles are actually bodies having sharp edges, as shown in the Figure (5.1). Therefore, considering them to be cubical shaped bodies is a more realistic assumption as compared to assuming them simply spherical. The model proposed in the present work addresses to all these shortcomings. It assumes the erodent particles to be rigid, cubical shaped bodies having side equal to the average grit size. It is further based on the assumption that the loss in kinetic energy of the impinging particles is utilized to cause micro-indentation in the composite material and the material loss is a measure of the indentation. The erosion is the result of cumulative damage of such non-interacting, single particle impacts. The model is developed with the simplified approach of energy conservation which equals the loss in erodent kinetic energy during impact with the work done in creating the indentation. It proceeds as follows.

At time  $t$  after initial contact, the particle of mass  $m$  will have indented the surface to a depth  $x$ ; the cross-sectional area of the indentation at the surface will be  $A(x)$ , where  $A(x)$  normally determined by the shape of the erodent particle. The upward force decelerating the particle will be that due to the plastic flow pressure acting over  $A(x)$ ; and the equation of motion of the particle can therefore be written as:

$$m \frac{d^2x}{dt^2} = -HA(x) \quad (5.3)$$

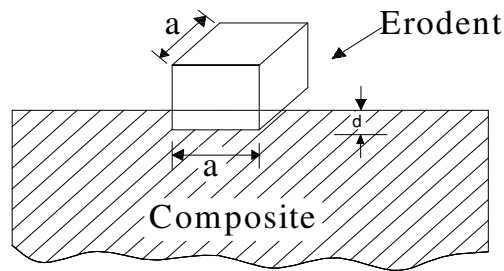


**Figure 5.2** Scheme of material removal mechanism

For simple particle shapes, this equation can readily be solved analytically. But to know the final volume of indentation when the particle comes to rest at a depth  $\delta$  at time  $t = T$ , the work done by the retarding force will equal to the sum of the kinetic energy and the loss of thermal energy of the particle.

The conservation of energy can be represented by the equation

$$\int_0^{\delta} HA(x)dx = \frac{1}{2} mU^2 \quad (5.4)$$

The impact velocity will have two components; one normal to the composite surface and one parallel to it. At zero impact angles, it is assumed that there is negligible wear because eroding particles do not practically impact the target surface [162]. Consequently, there will be no erosion due to the parallel component and the indentation is assumed to be caused entirely by the component normal to the composite surface as shown in Figure 5.3.

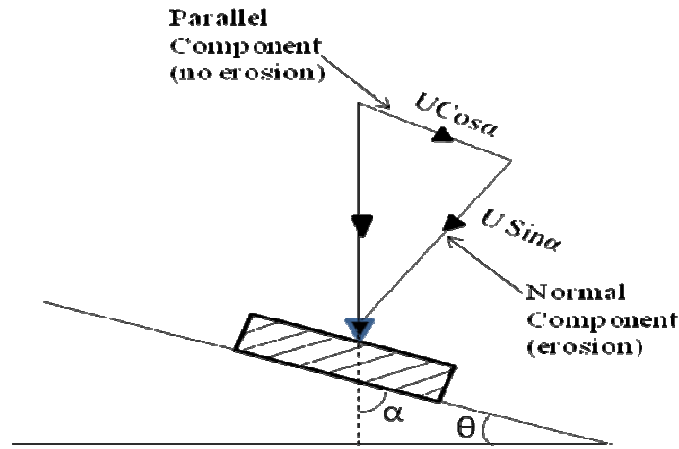


**Figure 5.3** Resolution of impact velocity in normal and parallel directions.

Now applying conservation of energy to the single impact erosion process, kinetic energy associated with the normal velocity component of a single erodent particle is equal to the work done in the indentation of composite. The energy of impact introduces a force  $P$  on the indenter to cause the indentation in the composite. Thus, in case of



oblique impact, the kinetic energy corresponding to the normal component of velocity is considered and Eq. (5.4) becomes:

$$\text{So, } \int_0^{\delta} HA(x)dx = \frac{1}{2} mU^2 \text{Sin}^2 \alpha \quad (5.5)$$

$$\text{Now, } \int_0^{\delta} A(x)dx = \int_0^{\delta} a^2 dx = a^2 \delta$$

So, the volumetric wear loss per particle impact is given by

$$\begin{aligned} e_v &= \text{Volume of indentation} \times \eta \\ &= \eta a^2 \delta \end{aligned}$$

Considering N number of particle impacts per unit time, the volumetric erosion wear loss will be

$$E_v = a^2 N \eta \delta$$

$$\text{Now, } \frac{1}{2} . P . \delta = \frac{1}{2} . m . U^2 . \text{Sin}^2 \alpha$$

$$\frac{1}{2} a^2 \delta . H = \frac{m U^2 . \text{Sin}^2 \alpha}{2}$$

$$e_v = \eta \cdot \left[ \frac{m . U^2 . \text{Sin}^2 \alpha}{H} \right]$$

For multiple impact

$$E_v = \eta . m N \left[ \frac{U^2 . \text{Sin}^2 \alpha}{H} \right]$$

$$\text{Or, } E_v = \eta . M \left[ \frac{U^2 . \text{Sin}^2 \alpha}{H} \right]$$

The non-dimensional erosion rate, defined as the composite mass lost per unit time due to erosion divided by the mass of the erodent causing the loss, is now expressed as

$$E_R = \frac{\eta \rho_c}{H} [U^2 \sin^2 \alpha] \quad (5.6)$$

The mathematical expression in Eq. 5.6 can possibly be used for predictive purpose to make an approximate assessment of the erosion damage from the composite surface.

### Chapter summary

- This chapter has provided a theoretical model for estimation of wear rate in an erosion process. But since, material removal by impact erosion wear involves complex mechanisms; a simplified theoretical model for such a process may appear inadequate unless its assessment against experimental results is made. So for the validation of the proposed model, erosion tests on the composites are to be conducted at various operating conditions.

The next chapter presents the erosion test results of the jute-epoxy-SiC composites under this study.

\*\*\*\*

# Chapter 6

## **Erosion Wear Characteristics of Jute-Epoxy Composites**

## EROSION WEAR CHARACTERISTICS OF JUTE-EPOXY COMPOSITES

---

The objective of this chapter is to validate the theoretical erosion model proposed in the previous chapter through systematic experimental investigation. The test results of erosion trials carried out on the three unfilled jute-epoxy composites A<sub>1</sub>, B<sub>1</sub> and C<sub>1</sub> and three particulate filled jute-epoxy composites C<sub>1</sub>, C<sub>2</sub> and C<sub>3</sub> are given in this part of the thesis. The Taguchi analysis of the experimental results is also presented.

### EROSION TEST RESULTS

#### **PART I** For Unfilled Jute-Epoxy Composites (A<sub>1</sub>, B<sub>1</sub> and C<sub>1</sub>)

##### **Steady state erosion**

Erosion wear behaviour of materials can be grouped as ductile and brittle categories although this grouping is not definitive. Thermoplastic matrix composites usually show ductile behaviour and have the peak erosion rate at around 30° impingement angle because cutting mechanism is dominant in erosion. While the thermosetting ones erode in a brittle manner with the peak erosion occurring at normal impact. However, there is a dispute about this failure classification as the erosive wear behaviour depends strongly on the experimental conditions and the composition of the target material [159]. In the present work, erosion curves are plotted in from the results of erosion tests conducted for different impingement angle keeping all other parameters constant (impact velocity = 32m/sec, stand-off distance = 100 mm and erodent size =200 μm). Figure 6.1 shows the dependence of the erosion rate of epoxy composites with different fiber content on the impingement angle. It can be seen that the peaks of erosion rates are located at an angle of 60° for all the samples irrespective of fiber content. This shows semi-ductile erosion behaviour of the composite. It is further noted that with increased fiber content the erosion rate of the composites is greater.

##### **Surface morphology**

To identify the mode of material removal, the morphologies of eroded surfaces are studied under scanning electron microscope. Figure 6.2 presents the microstructure of the

composite eroded at high impact velocity (58m/sec) and at an impingement angle of 60°. It shows local removal of resin material from the impacted surface resulting in exposure of the fibers to the erodent flux. This micrograph also reveals that due to sand particle impact on fibers there is formation of transverse cracks that break these fibers. The propagation of crack along transverse as well as longitudinal direction is well visualized.

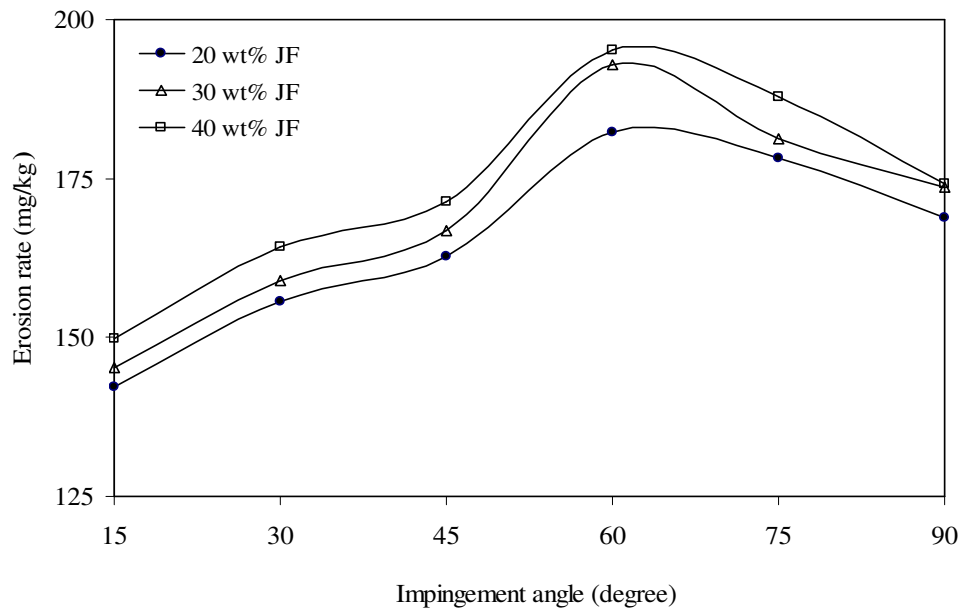


**Figure 6.1** Erosion rate vs. angle of impingement for different fiber loading

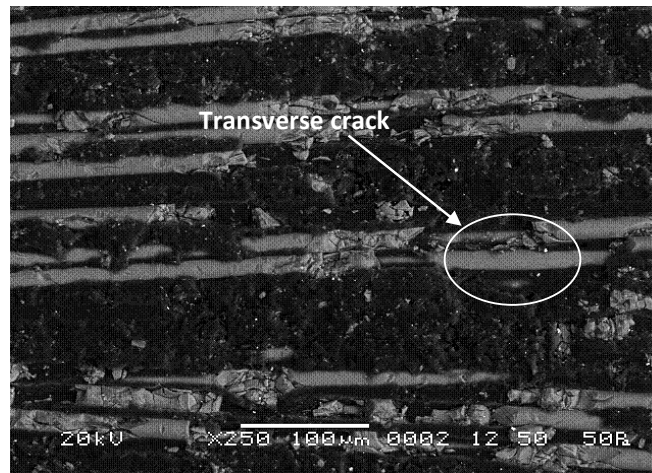


**Figure 6.2** SEM micrograph of eroded jute-epoxy composite surface (impact velocity 58m/sec, fiber loading 40 wt%, S.O.D 100mm, impingement angle 60° and erodent size 200µm).

A possible reason for the semi-ductile erosion behaviour exhibited by the epoxy based composites in the present investigation is that the erosion of jute fibers is caused mostly by damage mechanism such as micro-cracking. Such damage is supposed to increase with the increase of kinetic energy loss of the impinging sand particles. According to Hutchings et al. [162], kinetic energy loss is a maximum at normal impact, where erosion rates are highest for brittle materials. In the present study, however, the peak erosion rate shifts to an impingement angle of  $60^{\circ}$  and it is clearly due to the incorporation of jute fibers. So although neat epoxy exhibits a ductile erosion response, the presence of fibers makes the composite relatively more sensitive to impact energy which increases when the impact mode pattern changes from tangential ( $\alpha = 0^{\circ}$ ) to normal ( $\alpha = 90^{\circ}$ ). This explains the semi-ductile nature of the jute-epoxy composites with respect to solid particle erosion.

### Taguchi Analysis of the Erosion Test Results

The erosion wear rates of jute fiber reinforced epoxy matrix composites under various test conditions are given in Table 6.1. The theoretical erosion wear rates ( $E_{rth}$ ) of all the three unfilled composites are calculated using Eq. 5.6. These values are compared with those obtained from experiments ( $E_r$ ) conducted under similar operating conditions and the comparison curve has been given in Figure 6.3. Table 6.1 also presents the comparison between the theoretical and experimental results for the composites eroded under different test conditions. The errors associated with each comparison are found to lie in the range 0-12 %.

Test Run	Erodent Velocity (m/s)	Impingement Angle (Degrees)	Erodent size ( $\mu\text{m}$ )	Fiber Content (wt %)	Theoretical ER (mg/kg)	Experimental ER (mg/kg)	Error (%)
1	32	30	200	20	172.38	155.710	10.70
2	32	60	300	30	189.76	172.564	9.96
3	32	90	400	40	174.46	188.543	7.46
4	44	30	300	40	218.95	202.765	7.98
5	44	60	400	20	196.88	176.987	11.23
6	44	90	200	30	216.48	197.643	9.53
7	58	30	400	30	235.97	211.987	11.3
8	58	60	200	40	257.98	234.980	9.78
9	58	90	300	20	217.89	199.768	9.07

**Table 6.1** Erosion Test Results for Jute-Epoxy Composites

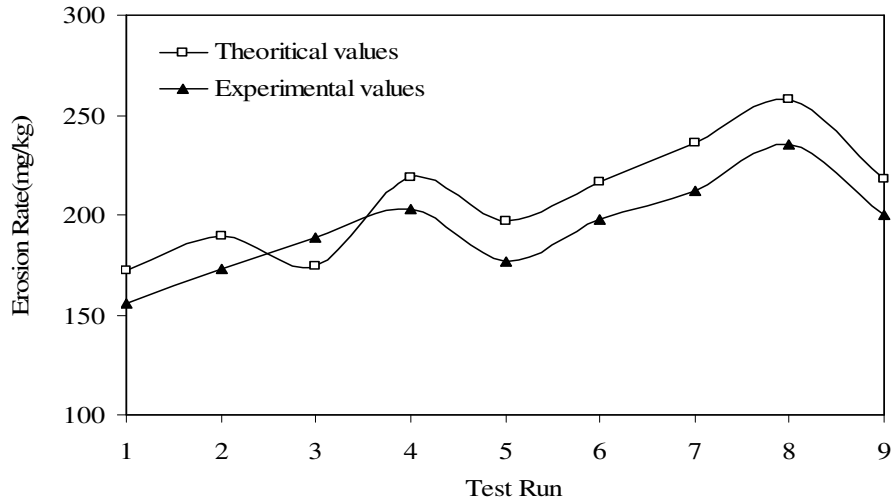


**Figure 6.3** Comparisons of Theoretical and Experimental Values of Erosion Rate

The experimental observations are transformed into a signal-to-noise (S/N) ratio. There are several S/N ratios available depending on the type of characteristics. The S/N ratio for minimum erosion rate coming under *smaller-is-better* characteristic, which can be calculated as logarithmic transformation of the loss function as shown below.

$$\text{Smaller is the better characteristic: } \frac{S}{N} = -10 \log \frac{1}{n} \left( \sum y^2 \right) \quad (6.1)$$

where n the number of observations, and y the observed data. “Lower is better” (LB) characteristic, with the above S/N ratio transformation, is suitable for minimization of erosion rate.

Test Run	A	B	C	D	E	S/N Ratio
1	32	30	200	20	155.710	-43.8463
2	32	60	300	30	172.564	-44.7390
3	32	90	400	40	188.543	-45.5082
4	44	30	300	40	202.765	-46.1399
5	44	60	400	20	176.987	-44.9588
6	44	90	200	30	197.643	-45.9176
7	58	30	400	30	211.987	-46.5262
8	58	60	200	40	234.980	-47.4206
9	58	90	300	20	199.768	-46.0105

**Table 6.2** S/N ratio and Erosion Rate for Different Test conditions

In Table 6.2, the last column represents S/N ratio of the erosion rate which is in fact the average of three replications. The overall mean for the S/N ratio of the erosion rate is found to be -45.674 db.

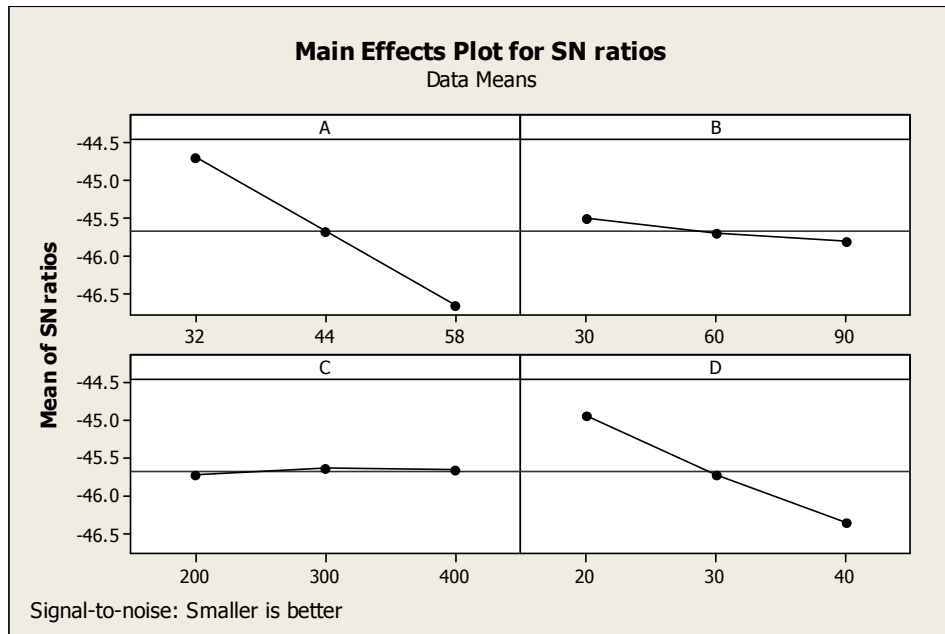


**Figure 6.4** Effect of control factors

Level	A	B	C	D
1	-44.70	-45.50	-45.73	-44.94
2	-45.67	-45.71	-45.63	-45.73
3	-46.65	-45.81	-45.66	-46.36
Delta	1.95	.31	0.10	1.42
Rank	<b>1</b>	<b>3</b>	<b>4</b>	<b>2</b>

**Table 6.3** Response Table for Signal to Noise Ratio (Smaller is better)

The analysis is made using the popular software specifically used for design of experiment applications known as MINITAB 14.

The effects of individual control factors are shown in Figure 6.2. The S/N ratio response are given in Table 6.3, from which it can be concluded that among all the factors, impact velocity is the most significant factor followed by fiber content and impingement angle while the erodent size has the least or almost no significance on erosion of the reinforced composite. It also leads to the conclusion that factor combination of A<sub>1</sub>, B<sub>1</sub>, and D<sub>1</sub> gives minimum erosion rate.



### **Factor Settings for Minimum Erosion Rate**

In this study, an attempt is made to derive a predictive equation in terms of the significant control factors for determination of erosion rate. The single-objective function requires quantitative determination of the relationship between erosion rates with combination of control factors. In order to express, erosion rate in the form of a mathematical model in the following correlation is suggested.

$$E = K_0 + K_1 \times A + K_2 \times B + K_3 \times D \quad (6.2)$$

Here,  $E$  is the performance output terms and  $K_i$  ( $i = 0, 1 \dots 3$ ) are the model constants. The constant are calculated using non-linear regression analysis with the help of SYSTAT 7 software and the following relations are obtained.

$$E = 66.984 + 1.665 \times A + 0.086 \times B + 1.564 \times D \quad (6.3)$$

$$r^2=0.99$$

The correctness of the calculated constants is confirmed as high correlation coefficients ( $r^2$ ) in the tune of 0.99 are obtained for Eq. (6.3).

### **PART II For Jute-Epoxy Composites Filled with SiC particulates ( $C_1, C_2$ & $C_3$ )**

#### **Steady state erosion**

Erosion behaviour of the composites is generally ascertained by correlating erosion rate with impingement angle, erodent velocity and composition of the material. Composites usually respond to solid particle erosion in two broad ways: ductile and brittle. The ductile response is characterized by maximum erosion rate occurring at 15–30° impingement angle and brittle behaviour is characterized by the peak erosion rate at 90°. Similarly, semi-ductile behaviour is characterized by the maximum erosion rate taking place at 45–60°. But as already mentioned, this grouping is not definitive because the erosion characteristics equally depend on the experimental conditions as on composition of the target material.

The erosion wear rates of jute-SiC-epoxy composites as a function of impingement angle ( $\alpha$ ) are shown in Figure 6.5. It can be seen that filling of composite with SiC particles reduces the wear rate of the jute-epoxy composites quite significantly. The unfilled composite, shows maximum erosion occurring at  $\alpha = 60^\circ$  while for both the filled composites (with 10wt% and 20wt% SiC content) the value of  $\alpha$  where the peak erosion occurs is found to be  $75^\circ$ . In the present study, the location of peak erosion has shifted to  $60^\circ$  from the usual  $15^\circ$ - $30^\circ$  (for purely ductile case) as it is reinforced with jute fiber (curve A). This shift in the erosion behaviour is an indication of loss of ductility and is obviously attributed to the presence of fibers. Further shifting of  $\alpha$  from  $60^\circ$  to  $75^\circ$  (curve B and C) proves that the composites tend to become still more brittle with incorporation of SiC particles. The trend is similar for both the composites with SiC filler. It is also important to note that the sample with higher filler content exhibits better erosion resistance. Thus it can be concluded that erosion performance of jute-epoxy composites improves with SiC filling and this improvement is a function of filler content within the limit of the present study.

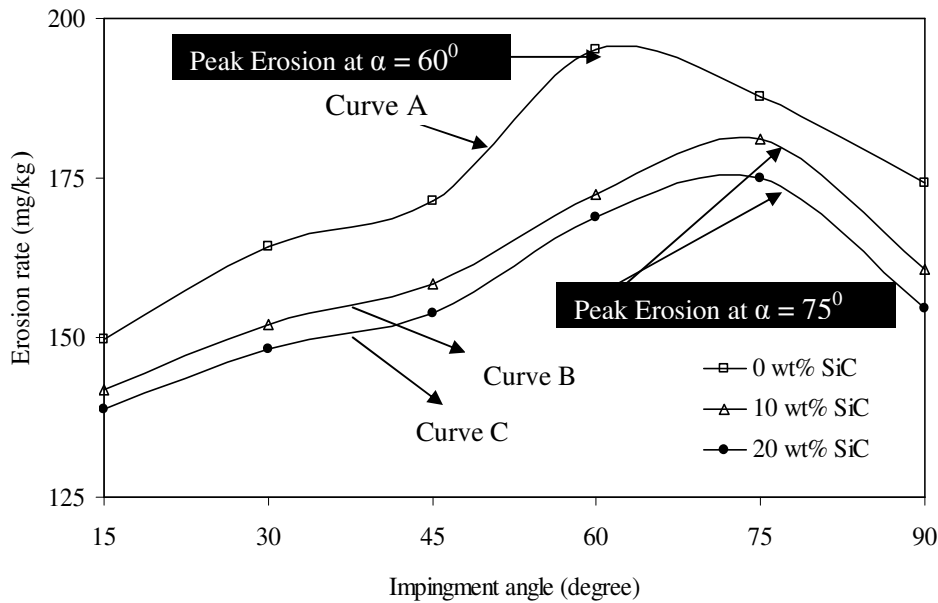


**Figure 6.5** Erosion rate vs. Angle of impingement for different weight fraction of SiC

### Surface morphology

To identify the mode of material removal, the morphologies of eroded surfaces are studied under scanning electron microscope. The surface micro-structures of some of the un-eroded composite samples are observed under scanning electron microscope basically

to get an insight to the features. As seen in Figures (6.6a) and (6.6b), the surfaces are reasonably homogeneous. No cracks are seen although some voids and pores are visible even at lower magnification. SiC particles are not seen in clusters within the matrix body. To identify the mode of material removal, the morphologies of eroded surfaces are studied under scanning electron microscope. Figure (6.6c) presents the microstructure of the composite eroded at high impact velocity (58m/sec) and at an impingement angle of  $60^{\circ}$ . It shows local removal of resin material from the impacted surface resulting in exposure of the fibers to the erodent flux. This micrograph also reveals that due to sand particle impact on fibers there is formation of transverse cracks that break these fibers. The propagation of crack along transverse as well as longitudinal direction is well visualized.

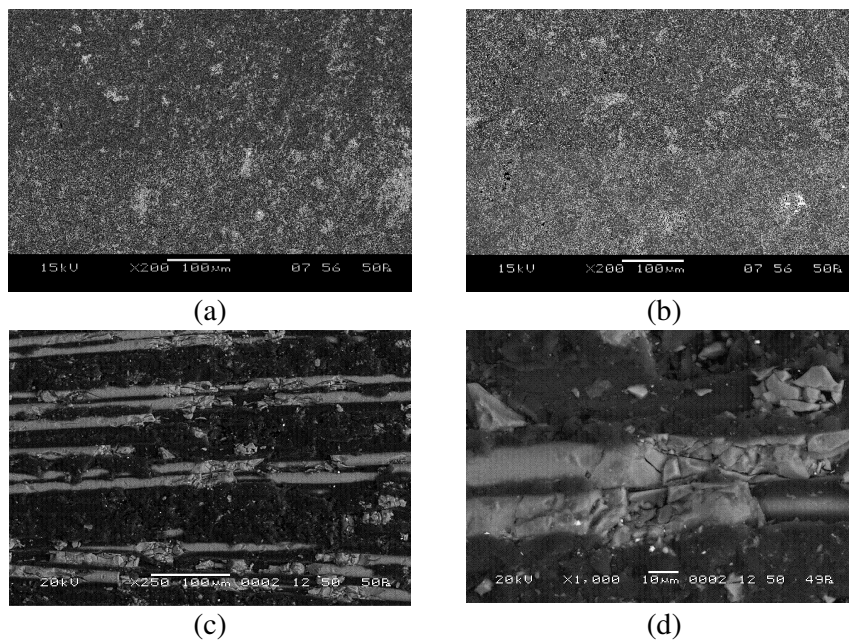


**Figure 6.6** SEM micrograph of SiC filled jute-epoxy composite surface

Figure (6.6d) presents the microstructure of the SiC filled composite eroded with high impact velocity (58m/sec) at an impingement angle of  $60^{\circ}$ . It shows local removal of resin material from the impacted surface resulting in exposure of the fibers to the erodent flux. This micrograph also reveals that due to sand particle impact on jute-fibers, there is formation of transverse cracks that break these fibers. The propagation of crack along transverse as well as longitudinal direction is well visualized. It appears that cracks have

grown on the fibers giving rise to breaking of the fibers into small fragments. Figure (6.6d) also shows the dominance of micro-chipping and micro-cracking phenomena. It can be seen that multiple cracks originate from the point of impact, intersect one another and form wear debris due to brittle fracture in the fiber body as well as in the silicon carbide particles present in the matrix body. After repetitive impacts, the debris in platelet form is removed and account for the measured wear loss.

### Taguchi Analysis of the Erosion Test Results

The erosion wear rates of jute fiber reinforced epoxy matrix composites filled with different proportions of silicon carbide under various test conditions are given in Table 6.4. The theoretical erosion wear rates ( $E_{rth}$ ) of all the three unfilled composites are calculated using Eq. 5.6. These values are compared with those obtained from experiments ( $E_r$ ) conducted under similar operating conditions and the comparison curve has been given in Figure 6.7. Table 6.4 also presents the comparison between the theoretical and experimental results for the composites eroded under different test conditions. The errors associated with each comparison lie in the range 0-12 %.

Test Run	Erodent Velocity (m/s)	Impingement Angle (Degrees)	Erodent size ( $\mu\text{m}$ )	Filler Content (wt %)	Theoretical ER (mg/kg)	Experimental ER (mg/kg)	Error (%)
1	32	30	200	0	142.83	135.170	5.66
2	32	60	300	10	144.68	133.980	7.89
3	32	90	400	20	114.46	106.667	7.30
4	44	30	300	20	121.95	131.320	7.13
5	44	60	400	0	226.81	204.778	10.75
6	44	90	200	10	199.40	189.874	5.01
7	58	30	400	10	235.297	211.493	11.25
8	58	60	200	20	217.297	197.765	9.87
9	58	90	300	0	247.892	258.370	4.05

**Table 6.4** Erosion Test Results for particulate filled Jute-Epoxy Composites

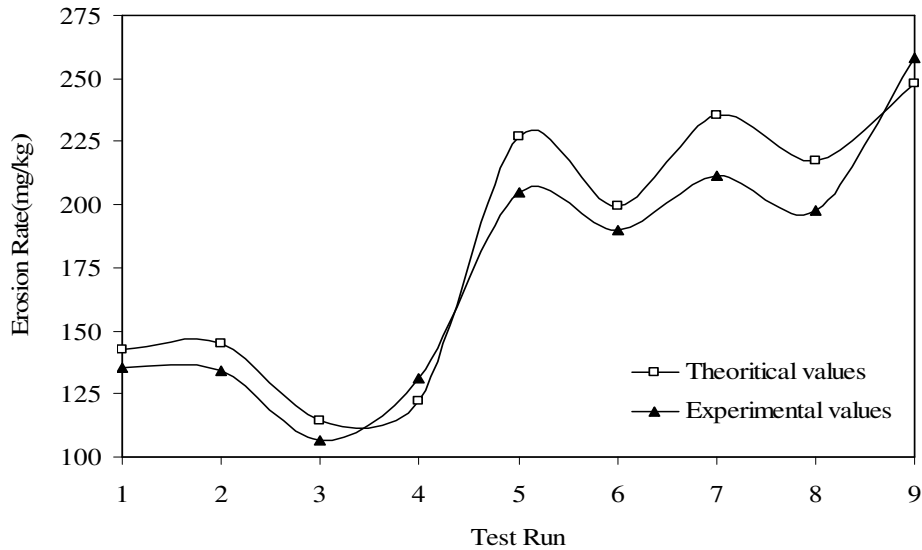


**Figure 6.7** Comparison of Theoretical and Experimental Values of Erosion Rate

The experimental observations are transformed into a signal-to-noise (S/N) ratio. There are several S/N ratios available depending on the type of characteristics. The S/N ratio for minimum erosion rate coming under *smaller-is-better* characteristic, which can be calculated as logarithmic transformation of the loss function as shown below.

$$\text{Smaller is the better characteristic: } \frac{S}{N} = -10 \log \frac{1}{n} (\sum y^2) \quad (6.4)$$

where n the number of observations, and y the observed data. “Lower is better” (LB) characteristic, with the above S/N ratio transformation, is suitable for minimization of erosion rate.

Test Run	A	B	C	D	E	S/N Ratio
1	32	30	200	0	135.170	-42.6176
2	32	60	300	10	133.980	-42.5408
3	32	90	400	20	106.667	-40.5606
4	44	30	300	20	131.320	-42.3666
5	44	60	400	0	204.778	-46.2257
6	44	90	200	10	189.874	-45.5693
7	58	30	400	10	211.493	-46.5059
8	58	60	200	20	197.765	-45.9230
9	58	90	300	0	258.370	-48.2448

**Table 6.5** S/N ratio and Erosion Rate for Different Test conditions

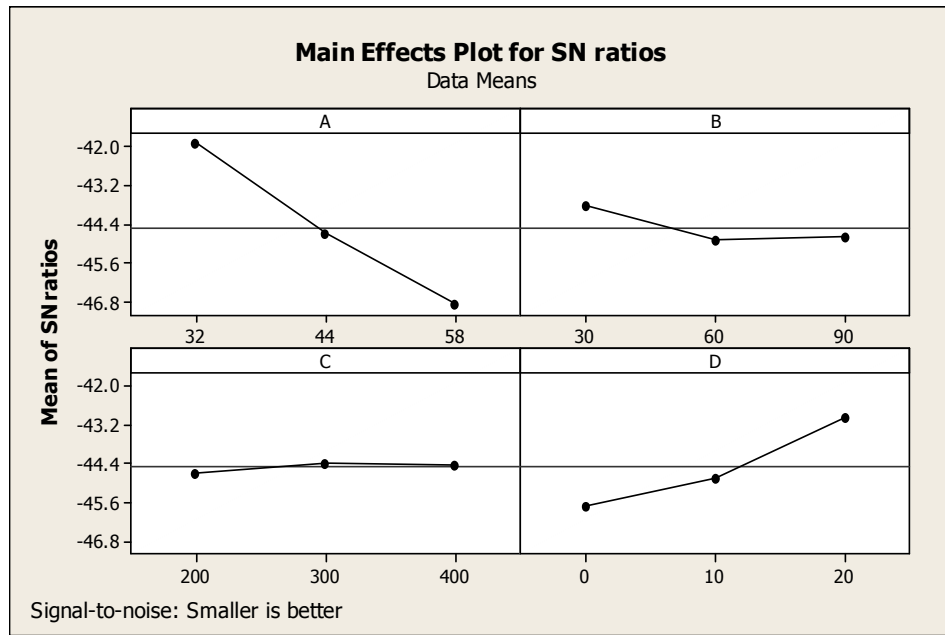


**Figure 6.8** Effect of control factors on erosion rate

In Table 6.5, the last column represents S/N ratio of the erosion rate which is in fact the average of three replications. The overall mean for the S/N ratio of the erosion rate is found to be - 44.506 db.

Level	A	B	C	D
1	-41.91	-43.83	-44.70	-45.70
2	-44.72	-44.90	-44.38	-44.87
3	-46.89	-44.79	-44.43	-42.95
Delta	4.98	1.07	0.32	2.75
Rank	1	3	4	2

**Table 6.6** Response Table for Signal to Noise Ratios (Smaller is better)

The analysis is made using the popular software specifically used for design of experiment applications known as MINITAB 14.

The effects of individual control factors are shown in Figure 6.8. The S/N ratio response are given in Table 6.6, from which it can be concluded that among all the factors, impact velocity is the most significant factor followed by filler content and impingement angle while the erodent size has the least or almost no significance on erosion of the reinforced composite. It also leads to the conclusion that factor combination of A<sub>1</sub>, B<sub>1</sub>, and D<sub>3</sub> gives minimum erosion rate.

### **Factor Settings for Minimum Erosion Rate**

In this study, an attempt is made to derive a predictive equation in terms of the significant control factors for determination of erosion rate. The single-objective function requires quantitative determination of the relationship between erosion rates with combination of control factors. In order to express, erosion rate in the form of a mathematical model in the following correlation is suggested.

$$E = K_0 + K_1 \times A + K_2 \times B + K_3 \times D \quad (6.5)$$

Here,  $E$  is the performance output terms and  $K_i$  ( $i = 0, 1 \dots 3$ ) are the model constants. The constant are calculated using non-linear regression analysis with the help of SYSTAT 7 software and the following relations are obtained.

$$E = 9.179 + 3.731 \times A + 0.427 \times B - 2.709 \times D \quad (6.6)$$

$$r^2 = 0.989$$

The correctness of the calculated constants is confirmed as high correlation coefficients ( $r^2$ ) in the tune of 0.989 are obtained for Eq. (6.6).

### **Chapter summary:**

This chapter has provided the findings that lead to the following conclusions:

1. Successful fabrication of multi-component hybrid jute-epoxy composites with reinforcement of SiC derived from rice husk by plasma processing route is possible.
2. It is demonstrated that if supported by an appropriate magnitude of erosion efficiency, the proposed theoretical model can perform well for epoxy based hybrid composites for normal as well as oblique impacts.

3. The presence of particulate fillers (silicon carbide) in these composites improves their erosion wear resistance and this improvement depends on the weight content of the filler.
4. Erosion characteristics of these composites have been successfully analyzed using Taguchi experimental design. Significant control factors affecting the erosion rate have been identified through successful implementation of this technique. Impact velocity, fiber/filler content and impingement angle in declining sequence are found to be significant for minimizing the erosion rate of all the composites. Erodent size is identified as the least influencing control factor for erosion rate.

The next chapter presents the executive summary and conclusions along with recommendations for future work.

\*\*\*\*\*



# Chapter 7

## Summary and Conclusions

#### **Summary**

The research reported in this thesis consists of two parts: the first part has provided the description of the experimental program and has presented the mechanical characteristics of the jute-epoxy composites under this study; the second part has reported the effect of SiC filler on the solid particle erosion characteristics of these composites.

By incorporating these particulate fillers into the jute-fiber reinforced epoxy, synergistic effects, as expected were achieved in the form of modified mechanical properties and improved erosion wear resistance. Inclusion of jute fiber in neat epoxy improved the load bearing capacity (tensile strength) and the ability to withstand bending (flexural strength) of the composites. But with the incorporation of silicon carbide fillers, the tensile strengths of the composites were found to be less. There can be two reasons for this decline in tensile strength of these particulate filled composites compared to the unfilled one. One possibility is that the chemical reaction at the interface between the filler particles and the matrix may be too weak to transfer the tensile stress; the other is that the corner points of the irregular shaped particulates result in stress concentration in the epoxy matrix.

Hardness values have been found to have improved for the particulate filled composites. The reduction in tensile strength and the improvement in hardness with the incorporation of fillers can be explained as follows: under the action of a tensile force the filler-matrix interface is vulnerable to debonding depending on interfacial bond strength and this may lead to a break in the composite. But in case of hardness test, a compression or pressing stress is in action. So the polymeric matrix phase and the solid filler phase would be pressed together and touch each other more tightly. Thus, the interface can transfer pressure more effectively although the interfacial bond may be poor. This might have resulted in an enhancement of hardness.

The presence of pores and voids in the composite structure significantly affect some of the mechanical properties and even the performance of the composites. Higher void contents usually mean lower fatigue resistance, greater susceptibility to water penetration

and weathering. However, presence of void is unavoidable in composite making particularly through hand-lay-up route. In the present investigation, it was noticed that the composites with particulate fillers have higher void fraction compared to the unfilled jute epoxy composites.

The possible wear mechanism during solid particle erosion of jute-epoxy composites, as evident from test results and scanning electron microscopy, can be characterized as follows.

- First, there is local removal of resin material from the impacted surface which results in exposure of the fibers to the erosive environment.
- Sand particles impact on the fibers and cause fibers to break because of the formation of cracks perpendicular to their length. These cracks are presumably caused by fibers-bending stresses due to the impact of erodent particles on the unsupported fibers.
- Further damage results when the interfaces between the broken fibers and the matrix resin are degraded until the fibers are removed by subsequent impacts.

The erosion wear rates of particulate filled jute-epoxy composites are found to be lower than those of the unfilled jute-epoxy composites under similar test conditions. This has led to the conclusion that the presence of silicon carbide particulates improves the erosion wear resistance of fiber reinforced epoxy. The reduction in material loss in these particulate filled composites can be attributed to two reasons. One is the improvement in the bulk hardness of the composite with addition of these hard ceramic particles. Secondly, during the erosion process, the filler particles absorb a good part of the kinetic energy associated with the erodent. This results in less amount of energy being available to be absorbed by the matrix body and the reinforcing jute fiber phase. These two factors together lead to the enhancement of erosion wear resistance of the composites. This study thus, shows that the filler content in the composite is significant in combating erosive wear.

The erosion wear rates of the composites were found to be dependent on the impingement angle. The findings of this research further suggest that, this dependency is also influenced by the weight percentage of the filler material. In fact, the angle of impact determines the relative magnitude of the two components of the impact velocity

namely, the component normal to the surface and parallel to the surface. The normal component will determine how long the impact will last (i.e. contact time) and the load. The product of this contact time and the tangential (parallel) velocity component determines the amount of sliding that takes place. The tangential velocity component also provides a shear loading to the surface, which is in addition to the normal load that the normal velocity component causes. Hence as this angle changes the amount of sliding that takes place also changes the nature and magnitude of the stress system. Both of these aspects influence the way a composite wears out.

## **Conclusions**

This analytical and experimental investigation on jute-epoxy composites (with and without SiC fillers) has led to the following specific conclusions:

1. Successful fabrication of multi-component hybrid jute-epoxy composites with reinforcement of SiC derived from rice husk by plasma processing route is possible.
2. Incorporation of these fillers modifies the tensile, flexural and inter-laminar shear strengths of the jute epoxy composites. The micro-hardness and density of the composites are also greatly influenced by the content of fillers. Hence, while fabricating a composite of specific requirements, there is a need for the choice of appropriate filler material and for optimizing its content in the composite system.
3. A mathematical model based on conservation of particle kinetic energy during multiple impact erosion process has been developed. To overcome the shortcomings of the existing theoretical models an ‘erosion efficiency’ term has been introduced. It is demonstrated that if supported by an appropriate magnitude of erosion efficiency, the model can perform well for polymer based hybrid composites for normal as well as oblique impacts.
4. The presence of particulate fillers (silicon carbide) in these composites improves their erosion wear resistance and this improvement depends on the weight content of the filler.

5. Erosion characteristics of these composites have been successfully analyzed using Taguchi experimental design. Significant control factors affecting the erosion rate have been identified through successful implementation of this technique. Impact velocity, fiber/filler content and impingement angle in declining sequence are found to be significant for minimizing the erosion rate of all the composites. Erodent size is identified as the least influencing control factor for erosion rate.

### **Recommendation for future work**

The present work leaves a wide scope for future investigators to explore many other aspects of particulate filled FRP composites. Some recommendations for future research include:

- The response of these composites to other wear modes such as sliding and abrasion.
- Possible use of other ceramic/metallic fillers, polymeric resins other than epoxy and natural fibers other than jute in the development of new hybrid composites.

\*\*\*\*\*

# References

## References

1. Agarwal B.D and Broutman L. J, (1990). Analysis and performance of fiber composites, Second edition, John Wiley & Sons, Inc, pp.2-16.
2. Jang B. Z, (1994). Advanced Polymer composites: principles and applications. ASM International.
3. Kuljanin J, Vuckovic M, Comor M.I, Bibic N, Djokovic V and Nedeljkovic J.M. (2002). Influence of CdS-filler on the thermal properties of polystyrene, *European Polymer Journal*, 38(8):1659–1662.
4. Weidenfeller B, Höfer M, Schilling F. (2004). Thermal conductivity, thermal diffusivity, and specific heat capacity of particle filled polypropylene, *Composites Part A: Applied Science and Manufacturing*, 35 (4):423–429
5. Stolarski T.A, (1990). Tribology in Machine Design, Heiman Newnes, UK.
6. Päivi Kivikytö-Reponen, (2006). Correlation of Material Characteristics and Wear of Powder Metallurgical Metal Matrix Composites, Doctoral Theses in Materials and Earth Sciences, Helsinki University of Technology, Laboratory of Materials Science, Espoo, 1-2.
7. Halling, (1975). Principles of tribology, The McMillan Press Ltd, NY, USA
8. Budinski K.G, (1998). Surface Engg. for Wear Resistance, N.J, USA.
9. Robinowicz E, (1965). Friction and wear of materials, Willey, NY, USA.
10. Thomas H. Kosel, (1992). ASM Handbook: Friction, Lubrication, and Wear Technology, ASM International Handbook Committee. 18, 371-372.
11. Pool K.V, Dharan C.K.H, and Finnie I, (1986). Erosion wear of composite materials, wear, vol. 107, 1-12
12. Aglan H.A and Chenock T.A Jr., (1993). Erosion damage features of polyimide Thermoset composites, *SAMPE Quarterly*, 41-47.
13. Rao P.V, (1995). Characterization of optical and surface parameters during particle impact damage, *ASME/Fluids engineering publications*, 23:87-96.
14. Tennyson, R.C, (1991). LDEF Mission update: composites in space, *Advance materials & processes*, 5:33-36.
15. Gregory Sawyer W, Freudenberg Kevin D, Bhimaraj Pravee and Schadler Linda S, (2003). A study on the friction and wear behavior of PTFE filled with alumina nanoparticles, *Wear*, 254:573–580.
16. Jung-il K., Kang P.H and Nho Y.C, (2004). Positive temperature coefficient behavior of polymer composites having a high melting temperature, *J Appl Poly Sci.*, 92:394–401.
17. Nikkeshi S, Kudo M and Masuko, T, (1998). Dynamic viscoelastic properties and thermal properties of powder-epoxy resin composites, *J Appl Poly Sci.*, 69:2593-8.
18. Zhu, K and Schmauder, S, (2003). Prediction of the failure properties of short fiber reinforced composites with metal and polymer matrix, *Comput Mater Sci.* 28:743–8.
19. Rusu M, Sofian N and Rusu D, (2001). Mechanical and thermal properties of zinc powder filled high density polyethylene composites, *Polym Test*, 20: 409–17.
20. Tavman I. H, (1997). Thermal and mechanical properties of copper powder filled poly (ethylene) composites, *Powder Technol*, 91: 63–7.
21. Rothon R.N, (1997). Mineral fillers in thermoplastics: filler manufacture, *J Adhesion*, 64:87–109.

22. Rothon R.N, (1999). Mineral fillers in thermoplastics: filler manufacture and characterization. *Adv. Polym. Sci.* 139: 67–107.
23. Nielsen L.E and Landel R.F, (1994). Mechanical properties of polymers and composites. 2nd ed. New York: Marcel Dekker, pp.377–459.
24. Peters S.T, (1998). Handbook of composites. 2nd ed. London: Chapman and Hall, pp. 242–243.
25. Wang H, Bai Y, Lui S, Wu J and Wong C.P, (2002). Combined effects of silica filler and its interface in epoxy resin. *Acta Mater.*, 50:4369–4377.
26. Yamamoto I, Higashihara T and Kobayashi T, (2003). Effect of silica-particle characteristics on impact/usual fatigue properties and evaluation of mechanical characteristics of silica-particle epoxy resins. *JSME Int J*, 46(2):145–153.
27. Nakamura Y, Yamaguchi M, Kitayama A, Okubo M and Matsumoto T, (1991). Effect of particle size on fracture toughness of epoxy resin filled with angular-shaped silica. *Polymer*, 32(12):2221–2229.
28. Nakamura Y, Yamaguchi M, Okubo M and Matsumoto T, (1991). Effect of particle size on impact properties of epoxy resin filled with angular shaped silica particles. *Polymer*, 32(16):2976–2979.
29. Nakamura Y, Yamaguchi M, Okubo M and Matsumoto T, (1992). Effects of particle size on mechanical and impact properties of epoxy resin filled with spherical silica. *J Appl Polym Sci*, 45:1281–1289.
30. Srivastava V.K, Prakash R and Shembekar P.S, (1988). Fracture behaviour of fly ash filled FRP composites. *Compos Struct.*, 10:271–9.
31. Srivastava V.K and Shembekar P.S, (1990). Tensile and fracture properties of epoxy resin filled with flyash particles. *J Mater Sci.*, 25:3513–3516.
32. Gracia R, Evans R.E and Palmer R.J, (1987). Toughened composites, STP 937, N.J.Johnson, Ed., ASTM. 397-412.
33. Gracia R, (1983). Nadc-83058-60, July.
34. Jang B.Z.,and Lin T.L (1989). Ann. Tech. Conf. (ANTEC) (New York), May.
35. Jang B.Z., Liau J.Y,Hwang L.R and Wilcox R.C, (1988). *Plast. Eng.*, Nov.
36. Bijwe J, Logani C.M and Tewari U.S, (1990). Influence of fillers and fiber reinforcement on abrasive wear resistance of some polymeric composites, *Wear*, 138:77–92.
37. Wang M, Gu B and Songhao Ge S, (2003). Investigation of the influence of MoS<sub>2</sub> filler on the tribological properties of carbon fiber reinforced nylon 1010 composites, *Wear*, 255:774–779.
38. Sunkara, (2000). The Role of Particulate Inorganic Fillers on the Tribological Behavior of Polyphenylene Sulfide, MS thesis, Iowa State University, Ames,
39. Hanmin Z, Guoren H and Guicheng Y, (1987). Friction and wear of poly (phenylene sulfide) and its carbon fiber composites: I Unlubricated, *Wear*, 116: 59–68.
40. Bahadur S, Gong D and Anderegg J.W, (1993). Tribochemical studies by XPS analysis of transfer films of nylon 11 and its composites containing copper compounds, *Wear*, 165:205–212.
41. Bahadur S, Gong D and Anderegg J, (1996). Investigation of the influence of CaS, CaO, and CaF<sub>2</sub> fillers on the transfer and wear of nylon by microscopy and XPS analysis, *Wear*, 197: 271–279.
42. Cutler I B 1973 US patent 3754079.
43. Janghorban K and Tazesh H R 1999 *Ceram. Int.* **25** 7.
44. Krishnarao R V, Mahajan Y R and Kumar T J 1998 *J. Euro. Ceram. Soc.* **18** 147.
45. Manosur N A L and Hanna S B 1979 *Trans. J. Br. Ceram. Soc* **78** 132.



46. Moustafa S F, Morsi M B and El-Din A 1997 *Can. Metall. Quar.* **36** 355.
47. Nutt S R 1988 *J. Am. Ceram. Soc.* **71** 149.
48. Padmaja G and Mukunda P G 1999 *J. Am. Ceram. Soc.* **82** 1393
49. Panigrahi M R and Overand R P 1997 in *Proceedings of the third biomass conference of the american* (ed.) R P Overend and E Chornet (New York: Elsevier Science, Inc.) p. 79.
50. Panigrahi B B, Roy G G and Godkhindi M M 2001 *Br. Ceram. Trans.* **100** 29.
51. Patel M 1991 *Silicon Ind.* **55** 30.
52. Ray A K, Mohanty G and Ghose A 1991 *J. Mater. Sci. Lett.* **10** 277.
53. Romera F J N and Reinso F R 1996 *J. Mater. Sci.* **31** 779
54. Singh S K, Stachowicz L, Girshick S L and Pfender E 1993 *J. Mater. Sci. Lett.* **12** 659.
55. Singh S K, Parida K M, Mohanty B C and Rao S B 1995 *Reac. Kinet. Catal. Lett.* **54** 29.
  
56. Mason J.S and Smith B.V, (1972). The erosion of bends by pneumatically conveyed suspensions of abrasive particles, *Powder Technol.*, 6: 323–335.
57. Tsai W, Humphrey J.A.C, Cornet I and Levy A.V, (1981). Experimental measurement of accelerated erosion in a slurry pot tester, *Wear*, 68: 289–303.
58. Hojo H, Tsuda K and Yabu T, (1986). Erosion damage of polymeric material by slurry, *Wear*, 112: 17–28.
59. Kumar R, Verma A.P and Lal G.K, (1983). Nozzle wear during the flow of a gas–particle mixture, *Wear*, 91: 33–43.
60. Crowley M.S, (1969). Influence of particle size on erosion resistance of refractory concretes, *Am. Ceram. Soc. Bull.* 48: 707–710.
61. Neilson J.H and Gilchrist A, (1968). An experimental investigation into aspects of erosion in rocket motor tail nozzles, *Wear* 11:123–143.
62. Hibbert W.A, (1965). Helicopter trials over sand and sea, *J. Roy. Aeronaut. Soc.* 69: 769–776.
63. Tilly G. P,(1969). Erosion caused by airborne particles, *Wear*, 14(1):63-79.
64. Zahavi J, Nadiv S and Schmitt Jr G. F, (1981). Indirect damage in composite materials due to raindrop impact, *Wear*, 72(3):305-313
65. Zahavi J, Nadiv S and Schmitt Jr G. F, (1981). Indirect damage in composite materials due to raindrop impact, *Wear*, 72(3):305-313
66. Tilly G. P and Wendy Sage, (1970). The interaction of particle and material behaviour in erosion processes, *Wear*, 16(6):447-465.
67. Tsiang T.H,(1989).Sand erosion of fiber composites: Testing and evaluation in CC. Chamis (Ed.), *Test methods for design allowables for fibrous composites*, Vol. 2, American Society for Testing and Materials, (ASTM) STP I003, Philadelphia, pp. 55-74.
68. Mathias P-J., Wu W, Goretta K.C, Routbort L.J, Groppi D.P and Karasek K.R, (1989). Solid particle erosion of a graphite-fiber reinforced bismaleimide polymer composite, *Wear*, 135: 161-169.
69. Abdul-Latif and Ali ahmed. (1987) Geostatistical estimation of reserves in the Abu-Tartur phosphate deposits western desert, Egypt. Masters thesis, King Fahd University of Petroleum and Minerals.
70. Karasek K.R, Goretta K.C, Helberg D.A and Routbort J.L, (1992). *J. Mater. Sci. Lett.*, II 1143.
71. Finnie I, (1960). An experimental study of erosion, *Proc. Sot. Exp. Stress Anal.*, 17:65 - 70.

72. Finnie I, (1960). Erosion of surface by solid particles, *Wear*, 3: 87 - 103.
73. Smeltzer C. E, Gulden M. E and Compton W. A, (1970). Mechanisms of material removal by impacting dust particles, *J. Basic Eng.*, 92: 639 - 654.
74. Schmitt G. P, (1970). The erosion behavior of polymeric coatings and composites at subsonic velocities. In A. A. Fyall and R. B. King (eds.), *Proc. 3rd Int. Conf. on Rain Erosion and Associated Phenomena*, Royal Aircraft Establishment, Farnborough, pp. 107 - 128.
75. Zahavi J and Schmitt, Jr., G. F, (1981). Solid particle erosion of polymeric coatings, *Wear*, 71: 191- 210.
76. Zahavi J and Schmitt Jr. G. F, (1981). Solid particle erosion of reinforced composite materials, *Wear*, 71: 179 - 190.
77. Ruff A.W and Wiederhorn S.M. (1979). Erosion by solid particle impact. In: Preece CM, editor. *Treatise on materials science and technology*, vol. 16. New York: Academic Press., pp. 69–125.
78. Sundararajan G, (1983). The solid particle erosion of metals and alloys. *Trans. Indian Inst. Met.* 36(6):474–495.
79. Evans A.G and Wilshaw T.R, (1976), Quasi-static solid particle damage in brittle solids, I. Observations, analysis and implications, *Acta Metal.*, 24:939-956.
80. Cousen A. K, Hutchings I. M, Field J. E and Comey N. S (eds.), (1983). *Proc. 6th Int. CM on Erosion by Liquid and Solid Impact*, Cavendish Laboratory, University of Cambridge, 1983, Cambridge, Paper 41.
81. Venugopal Reddy A and Sundararajan G, (1986). Erosion behaviour of ductile materials with a spherical non-friable erodent, *Wear*, 111(3):313-323.
82. Sheldon G.L and Finnie I, (1966). On the ductile behavior of nominally brittle materials during erosive cutting, *Trans ASME J Eng Ind.*, 88:387–392.
83. Ericson F, Johansson S and Schweitz, J.-Å. (1988). Hardness and fracture toughness of semiconducting materials studied by indentation and erosion techniques. *Mater. Sci. Eng. A*: 105/106:131-141.
84. Zum Gahr K. H, (1987). *Microstructure and Wear of Materials*, tribology Series, Vol. 10, Elsevier, Amsterdam.
85. Wiederhorn M and Hockey B. J, (1980). Effect of material parameters on the erosion resistance of brittle materials, *J. Mater. Sci.*, 18:766-780.
86. Lamy B, (1984). Effect of brittleness index and sliding speed on the morphology of surface scratching in abrasive or erosive processes, *Tribol. Int.*, 17(1):35-38.
87. Briscoe, B, (1981). *Wear of Polymers-An Essay on Fundamental-Aspects*, *Tribol Int*, 14: 231 –243.
88. Miyazaki N and Hamao T, (1996). Effect of interfacial strength on erosion behavior of FRPs, *J. Compos. Mater.*, 30: 35–50.
89. Miyazaki N and Hamao T, (1994). Solid particle erosion of thermoplastic resins reinforced by short fibers, *J. Compos. Mater.*, 28 (9): 871–883.
90. Haraki N, Tsuda K and Hojo H, (1992). Sand erosion behaviour of composites reinforced with glass cloth laminates, *Adv. Compos. Lett.*, 1 (1): 31–33.
91. Hovis S.K, Talia J.E and Scattergood R.O, (1986). Erosion in multiphase systems, *Wear*, 108:139–155.
92. Ballout Y.A, Hovis S.K and Talia J.E, (1990). Erosion in glass–fiber reinforced epoxy composite, *Scripta Metallurgicaet materialia*, 24: 195–200.
93. El-Tayeb N.S.M and Yousif B.F, (2007). Evaluation of glass fibre reinforced polyester composite for multi-pass abrasive wear applications, *Int. J. Wear*, 262:1140–1151.

94. Zum Gahr K.-H, (1987). Microstructure and wear of materials, Tribology Series 10, Elsevier, Amsterdam.
95. Chevallier P and Vannes A.B, (1995). Effect on a sheet surface of an erosive particle jet upon impact, *Wear* 184:87–91.
96. Tabakoff W, (1995). High-temperature erosion resistance of coatings for use in turbo machinery, *Wear* 186/187:224–229.
97. Tirupataiah Y, Venkataraman B and Sundararajan G, (1990). The nature of the elastic rebound of a hard ball impacting on ductile, metallic target materials, *Materials Science and Engineering: A*, 124(2):133-140.
98. Ballout Y.A, (1998). Erosion Mechanisms in Composite Materials and Ripple Formation Mechanism in Erosion, PhD Dissertation, Wichita State Univ.
99. Ibrahim A.T, (1990). A Mechanism for Solid Particle Erosion in Ductile and Brittle Materials, MS Thesis, Wichita State Univ.
100. Arnold J.C and Hutchings I.M. (1990). The mechanisms of erosion of unfilled elastomers by solid particle impact. *Wear*, 138:33–46.
101. Arnold J.C and Hutchings I.M. (1989). Flux rate effects in the erosive wear of elastomers. *J Mater Sci.*, 24:833–839.
102. Zahavi J. (1981). Solid particle erosion of polymeric coatings. *Wear*; 71:191–210.
103. Dhar S, Krajac T, Ciampini D and Papini M, (2005). Erosion mechanisms due to impact of single angular particles, *Wear*, 258(1–4):567–579.
104. Tilly G.P, (1973). A two stage mechanisms of ductile erosion. *Wear*, 23:87–96.
105. Wiederhorn S.M and Hockey B.J, (1983). Effect of material parameters on the erosion resistance of brittle materials. *J Mater Sci.*, 18:766–780.
106. Scattergood R.O and Routbort J.L, (1981). Velocity and size dependence of the erosion rate in silicon. *Wear*, 67:227.
107. Thai C.M, Tsuda K and Hojo H, (1981). Erosion behaviour of polystyrene. *J Test Eval*, 9(6):359–365.
108. Karasek K.R, Goretta K.C, Helberg D.A and Rourbort J.L. (1992). Erosion in bismaleimide polymers and bismaleimide-polymer composites. *J Mater Sci Lett*; 11:1143–1144.
109. Rao P.V and Buckley D.H, (1985). Angular particle impingement studies of thermoplastic materials at normal incidence. *ASLE Trans*, 29(3):283–298.
110. Humphrey J.A.C, (1990). Fundamentals of fluid motion in erosion by solid particle impact. *Int J Heat Fluid Flow*, 11(3):170–195.
111. Rochester M.C and Brunton J.H, (1974). Influences of physical properties of the liquid on the erosion of solids. Erosion, wear and interfaces with corrosion ASTM STP 567. American Society of Testing and Materials, pp. 128–151.
112. True M.E and Weiner P.D. (1976). A laboratory evaluation of sand erosion of oil and gas well production equipment. Annual API production division meeting. Los Angeles, CA, pp. I-1, I-27.
113. Glaeser W.A and Dow A, (1977). Mechanisms of erosion in slurry pipelines. In: Proceedings of the second international conference on slurry transportation. Las Vegas, NV: March 2–4, pp. 136–140.
114. Roco M.C, Nair P, Addie G.R and Dennis J, (1984). Erosion of concentrated slurries in turbulent flow. *J Pipelines*, 4:213–21.
115. Venkatesh E.S, (1986). Erosion damage in oil and gas wells, SPE paper 15183. Rocky mountain regional meeting of the society of petroleum engineers. Billings, MT.

116. Shook C.A, Mckibben M and Small M, (1987). Experimental investigation of some hydrodynamics factors affecting slurry pipeline wall erosion. ASME paper no. 87-PVP-9.
117. Soderberg S, Hogmark S and Swahn H, (1982). Mechanisms of material removal during erosion of a stainless steel, Paper no. 82-AM-4A-1. 37th ASLE Annual Meeting, Cincinnati, May 10–13.
118. Hutchings I.M, (1983). Monograph on the erosion of materials by solid particle impact. Materials Technology Institute of Chemical Process Industries, Inc.; MTI publ. no. 10.
119. McLaury B.S, Wang J, Shirazi S.A, Shadley J.R and Rybicki E.F,(1997). Solid particle erosion in long radius elbows and straight pipes. Society of Petroleum Engineers, Paper no. SPE 38842, pp. 977–986.
120. Edwards J.K, McLaury B.S and Shirazi S.A. (2000). Evaluation of alternative pipe bends fittings in erosive service. Proceedings of 2000 ASME fluids engineering summer meeting, June 11–15, Boston, MA: Paper no. FEDSM2000-11245,
121. Blanchard D.J, Griffith P and Rabinowicz E, (1984). Erosion of a pipe bend by solid particle entrained in water. *J Eng Indust.*, 106:213–217.
122. Finnie I, (1995). Some reflections on the past and future of erosion, *Wear*, 186/187:1–10.
123. Rabinowicz E, (1979). The wear equation for erosion of metals by abrasive particles, Department of ME, MIT.
124. Finnie I, (1958). The mechanism of erosion of ductile metals. In: Proceedings of 3rd US national congress of applied mechanics. pp. 527–532.
125. Nestic S, (1991).Computation of localized erosion-corrosion in disturbed two-phase flow, PhD thesis, University of Saskatchewan, Saskatoon, Canada.
126. Bitter J.G.A, (1963). A study of erosion phenomena, Part I. *Wear*, 6:5–21.
127. Laitone J.A, (1979). Erosion prediction near a stagnation point resulting from aerodynamically entrained solid particles. *J Aircraft*, 16(12):809–814.
128. Salama M.M and Venkatesh E.S, (1983). Evaluation of erosion velocity limitations of offshore gas wells. 15th Annual OTC. Houston, TX: May 2–5, OTC no. 4485.
129. Bourgoyne A.T, (1989). Experimental study of erosion in diverter systems due to sand production, Presented at the SPE/IADC Drilling Conference, New Orleans, LA, SPE/IADC 18716, 807–816.
130. Chase D.P, Rybicki E.F and Shadley J.R, (1992). A model for the effect of velocity on erosion of N80 steel tubing due to the normal impingement of solid particles. *Trans ASME J Energy Resour Technol.*, 114:54–64.
131. McLaury B.S, (1993). A model to predict solid particle erosion in oil field geometries. MS thesis, The University of Tulsa,
132. Svedeman S.J and Arnold K.E, (1993). Criteria for sizing Multiphase flow lines for erosive/corrosive services. Paper presented at the 1993 SPE conference, Houston SPE 265:69.
133. Jordan K, (1998). Erosion in multiphase production of oil and gas. *Corrosion* 98, Paper no. 58, NACE International Annual Conference, San Antonio.
134. Gomes Ferreira C, Ciampini D and Papini M, (2004). The effect of inter-particle collisions in erosive streams on the distribution of energy flux incident to a flat surface. *Tribology International*, 37:791–807.
135. Hutchings I.M, (1981). A model for the erosion of metals by spherical particles at normal incidence, *Wear*, 70:269–281.

136. Brown R, Jun E and Edington J, (1982). Mechanisms of solid particle erosive wear for 90° impact on copper and iron, *Wear*, 74:143–156.
137. Schimizu K, Noguchi T and Matubara Y, (1999). FEM analysis of erosive wear, *Int. J. Cast Metals Res.* 11:515–520.
138. Esteban Fernandez J, Ma del Rocio Fernandez M, Vijande Diaz R and Tucho Navarro R, (2003). *Wear*, 255:38–43.
139. Spuzic S, Zec M, Abhary K, Ghomashchi R and Reid I, (1997). Fractional design of experiments applied to a wear simulation, *Wear*, 212(1):131-139.
140. Prasad B. K, (2002). Abrasive wear characteristics of a zinc-based alloy and zinc-alloy/ SiC composite, *Wear*, 252(3-4):250-263.
141. Taguchi G and Konishi S, (1987). *Taguchi Methods: Orthogonal Arrays and Linear Graphs; Tools for Quality Engineering*, American Supplier Institute Inc., Dearborn, MI.
142. Taguchi G, (1990). *Introduction to Quality Engineering*, Asian Productivity Organization, Tokyo.
143. Phadke M.S, (1989). *Quality Engineering using Robust Design*, Prentice-Hall, Englewood Cliffs, NJ.
144. Wu Y and Moore W.H, (1986). *Quality Engineering: Product & Process Design Optimization*, American Supplier Institute Inc., Dearborn, MI.
145. Shoemaker A.C and Kackar R.N, (1988). A methodology for planning experiments in robust product and process design, *Qual. Reliab. Eng. Int.* 4:95–103.
146. Phadke M.S and Dehnad K, (1988). Optimization of product and process design for quality and cost. *Qual. Reliab. Eng. Int.* 4:105–112.
147. Modeling and Prediction of Erosion Response of Glass Reinforced Polyester-Flyash Composites-- Amar Patnaik, Alok Satapathy, S.S. Mahapatra and R.R.Dash., “*Journal of Reinforced Plastics and Composites* Mar 2009; vol. 28: pp. 513 - 536
148. A Taguchi Approach for Investigation of Erosion of Glass Fiber–Polyester Composites-- Amar Patnaik, Alok Satapathy, S.S. Mahapatra and R.R.Dash., *Journal of Reinforced Plastics and Composites* 2008, doi: 10.1177/0731684407085728.
149. Parametric Optimization of Erosion Wear of Polyester-GF-Alumina Hybrid Composites using Taguchi Method -- Amar Patnaik, Alok Satapathy, S.S. Mahapatra and R.R.Dash., *Journal of Reinforced Plastics and Composites* Jul 2008; vol. 27: pp. 1039 - 1058.
150. Implementation of Taguchi Design for Erosion of Fiber Reinforced Polyester Composite Systems with SiC Filler --- Amar Patnaik, Alok Satapathy, S.S. Mahapatra and R.R.Dash. *Journal of Reinforced Plastics and Composites*, Jul 2008; vol. 27: pp. 1093 - 1111.
151. A Comparative Study on Different Ceramic Fillers affecting Mechanical Properties of Glass-Polyester Composites---Amar Patnaik, Alok Satapathy, S.S. Mahapatra and R.R.Dash., *Journal of Reinforced Plastics and Composites* Jun 2009; vol. 28: pp. 1305 - 1318.
152. Erosive Wear Assesment of Glass Reinforced Polyester-Flyash Composites using Taguchi Method --- Amar Patnaik, Alok Satapathy, S.S. Mahapatra and R.R.Dash, *International Polymer Processing-2008*, DOI 10.3139/217.2113.
153. Taguchi Method Applied to Parametric Appraisal of Erosion Behavior of GF-Reinforced Polyester Composites--- S.S. Mahapatra, Amar Patnaik, Alok Satapathy, and R.R.Dash. 2007 *Wear*, 265 (2008) 214–222.

- 154.** A Modeling Approach for Prediction of Erosion Behavior of Glass Fiber-Polyester Composites --- Amar Patnaik, Alok Satapathy, S.S. Mahapatra and R.R.Dash, 2007-- Journal of Polymer Research, DOI 10.1007/s10965-007-9154-2.
- 155.** Modified Erosion Wear Characteristics of Glass-Polyester Composites by Silicon Carbide Filling: A Parametric Study using Taguchi Technique--- Amar Patnaik, Alok Satapathy, S.S. Mahapatra and R.R.Dash. International Journal of Materials and Product Technology (IJMPT) (Special Issue on: "Materials Processing Technology)-2007.
- 156.** Tribo-Performance of Polyester Hybrid Composites: Damage Assessment and Parameter Optimization using Taguchi Design ---- Amar Patnaik, Alok Satapathy, S.S. Mahapatra and R.R.Dash.---- Materials and Design-2007.
- 157.** Singh, S.K., Mohanty, B.C. and Basu S. (2002). Synthesis of SiC from rice husk in a plasma reactor, Bull. Materials Sci. **25**(6): 561-563.
- 158.** Ruff A W, Ives L K. (1975) Measurement of solid particle velocity in erosive wear. Wear; 35 (1): 195-199.
- 159.** Harsha A.P, Tewari U.S and Venkatraman B, (2003). Solid particle erosion behaviour of various polyaryletherketone composites, Wear, 254:693-712.
- 160.** Mishra, P.K. (1997). Non-conventional machining. Narosa Publishing House, New Delhi.
- 161.** Sundararajan G, Roy M and Venkataraman B, (1990). Erosion efficiency-a new parameter to characterize the dominant erosion micromechanism, Wear, 140: 369.
- 162.** Hutchings I.M, Winter R.E and Field J.E, (1976). Solid particle erosion of metals: the removal of surface material by spherical projectiles, Proc Roy Soc Lond, Ser A 348:379-392

\*\*\*\*\*

# Appendices

## Papers Communicated to Journals:

- 1. Processing and Characterization of Jute-Epoxy Composites Reinforced with SiC Derived from Rice Husk** --- Alok Satapathy, **Alok Kumar Jha**, Sisir Mantry, S.K. Singh --- Communicated to *Journal of Reinforced Plastics and Composites* (Sage Publications) Appendix I
- 2. Wear Performance Analysis of Jute-Epoxy-SiC Hybrid Composites** -- **Alok Kumar Jha**, Sisir Mantry, Alok Satapathy and Amar Patnaik --- Communicated to *Journal of Composite Materials* (Sage Publications) Appendix II

## Processing and Characterization of Jute-Epoxy Composites Reinforced with Silicon Carbide Derived from Rice Husk

Journal:	<i>Journal of Reinforced Plastics and Composites</i>
Manuscript ID:	JRP-09-0175
Manuscript Type:	Original Article
Date Submitted by the Author:	01-May-2009
Complete List of Authors:	Satapathy, Alok; N.I.T. Rourkela, Mechanical Engg Jha, Alok; N.I.T. Rourkela, Mechanical Engg. Mantry, Sisir; IMMT, Bhubaneswar, Advanced Materials Division Singh, S K; IMMT, Bhubaneswar, Advanced Materials Division
Keyword:	jute-epoxy, polymer composites, processing
Abstract:	<p>ABSTRACT</p> <p>This paper depicts the processing and mechanical characterization of a new class of multi-phase composites consisting of epoxy resin reinforced with jute fiber and filled with silicon carbide (SiC) particulates. The SiC used as filler material in this work has been prepared from rice husk through plasma processing technique. The effect of filler in modifying the physical and mechanical properties of jute-epoxy composites has been studied. It is found that the incorporation of rice husk derived SiC modifies the tensile, flexural and inter-laminar shear strengths of the jute-epoxy composites. The micro-hardness and density of the composites are also greatly influenced by the content of these fillers. Rice husk is considered as an agricultural waste and it is thus interesting to explore the utilization potential of SiC derived from rice husk in composite making. Moreover, being cheap, inexhaustible and easily available, it would hopefully provide a cost effective solution to composite manufacturers.</p>



1  
2  
3  
4  
5  
6  
7  
8  
9  
10  
11  
12  
13  
14  
15  
16  
17  
18  
19  
20  
21  
22  
23  
24  
25  
26  
27  
28  
29  
30  
31  
32  
33  
34  
35  
36  
37  
38  
39  
40  
41  
42  
43  
44  
45  
46  
47  
48  
49  
50  
51  
52  
53  
54  
55  
56  
57  
58  
59  
60

## Processing and Characterization of Jute-Epoxy Composites Reinforced with SiC Derived from Rice Husk

Alok Satapathy, Alok Kumar Jha, Sisir Mantry, S.K. Singh

### ABSTRACT

This paper depicts the processing and mechanical characterization of a new class of multi-phase composites consisting of epoxy resin reinforced with jute fiber and filled with silicon carbide (SiC) particulates. The SiC used as filler material in this work has been prepared from rice husk through plasma processing technique. The effect of filler in modifying the physical and mechanical properties of jute-epoxy composites has been studied. It is found that the incorporation of rice husk derived SiC modifies the tensile, flexural and inter-laminar shear strengths of the jute-epoxy composites. The micro-hardness and density of the composites are also greatly influenced by the content of these fillers. Rice husk is considered as an agricultural waste and it is thus interesting to explore the utilization potential of SiC derived from rice husk in composite making. Moreover, being cheap, inexhaustible and easily available, it would hopefully provide a cost effective solution to composite manufacturers.

**KEYWORDS:** Silicon carbide; Rice husk; Jute-Epoxy; Mechanical characterization;

## INTRODUCTION

Fiber reinforced polymer composites are now considered as an important class of engineering materials. They offer outstanding mechanical properties, unique flexibility in design capability and ease of fabrication. Additional advantages include light weight, corrosion and impact resistance and excellent fatigue strength. Today, fiber composites are routinely used in such diverse applications as automobiles, aircraft, space vehicles, off-shore structures, containers and piping, sporting goods, electronics and appliances. A fiber reinforced composite is not simply a mass of fibers dispersed within a polymer. It consists of fibers embedded in or bonded to a polymer matrix with distinct interfaces between the two constituent phases. The fibers are usually of high strength and modulus and serve as the principal load carrying members. The matrix acts as the load transfer medium between fibers and in less ideal cases where loads are complex, the matrix may even have to partly bear loads. The matrix also serves to protect the fibers from environmental damage before, during and after composite processing. In a composite, both fibers and matrix largely retain their identities and yet result in many properties that cannot be achieved with either of the constituents acting alone. A wide variety of fibers are available for use in composites. The most commonly used fibers are various types of carbon, glass and aramid fibers. Besides, natural fibers such as: jute, sisal and ceramic fibers like alumina, silicon carbide, mullite and silicon nitride are also used in composite making. The unique combinations of properties available in these fibers provide the outstanding functional and structural characteristics such as: high specific strength and specific stiffness to the fiber reinforced composites.

A key feature of fiber composites that makes them so promising as engineering materials is the opportunity to tailor the materials properties through the control of fiber and matrix combinations and the selection of processing techniques. In principle, an infinite range of

1  
2  
3 composite types exists, from randomly oriented chopped fiber based materials at the low  
4 property end to continuous, unidirectional fiber composites at the high performance end.  
5  
6  
7  
8 A judicious selection of matrix and the reinforcing phase can lead to a composite with a  
9  
10 combination of strength and modulus comparable to or even better than those of  
11  
12 conventional metallic materials [1]. The physical and mechanical characteristics can  
13  
14 further be modified by adding a solid filler phase to the matrix body during the  
15  
16 composite preparation. It has been observed that by incorporating filler particles into  
17  
18 fiber reinforced composites, synergistic effects may be achieved in the form of higher  
19  
20 modulus and reduced material cost, yet accompanied with decreased strength and impact  
21  
22 toughness [2, 3]. Garcia et al. [4, 5] suggested this kind of multi-phase composite  
23  
24 technique for improving the matrix dominated properties of continuous fiber reinforced  
25  
26 composites. In this technique a supplementary reinforcement such as particulates,  
27  
28 whiskers, or micro fibers is added to the matrix prior to resin impregnation. Jang et al.  
29  
30 [6,7] found a significant improvement in impact energy of hybrid composites  
31  
32 incorporating either particulates or ceramic whiskers. Hard particulate fillers consisting  
33  
34 of ceramic or metal particles and fiber fillers made of glass are being used these days to  
35  
36 dramatically improve the wear resistance of composites, even up to three orders of  
37  
38 magnitude [8].  
39  
40  
41  
42  
43  
44  
45  
46

47 The improved performance of polymers and their composites in industrial and structural  
48 applications by the addition of filler materials has shown a great promise and so has  
49 lately been a subject of considerable interest. Various kinds of polymers and polymer  
50 matrix composites reinforced with metal particles have a wide range of industrial  
51 applications such as heaters, electrodes [9], composites with thermal durability at high  
52 temperature [10] etc. These engineering composites are desired due to their low density,  
53 high corrosion resistance, ease of fabrication, and low cost [11, 12, 13]. Similarly,  
54  
55  
56  
57  
58  
59  
60

1  
2  
3 ceramic filled polymer composites have been the subject of extensive research in last two  
4  
5 decades. The inclusion of inorganic fillers into polymers for commercial applications is  
6  
7 primarily aimed at the cost reduction and stiffness improvement [14,15]. Along with  
8  
9 fiber-reinforced composites, the composites made with particulate fillers have been  
10  
11 found to perform well in many real operational conditions.  
12  
13

14  
15  
16 However, such multi-component hybrid composites form complex systems and there is  
17  
18 inadequate data available about phenomena behind the properties changes due to the  
19  
20 addition of particulate fillers to the fiber reinforced thermoplastic components. Hence the  
21  
22 objective of this paper is to know how the incorporation of silicon carbide (derived from  
23  
24 rice husk) particulates affects the mechanical properties of jute fiber reinforced epoxy  
25  
26 composites. Silicon carbide (SiC) is a ceramic material that has the potential to be used  
27  
28 as filler in various polymer matrices. It is an excellent abrasive used in grinding wheels  
29  
30 and other abrasive products for over one hundred years. Today the material has been  
31  
32 developed into a high quality technical grade ceramic with very good mechanical  
33  
34 properties. It is used in abrasives, refractories, ceramics, and numerous high-performance  
35  
36 applications. The high thermal conductivity coupled with low thermal expansion and  
37  
38 high strength gives this material exceptional thermal shock resistant qualities. Moreover,  
39  
40 silicon carbide has low density, low thermal expansion, high elastic modulus, high  
41  
42 strength, high hardness, and superior chemical inertness. Although the effect of SiC  
43  
44 (produced from mineral sources) as a filler material has been investigated earlier [16] in  
45  
46 glass-polyester composites, there is no report available on the potential of SiC particles  
47  
48 derived from a bio-resource like rice husk in jute fiber reinforced polymer composites. In  
49  
50 this investigation, SiC produced from rice husk by plasma processing route has been  
51  
52 used. The details of formation of SiC from rice husk by this route are described  
53  
54 elsewhere [17].  
55  
56  
57  
58  
59  
60

## EXPERIMENTAL DETAILS

### Matrix Material

Epoxy LY 556 is the resin which is used as the matrix material. Its common name is Bisphenol-A-Diglycidyl-Ether and it chemically belongs to the 'epoxide' family. The epoxy resin and the hardener are supplied by Ciba Geigy India Ltd.

### Fiber Material

Jute is a long, soft, shiny vegetable fiber that can be spun into coarse, strong threads. It is produced from plants in the genus *Corchorus*, family Tiliaceae. Jute is one of the cheapest natural fibres and is second only to cotton in amount produced and variety of uses. Jute fibres are composed primarily of the plant materials cellulose (major component of plant fibre) and lignin (major components wood fibre). It is thus a ligno-cellulosic fibre that is partially a textile fibre and partially wood. It falls into the bast fibre category (fibre collected from bast or skin of the plant) along with kenaf, industrial hemp, flax (linen), ramie, etc. Cross plied woven mats of this jute-fiber have been used as the reinforcing phase in the composites used in this work.

### Composite fabrication

Cross plied jute fibers are reinforced in epoxy resin in three different weight proportions (20 wt%, 30 wt% and 40 wt%) to prepare the composites A<sub>1</sub>, B<sub>1</sub> and C<sub>1</sub> respectively. Jute fibers and epoxy resin have modulus of about 55 GPa and 3.42 GPa respectively and possess density of 1300 kg/m<sup>3</sup> and 1100 kg/m<sup>3</sup> respectively. No particulate filler is used in these composites.

The other composite samples C<sub>2</sub> and C<sub>3</sub> with silicon carbide fillers of fixed weight percentage are fabricated by the same technique. The low temperature curing epoxy resin and corresponding hardener (HY951) are mixed in a ratio of 10:1 by weight as

1  
2  
3 recommended. The mix is stirred manually to disperse the particulate fillers in the  
4 matrix. The mixing is done thoroughly before the jute-fiber mats (40 wt%) are reinforced  
5 in the matrix body. Composites C<sub>2</sub> and C<sub>3</sub> contain SiC particles in 10 wt% and 20 wt%  
6 proportions respectively. Each ply of jute-fiber is of dimension 200 mm× 200 mm. The  
7 composite slabs are made by conventional hand-lay-up technique followed by light  
8 compression moulding technique. A stainless steel mould having dimensions of 210 ×  
9 210 × 40 mm<sup>3</sup> is used. A releasing agent (Silicon spray) is used to facilitate easy removal  
10 of the composite from the mould after curing. Care is taken to ensure a uniform sample  
11 since particles have a tendency to clump and tangle together when mixed. The cast of  
12 each composite is cured under a load of about 25kg for 24 h before it removed from the  
13 mould. Then this cast is post cured in the air for another 24 h after removing out of the  
14 mould. Specimens of suitable dimension are cut using a diamond cutter for physical  
15 characterization and mechanical testing. Utmost care has been taken to maintain  
16 uniformity and homogeneity of the composite. The designation and detailed composition  
17 of the composites are given in Table 1.

## MECHANICAL CHARACTERIZATION

### Density and Void Fraction

42  
43 The theoretical density of composite materials in terms of weight fraction can easily be  
44 obtained as for the following equations given by Agarwal and Broutman [18].  
45  
46  
47

$$\rho_{ct} = \frac{1}{(W_f / \rho_f) + (W_m / \rho_m)} \quad (1)$$

48  
49  
50  
51  
52  
53  
54 Where,  $W$  and  $\rho$  represent the weight fraction and density respectively. The suffix  $f$ ,  $m$   
55 and  $ct$  stand for the fiber, matrix and the composite materials respectively.  
56  
57  
58  
59  
60

The composites under this investigation consists of three components namely matrix, fiber and particulate filler. Hence the modified form of the expression for the density of the composite can be written as

$$\rho_{ct} = \frac{1}{(W_f / \rho_f) + (W_m / \rho_m) + (W_p / \rho_p)} \quad (2)$$

Where, the suffix 'p' indicates the particulate filler materials.

The actual density ( $\rho_{ce}$ ) of the composite, however, can be determined experimentally by simple water immersion technique. The volume fraction of voids ( $V_v$ ) in the composites is calculated using the following equation:

$$V_v = \frac{\rho_{ct} - \rho_{ce}}{\rho_{ct}} \quad (3)$$

The theoretical and measured densities of the composites along with the corresponding volume fraction of voids are presented in Table 2. It may be noted that the composite density values calculated theoretically from weight fractions using Eq.(2) are not equal to the experimentally measured values. This difference is a measure of voids and pores present in the composites. It is clearly seen that with the increase in fiber content from 20 wt% to 40 wt%, there is an increase in the void fraction. However, in all the three composites A<sub>1</sub>, B<sub>1</sub> and C<sub>1</sub>, the volume fractions of voids are reasonably small (< 1.5%) and this can be attributed to the absence of particulate fillers in these composites. With the addition of silicon carbide as the filler material, more voids are found in the composites. As the filler content increases from 0 wt% to 10 wt% and subsequently from 10 wt% to 20 wt% the volume fraction of voids is found to be increasing. This trend is observed in both the particulate filled composites (C<sub>2</sub> and C<sub>3</sub>).

Density of a composite depends on the relative proportion of matrix and reinforcing materials and this is one of the most important factors determining the properties of the

1  
2  
3 composites. The void content is the cause for the difference between the values of true  
4 density and the theoretically calculated one. The voids significantly affect some of the  
5 mechanical properties and even the performance of composites in the workplace. Higher  
6 void contents usually mean lower fatigue resistance, greater susceptibility to water  
7 penetration and weathering [18]. The knowledge of void content is desirable for  
8 estimation of the quality of the composites. It is understandable that a good composite  
9 should have fewer voids. However, presence of void is unavoidable in composite making  
10 particularly through hand-lay-up route.  
11  
12  
13  
14  
15  
16  
17  
18  
19  
20  
21

### 22 23 **Micro-hardness**

24  
25 Micro-hardness measurement is done using a Leitz micro-hardness tester. A diamond  
26 indenter, in the form of a right pyramid with a square base and an angle  $136^{\circ}$  between  
27 opposite faces, is forced into the material under a load of 24.54N. The variation of  
28 composite micro-hardness with the weight fraction of jute fiber and SiC particulates is  
29 shown in Figure (1). For the composite A<sub>1</sub> (20 wt% of JF), the micro-hardness value is  
30 recorded as 57 Hv while for C<sub>1</sub> (40 wt% of GF) this value is 63 Hv. It is thus seen that  
31 with the increase in fiber content in the composite, the hardness improves although the  
32 increment is marginal. Similarly, with the incorporation of filler particulates into the  
33 composites, the mean hardness is seen to have improved.  
34  
35  
36  
37  
38  
39  
40  
41  
42  
43  
44  
45  
46  
47

### 48 **Tensile, Flexural and Inter-laminar shear strength**

49  
50 The tensile test is generally performed on flat specimens. The commonly used specimens  
51 for tensile test are the dog-bone type and the straight side type with end tabs. During the  
52 test a uniaxial load is applied through both the ends of the specimen. The ASTM  
53 standard test method for tensile properties of fiber resin composites has the designation  
54 D 3039-76. The length of the test section should be 200 mm. The tensile test is  
55  
56  
57  
58  
59  
60



1  
2  
3 performed in the universal testing machine (UTM) Instron 1195 and results are analyzed  
4  
5 to calculate the tensile strength of composite samples.  
6  
7

8  
9 The short beam shear (SBS) tests are performed on the composite samples at room  
10 temperature to evaluate the value of inter-laminar shear strength (ILSS). It is a 3-point  
11 bend test, which generally promotes failure by inter-laminar shear. The SBS test is  
12 conducted as per ASTM standard (D2344-84) using the same UTM. Span length of 40  
13 mm and the cross head speed of 10 mm/min are maintained. The ILSS values are  
14 calculated as follows,  
15  
16  
17  
18  
19  
20  
21

$$22 \quad ILSS = \frac{3P}{4bt} \quad (4)$$

23  
24  
25  
26  
27 Where,  $P$  is maximum load,

28  
29  $b$  the width of specimen, and

30  
31  
32  $t$  the thickness of specimen  
33

34  
35 The data recorded during the 3-point bend test is used to evaluate the flexural strength  
36 also. The flexural strength (F.S.) of any composite specimen is determined using the  
37 following equation.  
38  
39  
40

$$41 \quad F.S = \frac{3PL}{2bt^2} \quad (5)$$

42  
43  
44  
45  
46 Where,  $L$  is the span length of the sample.  
47

48  
49  
50 It is well known that the strength properties of composites are mainly determined by the  
51 fiber content and the fiber strength. So variation in composite strength with different  
52 fiber loading is obvious. These variations in tensile and flexural strengths of the  
53 composites  $A_1$ ,  $B_1$  and  $C_1$  are presented in Table 2 and are shown in Figure (2). A  
54 gradual increase in both tensile strength as well as flexural strength with the fiber weight  
55 fraction is noticed. It clearly indicates that inclusion of jute fiber improves the load  
56  
57  
58  
59  
60

1  
2  
3 bearing capacity and the ability to withstand bending of the composites. Similar  
4 observations have been reported by Harsha et al. [19] for fiber reinforced thermoplastics  
5 such as poly-aryl-ether-ketone composites. It may be mentioned here that both tensile  
6 and flexural strengths are important for recommending any composite as a candidate for  
7 structural applications.  
8  
9

10  
11  
12  
13  
14  
15  
16 The test results for tensile and flexural strengths for the particulate filled composites C<sub>1</sub>,  
17 C<sub>2</sub> and C<sub>3</sub> are shown in Figure (3). It is seen that the tensile strength of the composite  
18 decreases with increase in the filler content. The unfilled jute epoxy composite has a  
19 strength of 349.6 MPa in tension and it may be seen from Table 4.2 that this value drops  
20 to 304.5 MPa and 279.4 MPa with addition of 10 wt% and 20 wt% of silicon carbide  
21 respectively. Similar trend is observed in case of flexural strength of these composites.  
22  
23  
24  
25  
26  
27  
28  
29  
30

31  
32 By incorporating these particulate fillers into the jute-fiber reinforced epoxy, synergistic  
33 effects, as expected were achieved in the form of modified mechanical properties and  
34 improved erosion wear resistance. Inclusion of jute fiber in neat epoxy improved the load  
35 bearing capacity (tensile strength) and the ability to withstand bending (flexural strength)  
36 of the composites. But with the incorporation of silicon carbide fillers, the tensile  
37 strengths of the composites were found to be less. There can be two reasons for this  
38 decline in tensile strength of these particulate filled composites compared to the unfilled  
39 one. One possibility is that the chemical reaction at the interface between the filler  
40 particles and the matrix may be too weak to transfer the tensile stress; the other is that the  
41 corner points of the irregular shaped particulates result in stress concentration in the  
42 epoxy matrix.  
43  
44  
45  
46  
47  
48  
49  
50  
51  
52  
53  
54  
55  
56

57  
58 Hardness values have been found to have improved for the particulate filled composites.

59  
60 The reduction in tensile strength and the improvement in hardness with the incorporation

1  
2  
3 of fillers can be explained as follows: under the action of a tensile force the filler-matrix  
4 interface is vulnerable to debonding depending on interfacial bond strength and this may  
5  
6 interface is vulnerable to debonding depending on interfacial bond strength and this may  
7  
8 lead to a break in the composite. But in case of hardness test, a compression or pressing  
9 stress is in action. So the polymeric matrix phase and the solid filler phase would be  
10 pressed together and touch each other more tightly. Thus, the interface can transfer  
11 pressure more effectively although the interfacial bond may be poor. This might have  
12 resulted in an enhancement of hardness.  
13  
14  
15  
16  
17  
18

19  
20 The stresses acting on the interface of the two adjacent laminae in a layered composite  
21 are called inter-laminar stresses. These stresses cause relative deformations between the  
22 consecutive laminae and if these are sufficiently high they may cause failure along the  
23 mid-plane between two adjacent laminae. It is therefore of considerable interest to  
24 evaluate inter-laminar shear strength through tests in which failure of the laminates of the  
25 composite initiates in a shear (delamination) mode. In the present work the ILSS values  
26 are measured for unfilled jute-epoxy composites  $A_1$ ,  $B_1$  and  $C_1$  and no improvement is  
27 recorded in the ILSS of the composites with increase in the fiber content in them.  
28  
29  
30  
31  
32  
33  
34  
35  
36  
37  
38  
39

40 The inter-laminar shear strength values of the particulate filled composites are shown  
41 along with that of the unfilled jute epoxy composite ( $C_1$ ) in the same Figure (4). It is seen  
42 that there is improvement of ILSS of jute-epoxy composites with particulate filling.  
43 Incorporation of silicon carbide is seen to have caused the substantial increase in the  
44 inter-laminar shear strength. In the present investigation, during flexural test, the span  
45 length is very short (40 mm). A large span to depth ratio in bending test increases the  
46 maximum normal stress without affecting the inter-laminar shear stress and thereby  
47 increases the tendency for longitudinal failure. If the span is short enough, failure  
48 initiates and propagates by inter-laminar shear failure. The maximum shear stress in a  
49  
50  
51  
52  
53  
54  
55  
56  
57  
58  
59  
60

1  
2  
3 beam occurs at the mid plane. So in the shear test, failure consists of a crack running  
4  
5 along the mid plane of the beam so that crack plane is parallel to the longitudinal plane.  
6  
7

### 8 9 **Surface morphology of composite samples**

10  
11 The surfaces of the specimens are examined directly by scanning electron microscope  
12  
13 JEOL JSM-6480LV. The composite samples are mounted on stubs with silver paste. To  
14  
15 enhance the conductivity of the samples, a thin film of platinum is vacuum-evaporated  
16  
17 onto them before the photomicrographs are taken. The surface micro-structures of some  
18  
19 of the composite samples are observed under scanning electron microscope basically to  
20  
21 get an insight to the features. As seen in Figures (5a) and (5b), the surfaces are  
22  
23 reasonably homogeneous. No cracks are seen although some voids and pores are visible  
24  
25 even at this lower magnification. SiC particles are not seen in clusters within the matrix  
26  
27 body.  
28  
29  
30  
31  
32

### 33 **CONCLUSIONS**

34  
35 Successful fabrication of jute-epoxy composites with reinforcement of SiC derived from  
36  
37 rice husk is possible. Incorporation of these fillers modifies the tensile, flexural and inter-  
38  
39 laminar shear strengths of the jute epoxy composites. The micro-hardness and density of  
40  
41 the composites are also greatly influenced by the content of fillers. Hence, while  
42  
43 fabricating a composite of specific requirements, there is a need for the choice of  
44  
45 appropriate filler material and for optimizing its content in the composite system.  
46  
47  
48

### 49 **REFERENCES**

- 50  
51  
52 1. Jang, B. Z. (1994). Advanced Polymer composites: principles and applications.  
53  
54 ASM International.  
55  
56 2. Pukanszky, B. (1995). Particulate filled polypropylene: structure and properties.  
57  
58 In: Karger-Kocsis J, editor. Polypropylene: Structure, blends and composites.  
59  
60 London: Chapman & Hall; 1-70.

- 1  
2  
3 3. Acosta, J.L, Morales E, Ojeda, M.C, Linares A. (1986).Effect of addition of  
4  
5 sepiolite on the mechanical properties of glass fiber reinforced polypropylene.  
6  
7  
8 Angew Makromol Chem. **138**:103-10.  
9
- 10 4. Gracia, R, Evans, R.E. and Palmer, R.J. (1987). Toughened composites, STP 937,  
11  
12 N.J.Johnson, Ed., ASTM. 397-412.  
13
- 14 5. Gracia, R. (1983). Nadc-83058-60, July.  
15
- 16 6. Lin, T.L and Jang, B.Z. (1989). Ann. Tech. Conf. (ANTEC) (New York),May.  
17
- 18 7. Liau, J.Y, Jang, B.Z, Hwang, L.R.and Wilcox, R.C. (1988). Plast. Eng., Nov.  
19
- 20 8. Gregory, S. W, Freudenberg K. D, Bhimaraj, P and Schadler, L.S. (2003). A  
21  
22 study on the friction and wear behavior of PTFE filled with alumina  
23  
24 nanoparticles, Wear. **254**: 573–580.  
25  
26
- 27 9. Jung-il, K., Kang, P.H and Nho, Y.C. (2004). Positive temperature coefficient  
28  
29 behavior of polymer composites having a high melting temperature, J Appl. Poly  
30  
31 Sci., **92**:394–401.  
32  
33
- 34 10. Nikkeshi, S, Kudo, M and Masuko, T. (1998). Dynamic viscoelastic properties  
35  
36 and thermal properties of powder-epoxy resin composites, J Appl Poly Sci.,  
37  
38 **69**:2593-8.  
39  
40
- 41 11. Zhu, K and Schmauder, S. (2003). Prediction of the failure properties of short  
42  
43 fiber reinforced composites with metal and polymer matrix, Comput Mater. Sci.  
44  
45 **28**:743–8.  
46  
47
- 48 12. Rusu, M., Sofian, N and Rusu, D.(2001). Mechanical and thermal properties of  
49  
50 zinc powder filled high density polyethylene composites', Polym Test, **20**: 409–  
51  
52 17.  
53  
54
- 55 13. Tavman, I H. (1997). Thermal and mechanical properties of copper powder filled  
56  
57 poly (ethylene) composites, Powder Technol, **91**: 63–7.  
58  
59  
60

14. Rotheron, R.N. (1997). Adhesion, **64**: 87.
15. Rotheron R.N. (1999). Adv. Polym. Sci., **139**: 67.
16. Patnaik, A., Satapathy, A., Mahapatra, S. and Dash, R.(2008). A Comparative Study on Different Ceramic Fillers affecting Mechanical Properties of Glass-Polyester Composites Journal of Reinforced Plastics and Composites
17. Singh, S.K., Mohanty, B.C. and Basu S.(2002). Synthesis of SiC from rice husk in a plasma reactor, Bull. Materials Sci. **25**(6): 561-563.
18. Agarwal, B.D, Broutman, L.J. (1990). Analysis and performance of fiber composites: Second Edition. John Wiley and Sons, Inc.
19. Suresh. A., and Harsha, A. P., 2006, "Study of erosion efficiency of polymers and polymer composites," Polymer testing, **25** (2), pp. 188-196.

**List of Figures**

**Figure 1** Micro-hardness values of composites with different fiber and filler content

**Figure 2** Effect of fiber loading on tensile & flexural strength of JF-epoxy composites

**Figure 3** Effect of filler content on tensile & flexural strength of JF-epoxy composites

**Figure 4** Comparison of Inter-laminar shear strength of different composites

**Figure 5** Surface morphology of composite samples

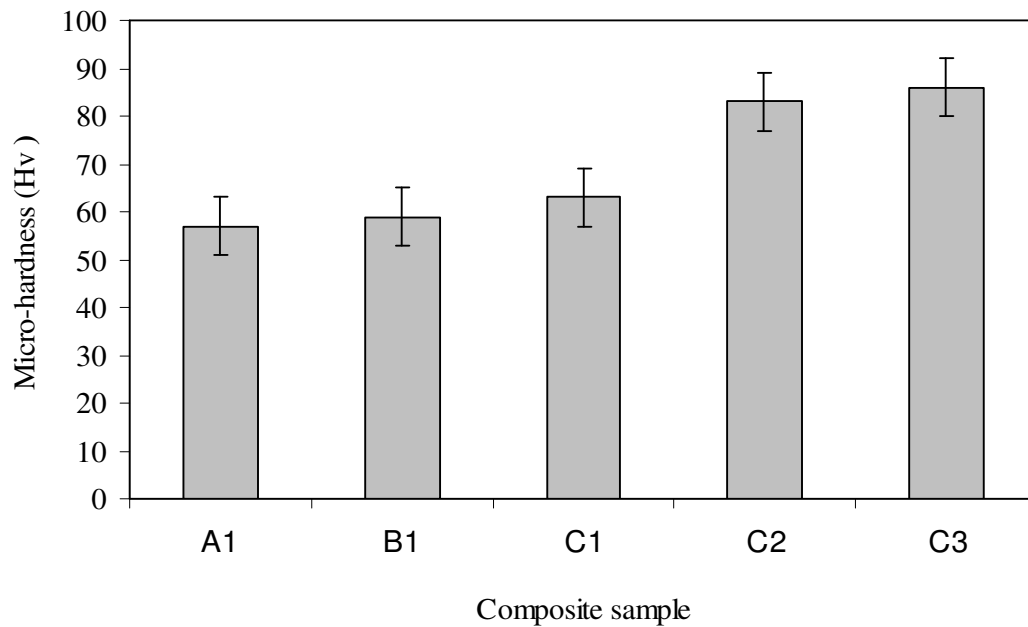


**Figure 1** Micro-hardness values of composites with different fiber and filler content

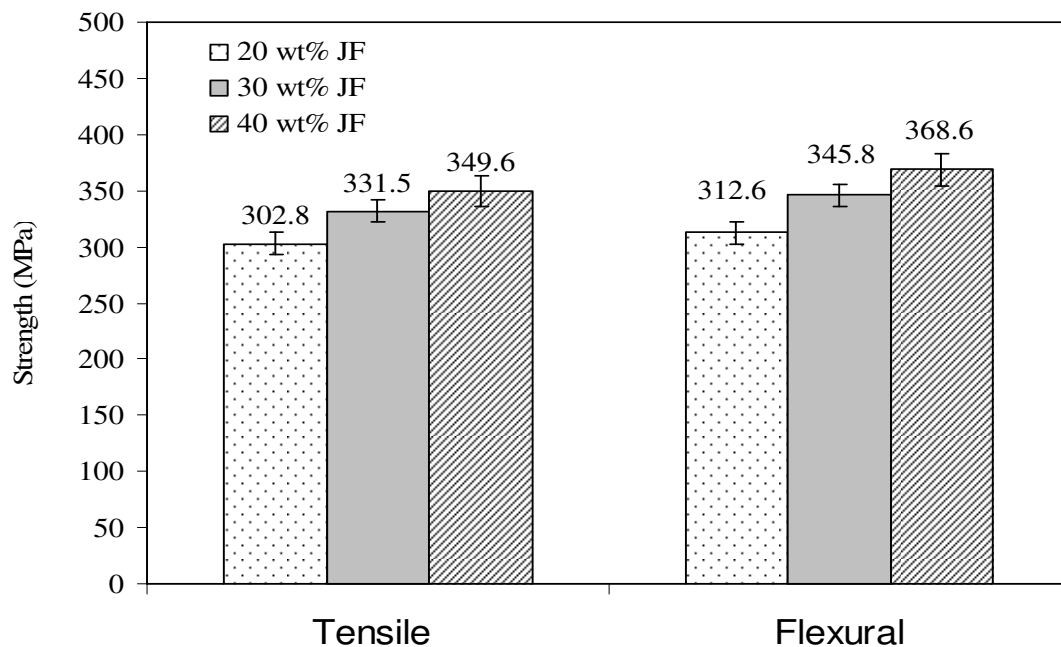


**Figure 2** Effect of fiber loading on tensile & flexural strength of JF-epoxy composites

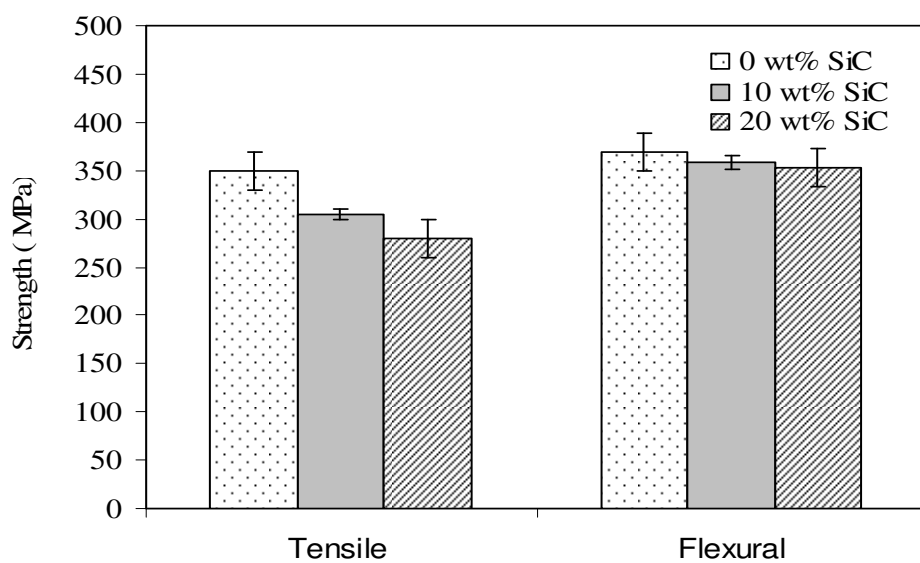


**Figure 3** Effect of filler content on tensile & flexural strength of JF-epoxy composites



1  
2  
3  
4  
5  
6  
7  
8  
9  
10  
11  
12  
13  
14  
15  
16  
17  
18  
19  
20  
21  
22  
23  
24  
25  
26  
27  
28  
29  
30  
31  
32  
33  
34  
35  
36  
37  
38  
39  
40  
41  
42  
43  
44  
45  
46  
47  
48  
49  
50  
51  
52  
53  
54  
55  
56  
57  
58  
59  
60

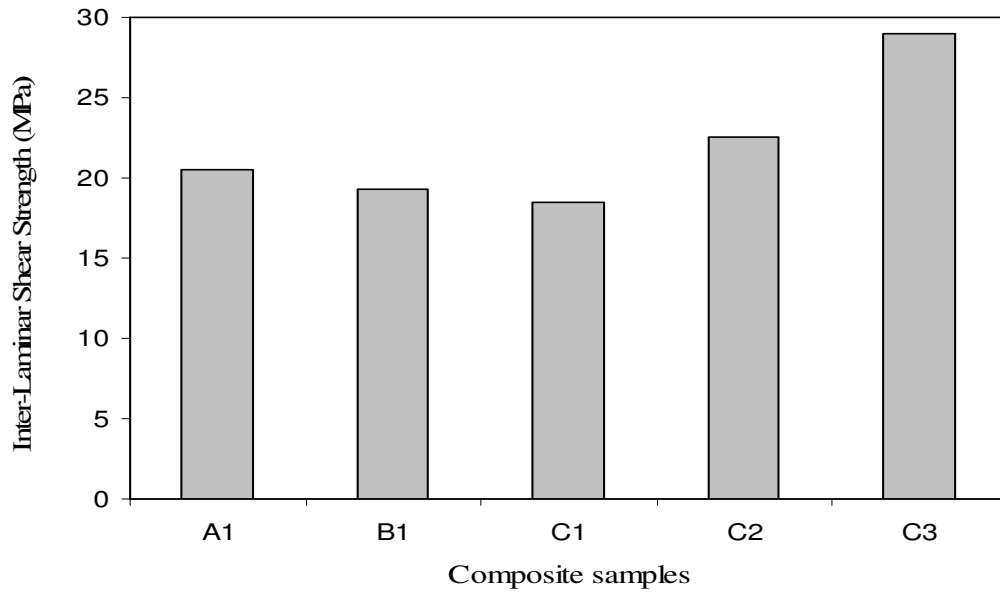


**Figure 4** Comparison of Inter-laminar shear strength of different composites

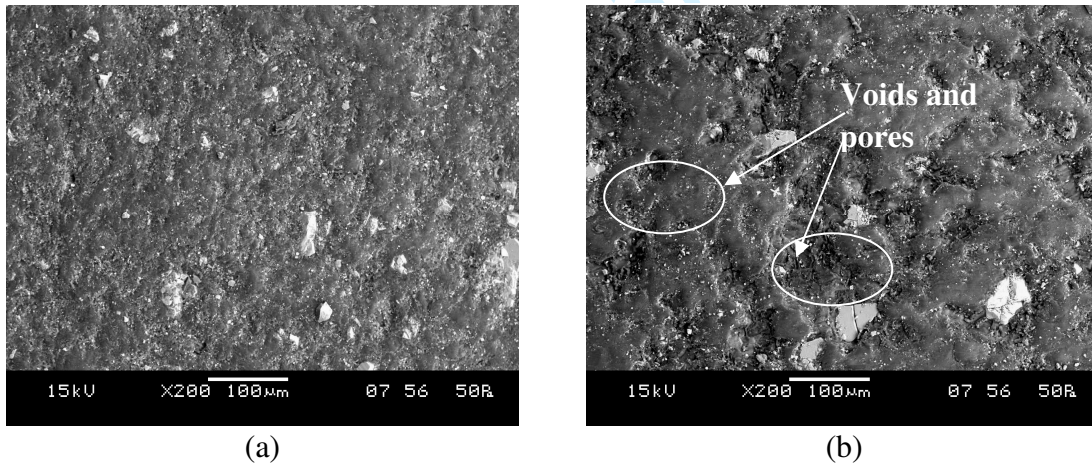


**Figure 5** Surface morphology of composite samples

1  
2  
3  
4  
5  
6  
7  
8  
9  
10  
11  
12  
13  
14  
15  
16  
17  
18  
19  
20  
21  
22  
23  
24  
25  
26  
27  
28  
29  
30  
31  
32  
33  
34  
35  
36  
37  
38  
39  
40  
41  
42  
43  
44  
45  
46  
47  
48  
49  
50  
51  
52  
53  
54  
55  
56  
57  
58  
59  
60

## List of Tables

**Table 1** Designation and detailed composition of the composites

**Table 2** Measured and Theoretical densities of the composites

**Table 3** Mechanical properties of the composites

Designation	Composition
A <sub>1</sub>	Epoxy + 20 wt% jute fiber
B <sub>1</sub>	Epoxy + 30 wt% jute fiber
C <sub>1</sub>	Epoxy + 40 wt% jute fiber
C <sub>2</sub>	Epoxy + 40 wt% jute fiber + 10wt% SiC
C <sub>3</sub>	Epoxy + 40 wt% jute fiber + 20wt% SiC

**Table 1** Designation and detailed composition of the composites

Composites	Measured density (gm/cc)	Theoretical density (gm/cc)	Volume fraction of voids (%)
A <sub>1</sub>	1.127	1.135	0.71
B <sub>1</sub>	1.139	1.153	1.35
C <sub>1</sub>	1.157	1.172	1.28
C <sub>2</sub>	1.199	1.258	4.68
C <sub>3</sub>	1.287	1.358	5.22

**Table 2** Measured and Theoretical densities of the composites

1  
2  
3  
4  
5  
6  
7  
8  
9  
10  
11  
12  
13  
14  
15  
16  
17  
18  
19  
20  
21  
22  
23  
24  
25  
26  
27  
28  
29  
30  
31  
32  
33  
34  
35  
36  
37  
38  
39  
40  
41  
42  
43  
44  
45  
46  
47  
48  
49  
50  
51  
52  
53  
54  
55  
56  
57  
58  
59  
60

Composites	Mean Hardness (Hv)	Tensile strength (MPa)	Flexural strength (MPa)	ILSS (MPa)
A <sub>1</sub>	57	302.8	312.6	20.52
B <sub>1</sub>	59	331.5	345.8	19.32
C <sub>1</sub>	63	349.6	368.6	18.42
C <sub>2</sub>	83	304.5	357.8	22.57
C <sub>3</sub>	86	279.4	353.2	28.99

**Table 3** Mechanical properties of the composites

## Wear Performance Analysis of Jute-Epoxy-SiC hybrid composites

Journal:	<i>Journal of Composite Materials</i>
Manuscript ID:	draft
Manuscript Type:	Original Manuscript
Date Submitted by the Author:	
Complete List of Authors:	Jha, Alok; N.I.T. Rourkela, Mechanical Engg Mantry, Sisir; Institute of Minerals and Materials Technology, Bhubaneswar, Advanced Materials Division Satapathy, Alok; N.I.T. Rourkela, Mechanical Engg. Patnaik, Amar; N.I.T. Hamirpur, Mechanical Engg
Keywords:	Jute-fiber, Epoxy, SiC filler, Hybrid composites, Theoretical model, Erosion wear
Abstract:	Fiber reinforced polymer composites are now considered as an important class of engineering materials. With the increased use of these materials in erosive work environments, it has become extremely important to investigate their erosion characteristics intensively. In view of this, the present article reports the solid particle erosion response of a new class of multi-component composite system consisting of epoxy resin reinforced with jute-fiber and SiC particles derived from a bio-resource like rice husk. Erosion trials are carried out at various test conditions. For this, an air jet type erosion test rig and Taguchi's orthogonal arrays are used. Significant control factors influencing the erosion wear rate are identified. This paper also presents the development of a theoretical model for estimating erosion damage caused by solid particle impact on the composites. The model is based upon conservation of particle kinetic energy and relates the erosion rate with some of the material properties and test conditions. The theoretical results are compared and are found to be in good agreement with the experimental values.

## Wear Performance Analysis of Jute-Epoxy-SiC Hybrid Composites

**Alok Kumar Jha, Sisir Mantry, Alok Satapathy and Amar Patnaik**

### ABSTRACT

Fiber reinforced polymer composites are now considered as an important class of engineering materials. With the increased use of these materials in erosive work environments, it has become extremely important to investigate their erosion characteristics intensively. In view of this, the present article reports the solid particle erosion response of a new class of multi-component composite system consisting of epoxy resin reinforced with jute-fiber and SiC particles derived from a bio-resource like rice husk. Erosion trials are carried out at various test conditions. For this, an air jet type erosion test rig and Taguchi's orthogonal arrays are used. Significant control factors influencing the erosion wear rate are identified. This paper also presents the development of a theoretical model for estimating erosion damage caused by solid particle impact on the composites. The model is based upon conservation of particle kinetic energy and relates the erosion rate with some of the material properties and test conditions. The theoretical results are compared and are found to be in good agreement with the experimental values.

**Keywords:** Jute-fiber; Epoxy; SiC filler; Composites; Erosion wear; Theoretical model;

## INTRODUCTION

Fiber-reinforced polymer (FRP) composites have many applications in automobile, marine and aerospace industries. They offer outstanding mechanical properties, unique flexibility in design capability and ease of fabrication. Additional advantages include light weight, corrosion and impact resistance and excellent fatigue strength. A fiber reinforced composite is not simply a mass of fibers dispersed within a polymer. It consists of fibers embedded in or bonded to a polymer matrix with distinct interfaces between the two constituent phases. The fibers are usually of high strength and modulus and serve as the principal load carrying members. The matrix acts as the load transfer medium between fibers and in less ideal cases where loads are complex, the matrix may even have to partly bear loads. The matrix also serves to protect the fibers from environmental damage before, during and after composite processing. In a composite, both fibers and matrix largely retain their identities and yet result in many properties that cannot be achieved with either of the constituents acting alone. A wide variety of fibers are available for use in composites. The most commonly used fibers are various types of carbon, glass and aramid fibers. Besides, natural fibers such as: jute, sisal and ceramic fibers like alumina, silicon carbide, mullite and silicon nitride are also used in composite making. The unique combinations of properties available in these fibers provide the outstanding functional and structural characteristics such as: high specific strength and specific stiffness to the fiber reinforced composites.

Fiber reinforced polymer composites are now considered as an important class of engineering materials. Due to operational requirements in dusty environments, the erosion characteristics of these composites are of vital importance. Since erosive wear of engineering components caused by abrasive particles is a major industrial problem, a full understanding of the effects of all system variables on the wear rate is necessary in order

1  
2  
3 to undertake appropriate steps in the design of machine or structural components, and to  
4  
5 choose the materials to reduce/control this wear mode. In recent years much research has  
6  
7 been devoted to exploring the potential advantages of thermoplastic polymers for  
8  
9 composite materials. Some of the commonly used thermoplastics are polyetheretherketone  
10  
11 (PEEK), polyetherketone (PEK), polyetherketoneketone (PEKK), polyester,  
12  
13 polypropylene (PP), etc. Several investigations on friction and wear properties of PEEK  
14  
15 and its composites filled with fibers, organic and inorganic fillers have been carried out  
16  
17 [1,2]. Cirino et al. [1, 3] reported the sliding as well as the abrasive wear behavior of  
18  
19 continuous carbon and aramid fiber-reinforced PEEK. Lhymn et al. [4] have studied the  
20  
21 abrasive wear of short carbon fiber-reinforced PEEK. Voss and Friedrich [5] investigated  
22  
23 the sliding and abrasive wear behavior of short fiber-reinforced PEEK composites at room  
24  
25 temperature. Briscoe et al. [6] described the friction and wear of PEEK-PTFE blends over  
26  
27 a wide composition range under several testing conditions. Bahadur and Gong [7]  
28  
29 investigated the action of various copper compounds as fillers on the tribological behavior  
30  
31 of PEEK. Wang et al. [2, 8, 9] investigated friction and wear properties of nanometric  
32  
33  $ZrO_2$  and  $SiC$ -filled PEEK composites with different filler proportions. However, most of  
34  
35 the above studies are confined to dry sliding wear of various polymers and their  
36  
37 composites. The erosive wear behavior of polymer composites reinforced with any fiber  
38  
39 and/or particulate has not adequately been reported in the literature.  
40  
41  
42  
43  
44  
45  
46  
47  
48

49 Hard particulate fillers consisting of ceramic or metal particles and fiber fillers made of  
50  
51 glass are being used these days to dramatically improve the wear resistance of composites,  
52  
53 even up to three orders of magnitude [10]. The improved performance of polymers and  
54  
55 their composites in tribological applications by the addition of filler materials has shown  
56  
57 great promise and so has lately been a subject of considerable interest. Various kinds of  
58  
59 polymers and polymer matrix composites reinforced with metal particles have a wide  
60

1  
2  
3 range of industrial applications, such as heaters, electrodes [11], composites with thermal  
4 durability at high temperature [12], etc. These engineering composites are desired due to  
5 their low density, high corrosion resistance, ease of fabrication, and low cost [13–15].  
6  
7 Similarly, ceramic-filled polymer composites have been the subject of extensive research  
8 in the last two decades. The inclusion of inorganic fillers into polymers for commercial  
9 applications is primarily aimed at cost reduction and stiffness improvement. Along with  
10 fiber-reinforced composites, the composites made with particulate fillers have been found  
11 to perform well in tribological conditions.  
12  
13  
14  
15  
16  
17  
18  
19  
20  
21

22  
23 Silicon carbide (SiC) is one such ceramic material that has the potential to be used as filler  
24 in various polymer matrices. It is an excellent abrasive and has been produced and made  
25 into grinding wheels and other abrasive products for over 100 years. It is the only  
26 chemical compound of carbon and silicon. It was originally produced by a high  
27 temperature electro-chemical reaction of sand and carbon. Today the material has been  
28 developed into a high quality technical grade ceramic with very good mechanical  
29 properties. It is used in abrasives, refractories, ceramics, and numerous high performance  
30 applications. The material can also be made an electrical conductor and has applications in  
31 resistance heating, flame igniters, and electronic components. Structural and wear  
32 applications are constantly developing. Silicon carbide is composed of tetrahedral of  
33 carbon and silicon atoms with strong bonds in the crystal lattice. This produces a very hard  
34 and strong material. It is not attacked by any acids, alkalis, or molten salts up to 800<sup>0</sup>C.  
35  
36 The high thermal conductivity coupled with low thermal expansion and high strength  
37 gives this material exceptional thermal shock resistant qualities. Silicon carbide has low  
38 density of about 3.1 g/cm<sup>3</sup>, low thermal expansion, high elastic modulus, high strength,  
39 high thermal conductivity, high hardness, excellent thermal shock resistance, and superior  
40 chemical inertness. Although the effects of SiC (produced from mineral sources) as a filler  
41  
42  
43  
44  
45  
46  
47  
48  
49  
50  
51  
52  
53  
54  
55  
56  
57  
58  
59  
60



1  
2  
3 material on the wear behavior have been investigated earlier [16] for glass-polyester  
4 composites, there is no report available on the potential of SiC particles derived from a  
5 bio-resource like rice husk in jute fiber reinforced composite system. In this investigation,  
6 SiC produced from rice husk by plasma processing route has been used. The details of  
7 formation of SiC from rice husk by this route are described elsewhere [17].  
8  
9

10  
11  
12  
13  
14  
15  
16 Erosion rate (E) depends on velocity by a power law, given as  $E = kV^n$ , where k is a  
17 material constant. However, the exponent n is found to be material independent and is  
18 governed by test condition including particle characteristics and the erosion test apparatus  
19 [18]. In addition to velocity, solid particle erosion is also governed by impact angle,  
20 particle size, particle shape and hardness [19]. The impact of the above parameters has  
21 been studied independently, keeping all parameters at fixed levels. Therefore, visualization  
22 of impact of various factors in an interacting environment really becomes difficult. To this  
23 end, an attempt has been made to analyze the impact of more than one parameter on solid  
24 particle erosion because, in actual practice, the resultant erosion rate is the combined effect  
25 of impact of more than one interacting variable. An inexpensive and easy-to-operate  
26 experimental strategy based on Taguchi's parameter design has been adopted to study the  
27 effect of various parameters and their interactions. This experimental procedure has  
28 already been successfully implemented for parametric appraisal in erosion of polyester  
29 based composites [20-25]. The Taguchi method helps to ease the process of analyzing the  
30 experimental results and get insight into the physical phenomenon of experimentation.  
31  
32  
33  
34  
35  
36  
37  
38  
39  
40  
41  
42  
43  
44  
45  
46  
47  
48  
49  
50  
51  
52  
53  
54  
55  
56  
57  
58  
59  
60

**MATHEMATICAL MODEL****Nomenclature**

**The following symbols are used in this paper:**

a	erodent height and base length (m)
$\delta$	indentation depth (m)
$e_v$	volumetric wear loss per particle impact ( $m^3$ )
$E_v$	total volumetric erosion wear rate ( $m^3/sec$ )
$\alpha$	angle of impingement (degree)
U	impact velocity (m/sec)
P	force on the indenter (N)
H	hardness ( $N/m^2$ )
m	mass of single erodent particle (kg)
M	mass flow rate of the erodent (kg/sec)
N	number of impact per unit time ( $sec^{-1}$ )
$\rho_c$	density of composite ( $kg/m^3$ )
$\rho$	density of erodent ( $kg/m^3$ )
$\eta_{nor}$	erosion efficiency with normal impact
$\eta$	erosion efficiency
$E_{rth}$	erosion wear rate (kg/kg)

1  
2  
3 Solid particle erosion is a wear process in which the material is removed from a surface by  
4  
5 the action of a high velocity stream of erodent particles entrained in a high velocity fluid  
6  
7 stream. The particles strike against the surface and promote material loss. During flight, a  
8  
9 particle carries momentum and kinetic energy which can be dissipated during the impact  
10  
11 due to its interaction with a target surface. As far as erosion study of polymer matrix  
12  
13 composites is concerned, no specific model has been developed and thus the study of their  
14  
15 erosion behaviour has been mostly experimental. However, Mishra [26] proposed a  
16  
17 mathematical model for material removal rate in abrasive jet machining process in which  
18  
19 the material is removed from the work piece in a similar fashion. This model assumes that  
20  
21 the volume of material removed is same as the volume of indentation caused by the  
22  
23 impact. This has a serious limitation as in a real erosion process the volume of material  
24  
25 removed is actually different from the indentation volume. Further, this model considers  
26  
27 only the normal impact i.e.  $\alpha = 90^0$  whereas in actual practice, particles may impinge on  
28  
29 the surface at any angle ( $0^0 \leq \alpha \leq 90^0$ ). The proposed model addresses these shortcomings  
30  
31 in an effective manner. It considers the real situation in which the volume of material  
32  
33 removed by erosion is not same as the volume of material displaced and therefore, an  
34  
35 additional term “erosion efficiency ( $\eta$ )” is incorporated in the erosion rate formulation. In  
36  
37 the case of a stream of particles impacting a surface normally (i.e. at  $\alpha=90^0$ ), erosion  
38  
39 efficiency ( $\eta_{normal}$ ) defined by Sundararajan et. al [27] is given as  
40  
41  
42  
43  
44  
45  
46  
47  
48

$$\eta_{normal} = \frac{2ErHv}{\rho U^2} \quad (1)$$

49  
50  
51  
52  
53

54 But considering impact of erodent at any angle  $\alpha$  to the surface, the actual erosion  
55  
56 efficiency can be obtained by modifying Eq. (1) as  
57  
58  
59  
60

$$\eta = \frac{2ErHv}{\rho U^2 \sin^2 \alpha} \quad (2)$$

Besides, while all previous models have been developed assuming the shape of erodent to be spherical, in the real situation, the erodent particles are actually bodies having sharp edges, as shown in the Figure (1). Therefore, considering them to be cubical shaped bodies is a more realistic assumption as compared to assuming them simply spherical. The model proposed in the present work addresses to all these shortcomings. It assumes the erodent particles to be rigid, cubical shaped bodies having side equal to the average grit size. It is further based on the assumption that the loss in kinetic energy of the impinging particles is utilized to cause micro-indentation in the composite material and the material loss is a measure of the indentation. The erosion is the result of cumulative damage of such non-interacting, single particle impacts. The material removal mechanism is shown schematically in Figure (2). The model is developed with the simplified approach of energy conservation which equals the loss in erodent kinetic energy during impact with the work done in creating the indentation. It proceeds as follows.

At time  $t$  after initial contact, the particle of mass  $m$  will have indented the surface to a depth  $x$ ; the cross-sectional area of the indentation at the surface will be  $A(x)$ , where  $A(x)$  normally determined by the shape of the erodent particle. The upward force decelerating the particle will be that due to the plastic flow pressure acting over  $A(x)$ ; and the equation of motion of the particle can therefore be written as:

$$m \frac{d^2 x}{dt^2} = -HA(x) \quad (3)$$

For simple particle shapes, this equation can readily be solved analytically. But to know the final volume of indentation when the particle comes to rest at a depth  $\delta$  at time  $t = T$ ,

the work done by the retarding force will equal to the sum of the kinetic energy and the loss of thermal energy of the particle.

The conservation of energy can be represented by the equation

$$\int_0^{\delta} HA(x)dx = \frac{1}{2} mU^2 \quad (4)$$

The impact velocity will have two components; one normal to the composite surface and one parallel to it. At zero impact angles, it is assumed that there is negligible wear because eroding particles do not practically impact the target surface [28]. Consequently, there will be no erosion due to the parallel component and the indentation is assumed to be caused entirely by the component normal to the composite surface as shown in Figure (3).

Now applying conservation of energy to the single impact erosion process, kinetic energy associated with the normal velocity component of a single erodent particle is equal to the work done in the indentation of composite. The energy of impact introduces a force P on the indenter to cause the indentation in the composite. Thus, in case of oblique impact, the kinetic energy corresponding to the normal component of velocity is considered and Eq. (4) becomes:

$$\text{So, } \int_0^{\delta} HA(x)dx = \frac{1}{2} mU^2 \sin^2 \alpha \quad (5)$$

$$\text{Now, } \int_0^{\delta} A(x)dx = \int_0^{\delta} a^2 dx = a^2 \delta$$

So, the volumetric wear loss per particle impact is given by

$$e_v = \text{Volume of indentation} \times \eta = \eta a^2 \delta$$

Considering  $N$  number of particle impacts per unit time, the volumetric erosion wear loss will be

$$E_v = a^2 N \eta \delta$$

$$\text{Now, } \frac{1}{2} \cdot P \cdot \delta = \frac{1}{2} \cdot m \cdot U^2 \cdot \sin^2 \alpha$$

$$\frac{1}{2} a^2 \delta \cdot H = \frac{m U^2 \cdot \sin^2 \alpha}{2}$$

$$e_v = \eta \cdot \left[ \frac{m U^2 \cdot \sin^2 \alpha}{3H} \right]$$

For multiple impact

$$E_v = \eta \cdot m N \left[ \frac{U^2 \cdot \sin^2 \alpha}{3H} \right]$$

$$\text{Or, } E_v = \eta \cdot M \left[ \frac{U^2 \cdot \sin^2 \alpha}{H} \right]$$

The non-dimensional erosion rate, defined as the composite mass lost per unit time due to erosion divided by the mass of the erodent causing the loss, is now expressed as

$$E_R = \frac{\eta \rho_c}{H} \left[ U^2 \sin^2 \alpha \right] \quad (6)$$

The mathematical expression in Eq. (6) can possibly be used for predictive purpose to make an approximate assessment of the erosion damage from the composite surface.

## EXPERIMENTAL DETAILS

### Composite fabrication

Cross plied jute fibers are reinforced in epoxy resin in three different weight proportions (20 wt%, 30 wt% and 40 wt %) to prepare the composites A<sub>1</sub>, B<sub>1</sub> and C<sub>1</sub> respectively. Jute fibers and epoxy resin have modulus of about 55 GPa and 3.42 GPa respectively and possess density of 1300 kg/m<sup>3</sup> and 1100 kg/m<sup>3</sup> respectively. No particulate filler is used in these composites.

The other composite samples C<sub>2</sub> and C<sub>3</sub> with silicon carbide fillers of fixed weight percentage are fabricated by the same technique. The low temperature curing epoxy resin and corresponding hardener (HY951) are mixed in a ratio of 10:1 by weight as recommended. The mix is stirred manually to disperse the particulate fillers in the matrix. The mixing is done thoroughly before the jute-fiber mats (40 wt %) are reinforced in the matrix body. Composites C<sub>2</sub> and C<sub>3</sub> contain SiC particles in 10 wt% and 20 wt% proportions respectively. Each ply of jute-fiber is of dimension 200 mm× 200 mm. The composite slabs are made by conventional hand-lay-up technique followed by light compression moulding technique. A stainless steel mould having dimensions of 210 × 210 × 40 mm<sup>3</sup> is used. A releasing agent (Silicon spray) is used to facilitate easy removal of the composite from the mould after curing. Care is taken to ensure a uniform sample since particles have a tendency to clump and tangle together when mixed. The cast of each composite is cured under a load of about 25kg for 24 h before it removed from the mould. Then this cast is post cured in the air for another 24 h after removing out of the mould. Specimens of suitable dimension are cut using a diamond cutter for physical characterization and mechanical testing. Utmost care has been taken to maintain

1  
2  
3 uniformity and homogeneity of the composite. The designation and detailed composition  
4  
5 of the composites are given in Table 1.  
6  
7

### 8 9 **Erosion Test Apparatus**

10  
11 The set up used in this study for the solid particle erosion wear test is capable of creating  
12  
13 reproducible erosive situations for assessing erosion wear resistance of the prepared  
14  
15 composite samples. It consists of an air compressor, an air particle mixing chamber and  
16  
17 accelerating chamber. The schematic diagram of the erosion test rig is given in Figure (4).  
18  
19 Dry compressed air is mixed with the erodent particles which are fed at constant rate from  
20  
21 a sand flow control knob through the nozzle tube and then accelerated by passing the  
22  
23 mixture through a convergent brass nozzle of 3mm internal diameter. These particles  
24  
25 impact the specimen which can be held at different angles with respect to the direction of  
26  
27 erodent flow using a swivel and an adjustable sample clip. The velocity of the eroding  
28  
29 particles is determined using standard double disc method [25]. The parameters  
30  
31 (confirming to ASTM G 76 test standards) which are considered for erosion tests are  
32  
33 listed in Table 2. In the present study, dry silica sand of different particle sizes (200 $\mu$ m,  
34  
35 300  $\mu$ m and 400 $\mu$ m) are used as erodent. The samples are cleaned in acetone, dried and  
36  
37 weighed to an accuracy of  $\pm 0.1$  mg before and after the erosion trials using a precision  
38  
39 electronic balance. The weight loss is recorded for subsequent calculation of erosion rate.  
40  
41 The process is repeated till the erosion rate attains a constant value called *steady state*  
42  
43 *erosion rate*. The ratio of this weight loss to the weight of the eroding particles causing  
44  
45 the loss is then computed as a dimensionless incremental erosion rate. The erosion rate is  
46  
47 defined as the weight loss of the specimen due to erosion divided by the weight of the  
48  
49 erodent causing the loss.  
50  
51  
52  
53  
54  
55  
56  
57  
58  
59  
60



## Parametric Appraisal and Taguchi Method

Statistical methods are commonly used to improve the quality of a product or process. Such methods enable the user to define and study the effect of every single condition possible in an experiment where numerous factors are involved. Solid particle erosion is such a process in which a number of control factors collectively determine the performance output i.e. the erosion rate. Hence, in the present work a technique called Taguchi method is used to optimize the process parameters leading to minimum erosion of the polymer composites under study. This part of the chapter presents the Taguchi experimental design methodology in detail.

### Taguchi Experimental Design

Every single discipline has researchers carrying out experiments to observe and understand a certain process or to discover the interaction and effect of different variables. From a scientific viewpoint, these experiments are either one or a series of tests to either confirm a hypothesis or to understand a process in further detail. Experiments from a manufacturing point of view, however, are concerned with finding the optimum product and process, which is both cost effective and of a high quality. In order to achieve a meaningful end result, several experiments are usually carried out. The investigator needs to know the factors involved, the range these factors are varied between, the levels assigned to each factor as well as a method to calculate and quantify the response of each factor. This *one-factor-at-a-time* approach will provide the most favorable level for each factor but not the optimum combination of all the interacting factors involved. Thus, experimentation in this scenario can be considered as an iterative process. Although it will provide a result, such methods are not time or cost effective. But the design of experiments is a scientific approach to effectively plan and perform experiments, using statistics. In

1  
2  
3 such designs, the combination of each factor at every level is studied to determine the  
4 combination that would yield the best result. The advantage of such design schemes is that  
5  
6 it will always determine the effect of factors and possible interactions (between factors) on  
7  
8 the performance output.  
9  
10

11  
12  
13 Taguchi design of experiment is a powerful analysis tool for modeling and analyzing the  
14 influence of control factors on performance output. The most important stage in the design  
15 of experiment lies in the selection of the control factors. Therefore, initially a large  
16 number of factors are included so that non-significant variables can be identified at earliest  
17 opportunity. Exhaustive literature review on erosion behavior of polymer composites  
18 reveal that parameters viz., impact velocity, impingement angle, fiber loading, filler  
19 content, erodent size etc largely influence the erosion rate of polymer composites [20-25].  
20  
21 In the present work, the impact of four such parameters are studied using  $L_9$  ( $3^4$ )  
22 orthogonal design. The operating parameters and the selected levels are given in Table 3.  
23  
24 The tests are conducted at room temperature as per experimental designs given in Table 4  
25 (for  $A_1, B_1, C_1$ ) and Table 5 (for  $C_1, C_2, C_3$ ) which gives the operating conditions under  
26 which each erosion test has been carried out.  
27  
28  
29  
30  
31  
32  
33  
34  
35  
36  
37  
38  
39  
40  
41  
42

43 Four parameters viz., impact velocity, impingement angle, erodent size, and fiber/filler  
44 loading, each at three levels, are considered in this study. In Tables 4 and 5, each column  
45 represents a test parameter and a row gives a test condition which is nothing but  
46 combination of parameter levels. Four parameters each at three levels would require  $3^4 =$   
47 81 runs in a full factorial experiment. Whereas, Taguchi's factorial experiment approach  
48 reduces it to 9 runs only offering a great advantage in terms of cost and time.  
49  
50  
51  
52  
53  
54  
55  
56  
57  
58  
59  
60

1  
2  
3 The plan of the experiments is as follows: the first column is assigned to impact velocity  
4 (A), the second column to impingement angle (B), third column to erodent size (C), and  
5  
6 the last column to fiber/filler loading (D).  
7  
8

9  
10  
11 The experimental observations are transformed into a signal-to-noise (S/N) ratio. There  
12 are several S/N ratios available depending on the type of characteristics. The S/N ratio for  
13  
14 minimum erosion rate coming under *smaller-is-better* characteristic, which can be  
15  
16 calculated as logarithmic transformation of the loss function as shown below.  
17  
18

19  
20  
21  
22 Smaller is the better characteristic: 
$$\frac{S}{N} = -10 \log \frac{1}{n} \left( \sum y^2 \right) \quad (7)$$
  
23  
24  
25

26 where n the number of observations, and y the observed data. “Lower is better” (LB)  
27  
28 characteristic, with the above S/N ratio transformation, is suitable for minimizations of  
29  
30 erosion rate.  
31  
32

## 33 34 RESULTS AND DISCUSSION

### 35 36 37 Steady state erosion

38  
39  
40 Erosion wear behavior of materials can be grouped as ductile and brittle categories  
41  
42 although this grouping is not definitive. Thermoplastic matrix composites usually show  
43  
44 ductile behavior and have the peak erosion rate at around 30<sup>0</sup> impingement angle because  
45  
46 cutting mechanism is dominant in erosion. While the thermosetting ones erode in a brittle  
47  
48 manner with the peak erosion occurring at normal impact. However, there is a dispute  
49  
50 about this failure classification as the erosive wear behavior depends strongly on the  
51  
52 experimental conditions and the composition of the target material. In the present work,  
53  
54 erosion curves are plotted in from the results of erosion tests conducted for different  
55  
56 impingement angle keeping all other parameters constant (impact velocity = 32m/sec,  
57  
58  
59  
60

1  
2  
3 stand-off distance = 100 mm and erodent size =200  $\mu\text{m}$ ). Figure (5) shows the dependence  
4 of the erosion rate of unfilled jute-epoxy composites with different fiber content on the  
5 impingement angle. It can be seen that the peaks of erosion rates are located at an angle of  
6  $60^\circ$  for all the samples irrespective of fiber content. This shows semi-ductile erosion  
7 behavior of the composite. It is further noted that with increased fiber content the erosion  
8 rate of the composites is greater.  
9

10  
11  
12 Erosion behaviour of the composites is generally ascertained by correlating erosion rate  
13 with impingement angle, erodent velocity and composition of the material. Composites  
14 usually respond to solid particle erosion in two broad ways: ductile and brittle. The ductile  
15 response is characterized by maximum erosion rate occurring at  $15\text{--}30^\circ$  impingement angle  
16 and brittle behaviour is characterized by the peak erosion rate at  $90^\circ$ . Similarly, semi-  
17 ductile behaviour is characterized by the maximum erosion rate taking place at  $45\text{--}60^\circ$ .  
18 But as already mentioned, this grouping is not definitive because the erosion  
19 characteristics equally depend on the experimental conditions as on composition of the  
20 target material.  
21  
22  
23  
24  
25  
26  
27  
28  
29  
30  
31  
32  
33  
34  
35  
36  
37  
38  
39

40  
41 The erosion wear rates of SiC filled jute-epoxy composites as a function of impingement  
42 angle ( $\alpha$ ) are shown in Figure (6). It can be seen that filling of composite with SiC  
43 particles reduces the wear rate of the jute-epoxy composites quite significantly. The  
44 unfilled composite, shows maximum erosion occurring at  $\alpha = 60^\circ$  while for both the filled  
45 composites (with 10wt% and 20wt% SiC content) the value of  $\alpha$  where the peak erosion  
46 occurs is found to be  $75^\circ$ . In the present study, the location of peak erosion has shifted to  
47  $60^\circ$  from the usual  $15^\circ\text{--}30^\circ$  (for purely ductile case) as it is reinforced with jute fiber (curve  
48 A). This shift in the erosion behavior is an indication of loss of ductility and is obviously  
49 attributed to the presence of fibers. Further shifting of  $\alpha$  from  $60^\circ$  to  $75^\circ$  (curve B and C)  
50  
51  
52  
53  
54  
55  
56  
57  
58  
59  
60

1  
2  
3 proves that the composites tend to become still more brittle with incorporation of SiC  
4 particles. The trend is similar for both the composites with SiC filler. It is also important to  
5 note that the sample with higher filler content exhibits better erosion resistance.  
6  
7  
8  
9

### 10 11 **Surface morphology**

12  
13  
14 The surface micro-structures of some of the un-eroded composite samples are observed  
15 under scanning electron microscope basically to get an insight to the features. As seen in  
16 Figures (7a) and (7b), the surfaces are reasonably homogeneous. No cracks are seen  
17 although some voids and pores are visible even at lower magnification. SiC particles are  
18 not seen in clusters within the matrix body.  
19  
20  
21  
22  
23  
24  
25  
26  
27

28 To identify the mode of material removal, the morphologies of eroded surfaces are studied  
29 under scanning electron microscope. Figure (7c) presents the microstructure of the  
30 composite eroded at high impact velocity (58m/sec) and at an impingement angle of 60°. It  
31 shows local removal of resin material from the impacted surface resulting in exposure of  
32 the fibers to the erodent flux. This micrograph also reveals that due to sand particle impact  
33 on fibers there is formation of transverse cracks that break these fibers. The propagation of  
34 crack along transverse as well as longitudinal direction is well visualized.  
35  
36  
37  
38  
39  
40  
41  
42  
43  
44  
45

46 A possible reason for the semi-ductile erosion behavior exhibited by the epoxy based  
47 composites in the present investigation is that the erosion of jute fibers is caused mostly by  
48 damage mechanism such as micro-cracking. Such damage is supposed to increase with the  
49 increase of kinetic energy loss of the impinging sand particles. According to Hutchings et  
50 al. [29], kinetic energy loss is a maximum at normal impact, where erosion rates are  
51 highest for brittle materials. In the present study, however, the peak erosion rate shifts to  
52 an impingement angle of 60° and it is clearly due to the incorporation of jute fibers. So  
53  
54  
55  
56  
57  
58  
59  
60

1  
2  
3 although neat epoxy exhibits a ductile erosion response, the presence of fibers makes the  
4 composite relatively more sensitive to impact energy which increases when the impact  
5 mode pattern changes from tangential ( $\alpha = 0^{\circ}$ ) to normal ( $\alpha = 90^{\circ}$ ). This explains the  
6 semi-ductile nature of the jute-epoxy composites with respect to solid particle erosion.  
7  
8  
9

10  
11 Figure (7d) presents the microstructure of the SiC filled composite eroded with high  
12 impact velocity (58m/sec) at an impingement angle of  $60^{\circ}$ . It shows local removal of resin  
13 material from the impacted surface resulting in exposure of the fibers to the erodent flux.  
14 This micrograph also reveals that due to sand particle impact on jute-fibers, there is  
15 formation of transverse cracks that break these fibers. The propagation of crack along  
16 transverse as well as longitudinal direction is well visualized. It appears that cracks have  
17 grown on the fibers giving rise to breaking of the fibers into small fragments. Further the  
18 cracks have been annihilated at the fiber matrix interface and seem not to have penetrated  
19 through the matrix. Figure (7d) also shows the dominance of micro-chipping and micro-  
20 cracking phenomena. It can be seen that multiple cracks originate from the point of  
21 impact, intersect one another and form wear debris due to brittle fracture in the fiber body  
22 as well as in the silicon carbide particles present in the matrix body. After repetitive  
23 impacts, the debris in platelet form is removed and account for the measured wear loss.  
24  
25  
26  
27  
28  
29  
30  
31  
32  
33  
34  
35  
36  
37  
38  
39  
40  
41  
42  
43

#### 44 45 **Taguchi Analysis of the Erosion Test Results**

46  
47 The erosion wear rates of unfilled jute fiber reinforced epoxy matrix composites under  
48 various test conditions are given in Table 6. The theoretical erosion wear rates ( $E_{rth}$ ) of all  
49 the three unfilled composites are calculated using Eq. (7). These values are compared with  
50 those obtained from experiments ( $E_r$ ) conducted under similar operating conditions and the  
51 comparison curve has been given in Figure (8). Table 6 also presents the values of  
52 theoretical and experimental results for the composites eroded under different test  
53  
54  
55  
56  
57  
58  
59  
60

1  
2  
3 conditions. The errors associated with each comparison are found to lie in the range 0-12  
4  
5  
6  
7  
8  
9  
10  
11  
12  
13  
14  
15  
16  
17  
18  
19  
20  
21  
22  
23  
24  
25  
26  
27  
28  
29  
30  
31  
32  
33  
34  
35  
36  
37  
38  
39  
40  
41  
42  
43  
44  
45  
46  
47  
48  
49  
50  
51  
52  
53  
54  
55  
56  
57  
58  
59  
60

conditions. The errors associated with each comparison are found to lie in the range 0-12  
%. Similarly, the erosion wear rates of jute fiber reinforced epoxy matrix composites filled  
with different proportions of silicon carbide under various test conditions are given in  
Table 9. These values are compared with those obtained from experiments ( $E_r$ ) conducted  
under similar operating conditions and the comparison curve has been given in Figure (9).  
The errors associated with each comparison, in this case also lie in the range 0-12 %.

The experimental observations are transformed into a signal-to-noise (S/N) ratio. There  
are several S/N ratios available depending on the type of characteristics. The S/N ratio for  
minimum erosion rate coming under *smaller-is-better* characteristic, which can be  
calculated as logarithmic transformation of the loss function as shown below.

Smaller is the better characteristic: 
$$\frac{S}{N} = -10 \log \frac{1}{n} (\sum y^2) \quad (8)$$

where n the number of observations, and y the observed data. “Lower is better” (LB)  
characteristic, with the above S/N ratio transformation, is suitable for minimization of  
erosion rate.

In Tables 7 and 10, the last columns represents S/N ratio of the erosion rate which is in  
fact the average of three replications. The overall mean for the S/N ratio of the erosion rate  
is found to be -45.674 db in case of unfilled composites (Table 7) and- 44.506 db in case  
of silicon carbide composites (Table 10). The analysis is made using the popular software  
specifically used for design of experiment applications known as MINITAB 14.

The effects of individual control factors influencing the erosion wear rates of unfilled jute-  
epoxy composites are shown in Figure (10). The S/N ratio response is given in Table 8,  
from which it can be concluded that among all the factors, impact velocity is the most  
significant factor followed by fiber content and impingement angle while the erodent size

has the least or almost no significance on erosion of the reinforced composite. It also leads to the conclusion that factor combination of  $A_1$ ,  $B_1$ , and  $D_1$  gives minimum erosion rate.

Similarly, the effects of individual control factors influencing the erosion wear rates of SiC filled jute-epoxy composites are shown in Figure (11). The S/N ratio response is given in Table 11, from which it can be concluded that among all the factors, impact velocity is the most significant factor followed by filler content and impingement angle while the erodent size has the least or almost no significance on erosion of the reinforced composite. It also leads to the conclusion that factor combination of  $A_1$ ,  $B_1$ , and  $D_3$  gives minimum erosion rate.

### Factor Settings for Minimum Erosion Rate

In this study, an attempt is made to derive predictive equations in terms of the significant control factors for determination of erosion rate of both the filled and unfilled composites. The single-objective function requires quantitative determination of the relationship between erosion rates with combination of control factors. In order to express, erosion rate in the form of a mathematical model in the following correlation is suggested.

$$E = K_0 + K_1 \times A + K_2 \times B + K_3 \times D \quad (9)$$

Here,  $E$  is the performance output terms and  $K_i$  ( $i = 0, 1 \dots 3$ ) are the model constants. The constants are calculated using non-linear regression analysis with the help of SYSTAT 7 software and the following relations are obtained

$$E = 66.984 + 1.665 \times A + 0.086 \times B + 1.564 \times D \quad (10)$$

$(r^2=0.99)$

$$E = 9.179 + 3.731 \times A + 0.427 \times B - 2.709 \times D \quad (11)$$

$(r^2=0.989)$



1  
2  
3 The correctness of the calculated constants is confirmed as high correlation coefficients  
4  
5 ( $r^2$ ) in the tune of 0.99 and 0.989 are obtained for Eq. (10) and for Eq. (11) respectively.  
6  
7  
8  
9

## 10 11 12 **CONCLUSIONS**

13  
14 Successful fabrication of multi-component hybrid jute-epoxy composites with  
15  
16 reinforcement of SiC derived from rice husk by plasma processing route is possible. It is  
17  
18 demonstrated that if supported by an appropriate magnitude of erosion efficiency, the  
19  
20 proposed theoretical model can perform well for epoxy based hybrid composites for  
21  
22 normal as well as oblique impacts. The presence of particulate fillers (silicon carbide) in  
23  
24 these composites improves their erosion wear resistance and this improvement depends on  
25  
26 the weight content of the filler. Erosion characteristics of these composites have been  
27  
28 successfully analyzed using Taguchi experimental design. Significant control factors  
29  
30 affecting the erosion rate have been identified through successful implementation of this  
31  
32 technique. Impact velocity, fiber/filler content and impingement angle in declining  
33  
34 sequence are found to be significant for minimizing the erosion rate of all the composites.  
35  
36 Erodent size is identified as the least influencing control factor for erosion rate.  
37  
38  
39  
40  
41  
42  
43  
44

## 45 **REFERENCES**

- 46  
47  
48 1. Cirino, M., Pipes, R. B., and Friedrich, K. (1987). The Abrasive Wear Behaviour  
49  
50 of Continuous Fibre Polymer Composites. *Journal of Materials Science*, **22**: 2481.  
51  
52  
53 2. Wang, Q. H., Xue, Q. J., Liu, W. M., and Chen, J. M. (2000). The Friction and  
54  
55 Wear Characteristics of Nanometer SiC and PTFE filled PEEK. *Wear*, **243**: 140.  
56  
57  
58 3. Cirino, M., Friedrich, K. and Pipes, R. B. (1988). Evaluation of Polymer  
59  
60 Composites for Sliding and Abrasive Wear Application. *Composites*, **19**: 383.

- 1  
2  
3 4. Lhymn, C., Tempelmeyer, K. E. and Davis, P. K. (1985). The Abrasive Wear of  
4 Short Fibre Composites. *Composites*, **16**: 127.
- 5  
6  
7  
8 5. Voss, H. and Friedrich, K. (1987). On the Wear Behaviour of Short Fibre  
9 Reinforced PEEK Composites. *Wear*, **116**: 1.
- 10  
11  
12  
13 6. Briscoe, B. J., Yao, L. H. and Stolarski, T. A. (1986). The Friction and Wear of  
14 PTFE and PEEK Composites: An Initial Appraisal of the Optimum Composition.  
15  
16  
17  
18  
19  
20  
21 7. Bahadur, S. and Gong, D. (1992). The Role of Copper Compounds as Fillers in the  
22 Transfer and Wear Behaviour of PEEK. *Wear*, **154**: 151.
- 23  
24  
25  
26  
27 8. Wang, Q. H., Xue, Q. J., Shen, W. C. and Zhang, J. (1998). The Friction and Wear  
28 Properties of Nanometer ZrO<sub>2</sub>-Filled PEEK. *Journal of Applied Polymer Science*,  
29  
30  
31  
32  
33  
34  
35  
36  
37 9. Wang, Q. H., Xue, Q. J. and Shen, W. C. (1998). The Tribological Properties of  
38 SiC Whisker Reinforced PEEK. *Journal of Applied Polymer Science*, **69**: 2341.
- 39  
40  
41  
42  
43  
44  
45  
46  
47  
48  
49  
50  
51  
52  
53  
54  
55  
56  
57  
58  
59  
60 10. Gregory, S. W., Freudenberg, K. D., Bhimaraj, P. and Schadler, L. S. (2003). A  
Study on the Friction and Wear Behavior of PTFE Filled with Alumina  
Nanoparticles. *Wear*, **254**: 573–580.
11. Jung-II, K., Kang, P. H. and Nho, Y. C. (2004). Positive Temperature Coefficient  
Behavior of Polymer Composites Having a High Melting Temperature. *Journal of  
Applied Polymer Science*, **92**: 394–401.
12. Nikkeshi, S., Kudo, M. and Masuko, T. (1998). Dynamic Viscoelastic Properties  
and Thermal Properties of Powder-Epoxy Resin Composites. *Journal of Applied  
Polymer Science*, **69**: 593–598.

- 1  
2  
3  
4  
5  
6  
7  
8  
9  
10  
11  
12  
13  
14  
15  
16  
17  
18  
19  
20  
21  
22  
23  
24  
25  
26  
27  
28  
29  
30  
31  
32  
33  
34  
35  
36  
37  
38  
39  
40  
41  
42  
43  
44  
45  
46  
47  
48  
49  
50  
51  
52  
53  
54  
55  
56  
57  
58  
59  
60
13. Zhu, K., and Schmauder, S. (2003). Prediction of the Failure Properties of Short Fiber Reinforced Composites with Metal and Polymer Matrix. *Computation Material Science*, **28**: 743–758.
  14. Rusu, M., Sofian, N. and Rusu, D. (2001). Mechanical and Thermal Properties of Zinc Powder Filled High Density Polyethylene Composites. *Polymer Testing*, **20**: 409–417.
  15. Tavman, I. H. (1997). Thermal and Mechanical Properties of Copper Powder Filled Poly (ethylene) Composites, *Powder Technology*, **91**: 63–76.
  16. Patnaik, A., Satapathy, A., Mahapatra, S. S., Dash, R. R. (2008). Implementation of Taguchi Design for Erosion of Fiber Reinforced Polyester Composite Systems with SiC Filler. *Journal of Reinforced Plastics and Composites*. **27**:1093 - 1111.
  17. Singh, S.K., Mohanty, B.C. and Basu S. (2002). Synthesis of SiC from rice husk in a plasma reactor, *Bull. Materials Sci.* **25**(6): 561-563.
  18. Chen, Q., and Li, D. Y. (2003). Computer Simulation of Solid Particle Erosion, *Wear*, **254**: 203–210.
  19. Sundararajan, G. and Manish, R. (1997). Solid Particle Erosion Behaviour of Metallic Materials at Room and Elevated Temperatures. *Tribology International*, **30**(5): 339–359.
  20. Patnaik, A., Satapathy, A., Mahapatra, S. S., Dash, R. R. (2008). Tribo-Performance of Polyester Hybrid Composites: Damage Assessment and Parameter Optimization using Taguchi Design. *Materials and Design*, **30**: 57-67.
  21. Patnaik, A., Satapathy, A., Mahapatra, S. S., Dash, R. R. (2008). A Taguchi Approach for Investigation of Erosion of Glass Fiber -Polyester Composites. *Journal of Reinforced Plastics and Composites*, **27**: 871 - 888.

- 1  
2  
3  
4  
5  
6  
7  
8  
9  
10  
11  
12  
13  
14  
15  
16  
17  
18  
19  
20  
21  
22  
23  
24  
25  
26  
27  
28  
29  
30  
31  
32  
33  
34  
35  
36  
37  
38  
39  
40  
41  
42  
43  
44  
45  
46  
47  
48  
49  
50  
51  
52  
53  
54  
55  
56  
57  
58  
59  
60
22. Patnaik, A., Satapathy, A., Mahapatra, S. S., Dash, R. R. (2008). Parametric Optimization Erosion Wear of Polyester-GF-Alumina Hybrid Composites using the Taguchi Method. *Journal of Reinforced Plastics and Composites*, **27**:1039 - 1058.
  23. Patnaik, A., Satapathy, A., Mahapatra, S. S., Dash, R. R. (2008). Erosive Wear Assesment of Glass Reinforced Polyester-Flyash Composites using Taguchi Method. *International Polymer Processing*. DOI 10.3139/217.2113.
  24. Mahapatra, S. S, Patnaik, A, Satapathy, A. (2008) Taguchi Method Applied to Parametric Appraisal of Erosion Behavior of GF-Reinforced Polyester Composites. *Wear*, **265**: 214–222.
  25. Patnaik, A., Satapathy, A., Mahapatra, S. S., Dash, R. R. (2007).A Modeling Approach for Prediction of Erosion Behavior of Glass Fiber- Polyester Composites. *Journal of Polymer Research*, DOI 10.1007/s10965-007-9154-2.
  26. Mishra, P. K. (1997). Non-conventional Machining, Narosa Publishing House, New Delhi.
  27. Sundararajan, G., Roy, M. and Venkataraman, B. (1990). Erosion Efficiency - a New Parameter to Characterize the Dominant Erosion Micro-mechanism. *Wear*, **140**: 369.
  28. Stachowiak, G.W and Batchelor, A.W. (1993). Engineering tribology, *Tribology Series 24, Elseiver*. Amsterdam. 588.
  29. Hutchings I.M, Winter R.E, Field J.E, (1976). Solid particle erosion of metals: the removal of surface material by spherical projectiles. *Proc Roy Soc Lond, Ser A* **348**:379-392.

1  
2  
3 **List of Figures:**  
4  
5  
6  
7

8 **Figure 1** SEM Micrograph of the erodent used  
9

10 **Figure 2** Scheme of material removal mechanism  
11

12 **Figure 3** Resolution of impact velocity in normal and parallel directions.  
13  
14

15 **Figure 4** A schematic diagram of the erosion test rig  
16  
17

18 **Figure 5** Erosion rate vs. angle of impingement for different fiber loading  
19

20 **Figure 6** Erosion rate vs. angle of impingement for different weight fraction of SiC  
21  
22

23 **Figure 7** SEM micrograph of SiC filled jute-epoxy composite surface  
24  
25

26 **Figure 8** Comparison of theoretical and experimental values of erosion rate for unfilled jute-  
27 epoxy composites  
28  
29

30 **Figure 9** Comparison of theoretical and experimental values of erosion rate for SiC filled jute-  
31 epoxy composites  
32  
33  
34

35 **Figure 10** Effect of control factors on erosion rate (for unfilled composites)  
36  
37

38 **Figure 11** Effect of control factors on erosion rate (for particulate filled composites)  
39  
40  
41  
42  
43  
44  
45  
46  
47  
48  
49  
50  
51  
52  
53  
54  
55  
56  
57  
58  
59  
60

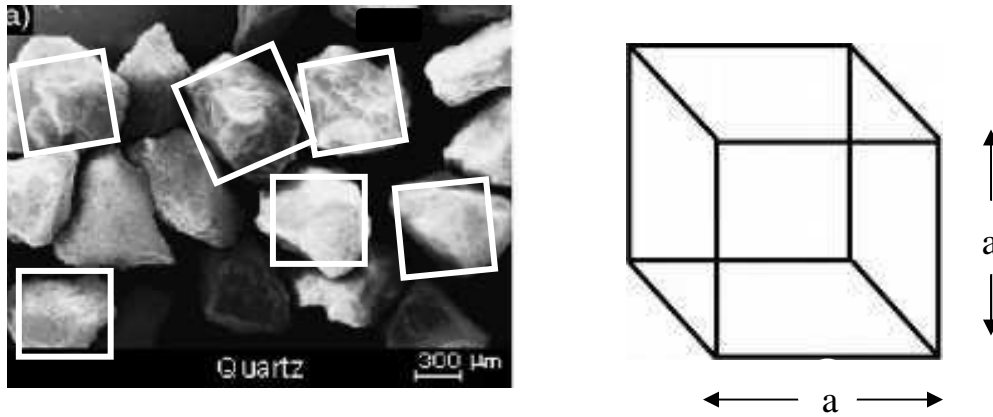


**Figure 1** SEM Micrograph of the erodent used

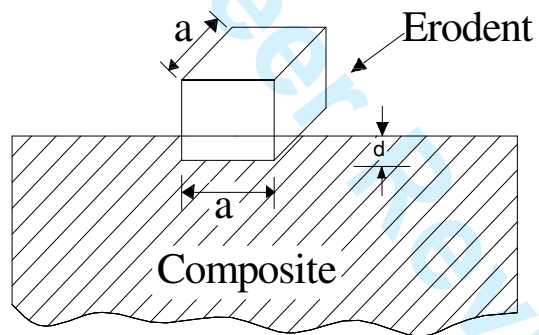


**Figure 2** Scheme of material removal mechanism

1  
2  
3  
4  
5  
6  
7  
8  
9  
10  
11  
12  
13  
14  
15  
16  
17  
18  
19  
20  
21  
22  
23  
24  
25  
26  
27  
28  
29  
30  
31  
32  
33  
34  
35  
36  
37  
38  
39  
40  
41  
42  
43  
44  
45  
46  
47  
48  
49  
50  
51  
52  
53  
54  
55  
56  
57  
58  
59  
60

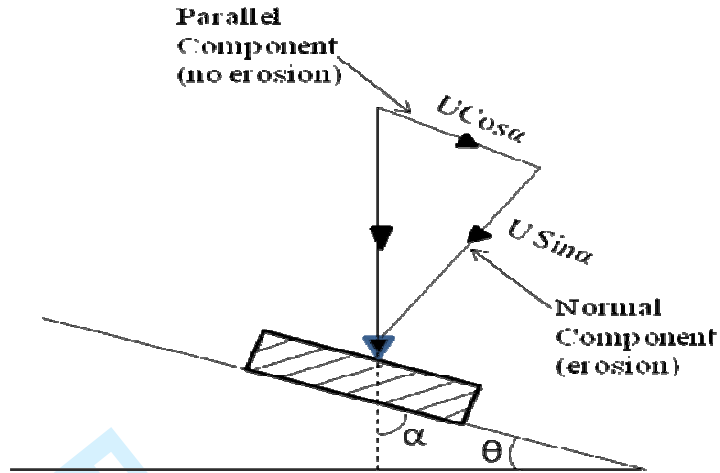


Figure 3 Resolution of impact velocity in normal and parallel directions.

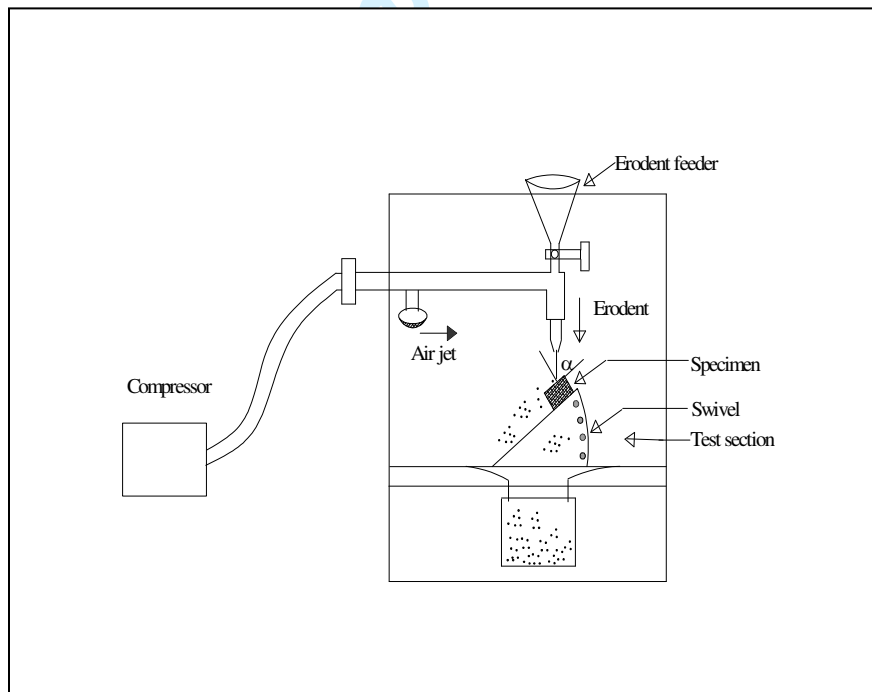
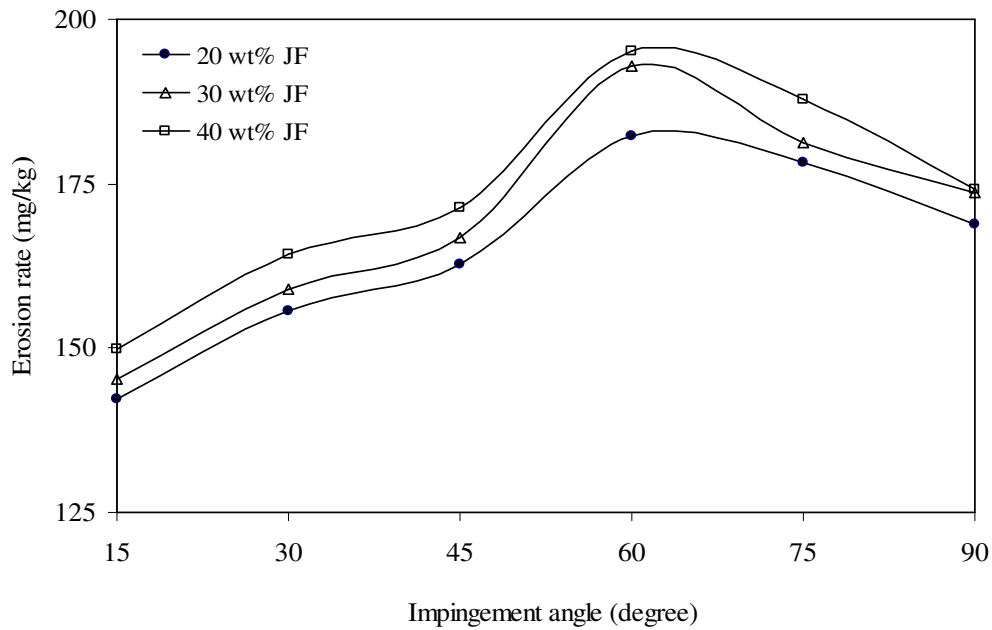
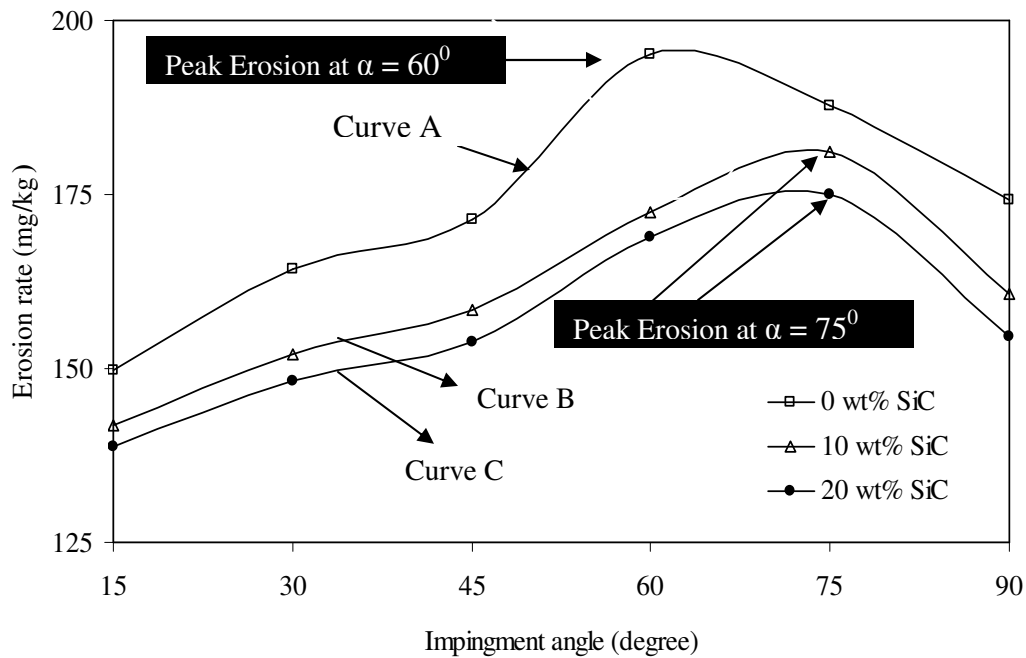


Figure 4 A schematic diagram of the erosion test rig



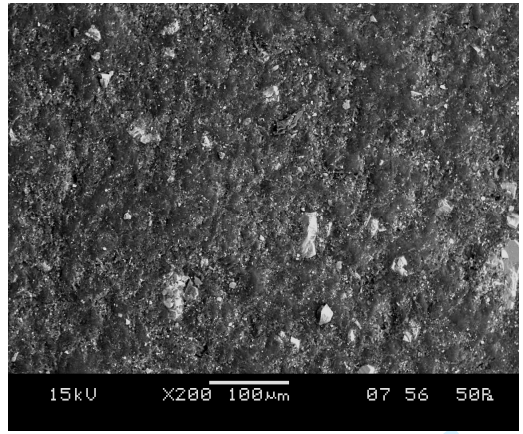
**Figure 5** Erosion rate vs. angle of impingement for different fiber loading



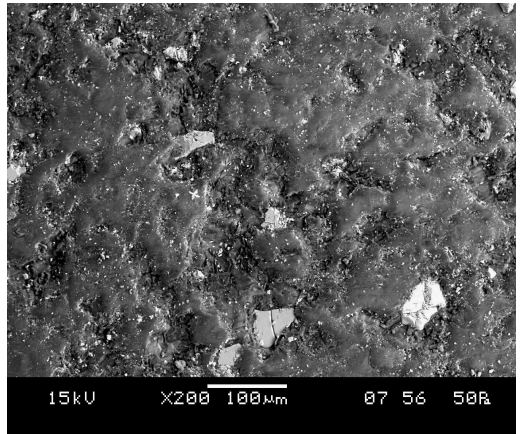
**Figure 6** Erosion rate vs. angle of impingement for different weight fraction of SiC



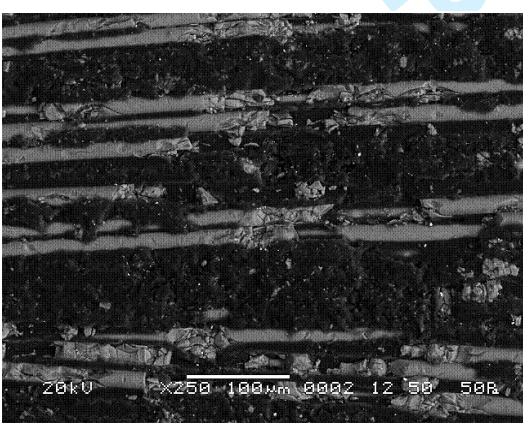
1  
2  
3  
4  
5  
6  
7  
8  
9  
10  
11  
12  
13  
14  
15  
16  
17  
18  
19  
20  
21  
22  
23  
24  
25  
26  
27  
28  
29  
30  
31  
32  
33  
34  
35  
36  
37  
38  
39  
40  
41  
42  
43  
44  
45  
46  
47  
48  
49  
50  
51  
52  
53  
54  
55  
56  
57  
58  
59  
60



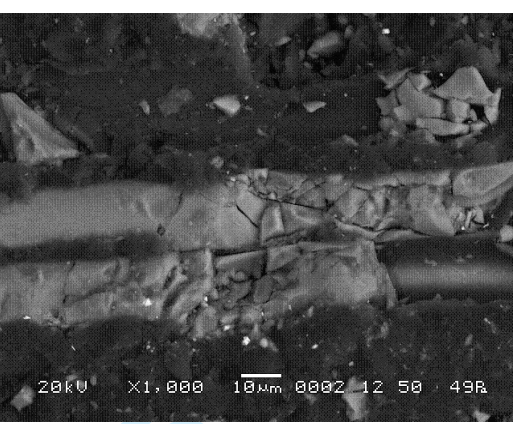
(a)



(b)



(c)



(d)

**Figure 7** SEM micrograph of SiC filled jute-epoxy composite surface

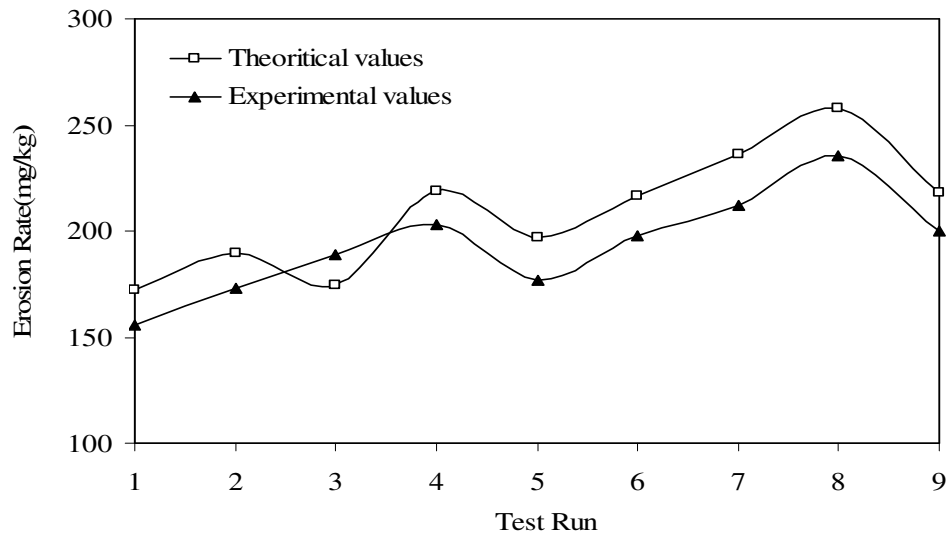


**Figure 8** Comparison of theoretical and experimental values of erosion rate for unfilled jute-epoxy composites

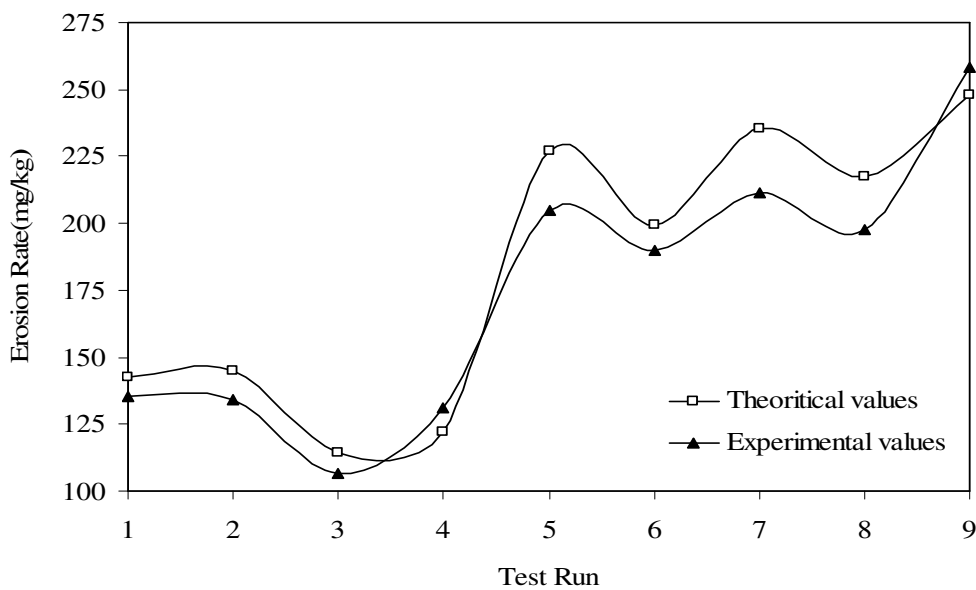


**Figure 9** Comparison of theoretical and experimental values of erosion rate for SiC filled jute-epoxy composites

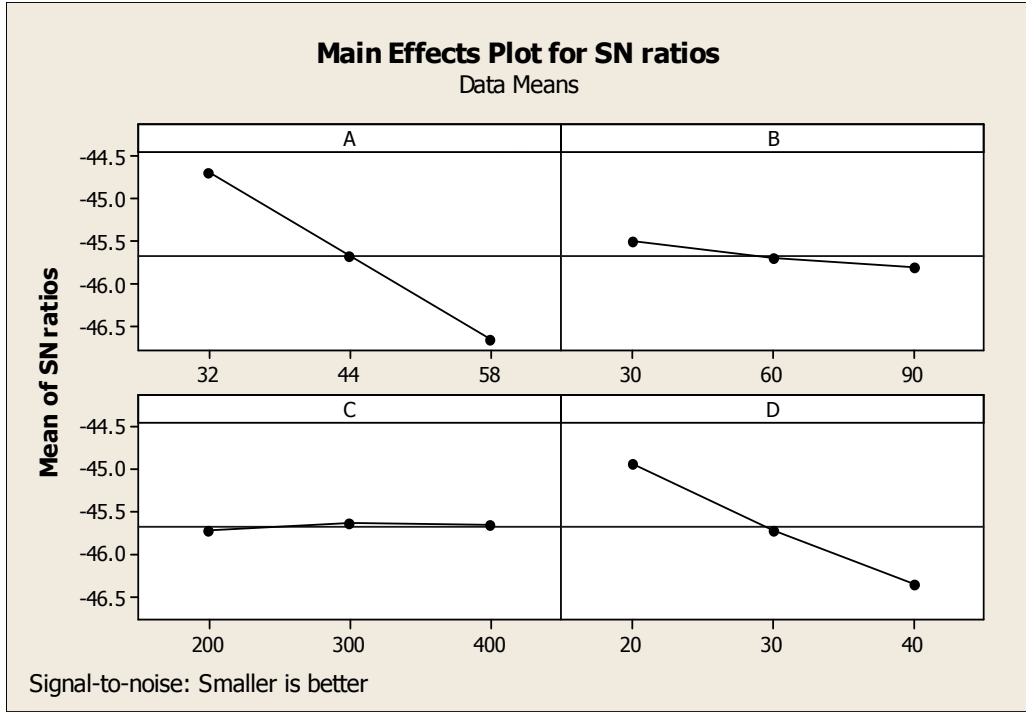


Figure 10 Effect of control factors on erosion rate (for unfilled composites)

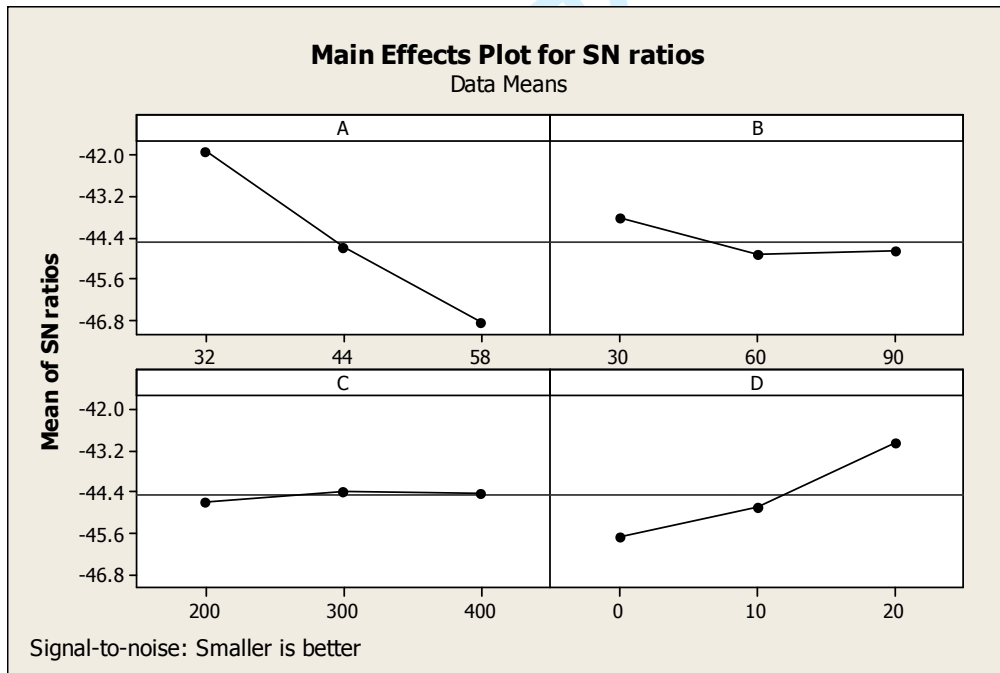


Figure 11 Effect of control factors on erosion rate (for particulate filled composites)

1  
2  
3 **List of Tables**  
4  
5  
6  
7

8 **Table 1** Designation and detailed composition of the composites  
9

10 **Table 2** Parameters considered during erosion test  
11

12 **Table 3** Levels for various control factors  
13

14 **Table 4** Orthogonal array for L<sub>9</sub> Taguchi Design for composites A<sub>1</sub>, B<sub>1</sub>, C<sub>1</sub>  
15

16 **Table 5** Orthogonal array for L<sub>9</sub> Taguchi Design composites C<sub>1</sub>, C<sub>2</sub>, C<sub>3</sub>  
17

18 **Table 6** Erosion Test Results for Jute-Epoxy Composites  
19

20 **Table 7** S/N ratio and Erosion Rate for Different Test conditions  
21

22 **Table 8** Response Table for Signal to Noise Ratio (Smaller is better)  
23

24 **Table 9** Erosion Test Results for particulate filled Jute-Epoxy Composites  
25

26 **Table 10** S/N ratio and Erosion Rate for Different Test conditions  
27

28 **Table 11** Response Table for Signal to Noise Ratios (Smaller is better)  
29  
30  
31  
32  
33  
34  
35  
36  
37  
38  
39  
40  
41  
42  
43  
44  
45  
46  
47  
48  
49  
50  
51  
52  
53  
54  
55  
56  
57  
58  
59  
60

Designation	Composition
A <sub>1</sub>	Epoxy + 20 wt% jute fiber
B <sub>1</sub>	Epoxy + 30 wt% jute fiber
C <sub>1</sub>	Epoxy + 40 wt% jute fiber
C <sub>2</sub>	Epoxy + 40 wt% jute fiber + 10wt% SiC
C <sub>3</sub>	Epoxy + 40 wt% jute fiber + 20wt% SiC

**Table 1.** Designation and detailed composition of the composites

Control Factors	Symbols	Fixed parameters	
Velocity of impact	Factor A	Erodent	Silica sand
Impingement angle	Factor B	Erodent feed rate (g/min)	10.0 ± 1.0
Erodent size	Factor C	Test temperature	RT
Fiber/Filler loading	Factor D	Nozzle diameter (mm)	3
		Length of nozzle (mm)	80
		Stand-off distance (mm)	100

**Table 2** Parameters considered during erosion test

Control factor	Level			Units
	I	II	III	
A: Velocity of impact	32	44	58	m/sec
B: Impingement angle	30	60	90	degree
C: Erodent size	200	300	400	$\mu\text{m}$
D: Fiber loading (for composites A <sub>1</sub> ,B <sub>1</sub> ,C <sub>1</sub> )  Filler content (for composites C <sub>1</sub> ,C <sub>2</sub> ,C <sub>3</sub> )	20   0	30   10	40   20	wt%   wt%

**Table 3** Levels for various control factors

Test Run	Erodent Velocity (m/s)	Impingement Angle (Degrees)	Erodent Size ( $\mu\text{m}$ )	Fiber Content (wt %)
	A	B	C	D
1	32	30	200	20
2	32	60	300	30
3	32	90	400	40
4	44	30	300	40
5	44	60	400	20
6	44	90	200	30
7	58	30	400	30
8	58	60	200	40
9	58	90	300	20

**Table 4** Orthogonal array for L<sub>9</sub> Taguchi Design for composites A<sub>1</sub>,B<sub>1</sub>,C<sub>1</sub>

Test Run	Erodent Velocity (m/s) A	Impingement Angle (Degrees) B	Erodent size ( $\mu\text{m}$ ) C	Filler Content (wt %) D
1	32	30	200	0
2	32	60	300	10
3	32	90	400	20
4	44	30	300	20
5	44	60	400	0
6	44	90	200	10
7	58	30	400	10
8	58	60	200	20
9	58	90	300	0

**Table 5** Orthogonal array for  $L_9$  Taguchi Design composites  $C_1, C_2, C_3$

Test Run	Erodent Velocity (m/s)	Impingement Angle (Degrees)	Erodent size ( $\mu\text{m}$ )	Fiber Content (wt %)	Theoretical ER (mg/kg)	Experimental ER (mg/kg)	Error (%)
1	32	30	200	20	172.38	155.710	10.70
2	32	60	300	30	189.76	172.564	9.96
3	32	90	400	40	174.46	188.543	7.46
4	44	30	300	40	218.95	202.765	7.98
5	44	60	400	20	196.88	176.987	11.23
6	44	90	200	30	216.48	197.643	9.53
7	58	30	400	30	235.97	211.987	11.3
8	58	60	200	40	257.98	234.980	9.78
9	58	90	300	20	217.89	199.768	9.07

**Table 6** Erosion Test Results for Jute-Epoxy Composites

Test Run	A	B	C	D	E	S/N Ratio
1	32	30	200	20	155.710	-43.8463
2	32	60	300	30	172.564	-44.7390
3	32	90	400	40	188.543	-45.5082
4	44	30	300	40	202.765	-46.1399
5	44	60	400	20	176.987	-44.9588
6	44	90	200	30	197.643	-45.9176
7	58	30	400	30	211.987	-46.5262
8	58	60	200	40	234.980	-47.4206
9	58	90	300	20	199.768	-46.0105

**Table 7** S/N ratio and Erosion Rate for Different Test conditions (for unfilled composites)

Level	A	B	C	D
1	-44.70	-45.50	-45.73	-44.94
2	-45.67	-45.71	-45.63	-45.73
3	-46.65	-45.81	-45.66	-46.36
Delta	1.95	.31	0.10	1.42
Rank	<b>1</b>	<b>3</b>	<b>4</b>	<b>2</b>

**Table 8** Response Table for Signal to Noise Ratio (Smaller is better) for unfilled composites



Test Run	Erodent Velocity (m/s)	Impingement Angle (Degrees)	Erodent size ( $\mu\text{m}$ )	Filler Content (wt %)	Theoretical ER (mg/kg)	Experimental ER (mg/kg)	Error (%)
1	32	30	200	0	142.83	135.170	5.66
2	32	60	300	10	144.68	133.980	7.89
3	32	90	400	20	114.46	106.667	7.30
4	44	30	300	20	121.95	131.320	7.13
5	44	60	400	0	226.81	204.778	10.75
6	44	90	200	10	199.40	189.874	5.01
7	58	30	400	10	235.297	211.493	11.25
8	58	60	200	20	217.297	197.765	9.87
9	58	90	300	0	247.892	258.370	4.05

**Table 9** Erosion Test Results for particulate filled jute-epoxy Composites

Test Run	A	B	C	D	E	S/N Ratio
1	32	30	200	0	135.170	-42.6176
2	32	60	300	10	133.980	-42.5408
3	32	90	400	20	106.667	-40.5606
4	44	30	300	20	131.320	-42.3666
5	44	60	400	0	204.778	-46.2257
6	44	90	200	10	189.874	-45.5693
7	58	30	400	10	211.493	-46.5059
8	58	60	200	20	197.765	-45.9230
9	58	90	300	0	258.370	-48.2448

**Table 10** S/N ratio and erosion rate for different test conditions for particulate filled jute-epoxy composites

Level	A	B	C	D
1	-41.91	-43.83	-44.70	-45.70
2	-44.72	-44.90	-44.38	-44.87
3	-46.89	-44.79	-44.43	-42.95
Delta	4.98	1.07	0.32	2.75
Rank	<b>1</b>	<b>3</b>	<b>4</b>	<b>2</b>

**Table 11** Response Table for Signal to Noise Ratios (Smaller is better) for particulate filled jute-epoxy Composites